Nonlinear Control of Autonomous Underwater Vehicle in Shallow Water Environment

Liu Shuyong

School of Electrical & Electronic Engineering

A thesis submitted to the Nanyang Technological University

in fulfillment of the requirements for the degree of

Doctor of Philosophy

2008

Statement of Originality

I hereby certify that the content of this thesis is the result of work done by me and has not been submitted for a higher degree to any other University or Institution.

....

Date Liu Shuyong

Acknowledgments

I would like to express my sincere gratitude to all the people who have assisted me during the years of my postgraduate study at Nanyang Technological University. I am most grateful to my supervisors, Professor Wang Danwei and Associate Professor Poh Engkee, for their professional guidance, constant support, encouragement and trust. Their insightful comments have been an inspiration for my work. It has been a great pleasure to have Professor Wang and Poh as my advisors.

Thanks my colleagues in Intelligent Robotics Lab, they are friendly and helpful.

At last, my sincere thanks go to all the members of my family. Thank for your love, care, understanding and encouragement.

Summary

This dissertation presents new results on the design of output feedback control systems for Autonomous Underwater Vehicles (AUVs) operating in very shallow water/surface zone (VSW/SZ) areas. The VSW and SZ areas are defined as water depths of 40 feet to 10 feet and 10 feet to water surface, respectively.

The AUVs operating in shallow water environments are exposed to continuous time-varying environmental disturbances due to shallow water waves. There are various missions for the AUVs in shallow water which requires different corresponding control strategies, such as station keeping (SK) which has precise control requirement, dynamic positioning (DP) and trajectory tracking which concern energy efficiency problems. The unmeasurable wave velocities or wave displacements are estimated by nonlinear observer which will be used to accomplish these various control objectives. This thesis will investigate the nonlinear observer and corresponding controller designs for various control objectives.

The main contributions of this thesis include:

- Nonlinear observer designs: A nonlinear observer is firstly designed for tracking control of an AUV in shallow water area with known wave parameters. The low frequency (LF) positions and velocities of the vehicle, along with the wave frequency (WF) positions in the earth-fixed frame are well estimated. The global exponential stability (GES) of the observer is proved. An adaptive observer is then designed for tracking control of an AUV in shallow water area concerning unknown constant wave parameters. The adaptive

observer is proved to be globally asymptotically stable (GAS). Simulations are conducted to demonstrate the performance of proposed observers. With these observer designs, we can derive different output feedback controller for various mission requirements.

- Station keeping controller designs: The mission of station keeping is to maintain the position of an AUV at a fixed point in shallow water environments by counteracting external wave disturbances. Based on some separation principle and observer backstepping techniques, two output feedback controllers are developed, respectively. The nonlinear output feedback controllers are shown to maintain the AUV at a fixed position by effectively counteracting high frequency wave disturbance. The stability of the proposed observers are proven by using Lyapunov stability analysis. Simulation results of a representable AUV show that the output feedback controller indeed performs well with good stability and robustness properties. With these designed approaches, AUVs can be used for Mine Countermeasures (MCM) for force protection and counter-terrorism with precision requirement.

- Dynamic positioning controller design: An energy efficient control strategy for AUVs operating at low speed motion in shallow water environment is formulated and an observer backstepping controller is designed to maintain AUVs at a position without counteracting the wave disturbances. Also using the Lyapunov stability analysis, the GES of the whole observer-controller system is proven. Case study and simulation results are presented to show the performance of the output feedback controller.

- Trajectory tracking controller design: An output feedback controller for trajectory tracking for high speed AUVs in shallow water area concerning the energy efficiency problem is developed. The global exponential stability (GES) of the observer-controller system is proved by Lyapunov stability theory. Simulation results are also presented to demonstrate the performance of the proposed controller.

Table of Contents

List of Figures

List of Tables

Chapter 1

Introduction

1.1 Motivation

Autonomous underwater vehicles (AUVs) are unmanned, untethered, self-contained systems designed for applications in marine environment. The technologies in connection with the development of AUVs, due primarily to the continual improvement in computer technology, have advanced to the point where such vehicles now provide a promising solution for ocean science and engineering applications.

Unlike remotely operated vehicles (ROVs), which are manipulated by operators on the mother ships through a power and communications umbilical cable, AUVs are free-swimming vehicles which carry their own on-board power and sensors and automatically interact with the environment through the intelligent control algorithms stored in the on-board computers. The lack of an umbilical cable allows AUVs to operate at ranges unreachable by ROVs, such as missions of over a 1000 kilometers distance in areas fully covered by ice [26]. The potential applications of AUVs include military (mine warfare, mine countermeasures, tactical information gathering, smart weapons, harbor protection, etc) [16, 42, 53], scientific (oceanography, geophysics, geology, etc) [6, 77, 96], environmental (sub-ice monitoring,

waste disposal monitoring, wetland surveillance, etc) [26, 35, 39, 57], commercial (cable inspection, oil and gas, etc) [7, 43].

Recently, AUVs have also become a critical cornerstone for many countries's naval warfare strategy. With increased amphibious operations in littoral environments and an increased need for force protection of ports, it is critical to be able to characterize the undersea battlefield and an enemy's coastal defenses. The undersea battlefield has undergone considerable changes with the advent of improved mines, submarine quieting, and other littoral threats from enemy nations and terrorists. The U.S. naval strategic commanders accorded the highest priority to Mine Countermeasures (MCM) for force protection and counter-terrorism [8]. Given the inherent danger in dealing with the naval mine threat coupled with low public tolerance for casualties and overall initiatives to replace manpower with technology, AUVs have assumed an increasingly important role in the MCM missions.

The totally submersible Autonomous Underwater Vehicle (AUV) is an alternative option for MCM missions because of the harsh environment in very shallow water (VSW) and surface zone (SZ) domains. AUVs not only provide safety to military forces by removing the human swimmer from the hostile minefield environment, but they also provide a more maneuverable asset in the random and turbulent water of the shallow water environments.

Due to the highly nonlinearity in motion dynamics and significant environment disturbances, it is a great challenge to design control systems for AUVs operating in very shallow water/surface zone (VSW/SZ) domains. This thesis focuses on output feedback controller designs of AUVs operating in shallow water environment for different mission objectives.

1.2 Literature Review and Research Formulation

In this section we will summarize available results in the control aspects of AUVs.

Since the first modern use of unmanned underwater vehicles (UUVs) in the early 70's, unmanned underwater vehicle technology has almost attained maturity.

From being a vehicle mainly used by scientists for research purposes, AUVs have become increasingly popular due to various mission requirements, such as military operations, environmental monitoring, inspections of cables and sub sea installations. These have fuelled demands on the motion capabilities of the AUVs for station keeping, dynamic positioning, way-point tracking, path following and high speed manoeuvering. In particular the requirements on the control system have increased correspondingly. To design the control systems, the dynamic models of underwater vehicles are required, and models of underwater vehicles have been investigated by many authors [3, 27, 45, 79, 112]. The autopilot controller designs for AUVs present several difficulties due to:

(1) the fundamentally nonlinear dynamics of the vehicle.

(2) the external disturbances such as underwater currents and wave disturbances

The essential features of AUVs are more advanced and more sophisticated than surface ships due to their nonlinear dynamics and challenging mission requirements. Due to their operating environments and their inherent nonlinear behaviors, significant challenges present in the autopilot controller designs of AUVs. Various kinds of autopilot controllers have been investigated for underwater vehicle control systems, such as LQG/LTR control [75, 104] sliding control [45, 111] , nonlinear control [76], adaptive control [13, 37, 60, 81, 103, 112, 115], neural network control [47, 70, 106, 113, 114], fuzzy control [18, 52, 97], and combination of them [32, 41, 61, 109]. Various control architectures for autonomous underwater vehicles were also discussed in [31, 41, 61, 105].

Naeem *et al.* proposed an integrated guidance and control approach using a hybrid guidance law and an LQG/LTR controller [75]. The LQR/LTR controller is synthesized in discrete-time and a hybrid guidance law is proposed which uses different vehicle speeds in different phases of the mission. Triantafyllou and Grosenbaugh applied a multi input-multi output (MIMO) self-tuning controller to the difficult problem of automatic guidance of an AUV with time delays by manipulating thruster outputs to produce the desired translational and yaw velocities in [104].

Yoerger and Slotine [111] designed a sliding mode controller for an underwater vehicle to track trajectory. They investigated the effects of uncertainty in the hydrodynamic coefficients and negligence of cross-coupling terms. Healey and Lienard used similar approach to independently control the speed, yaw and depth channels of an AUV based on linearized model in [45]. This work was then extended to develop a combined channel autopilot for the AUVs at high speed. Results show robust performance in each of the individually controlled channel at low speed, and robust control in the combined autopilot for acceleration up to the chosen operational speed.

Nakamura and Savant [76] proposed a nonlinear tracking control of a 4 DOF (surge, roll, pitch and yaw) AUV considering kinematic motion. They made use of the nonholonomic nature of the system without considering the dynamics of the system.

Goheen and Jefferys [37] proposed a multivariable self-tuning controller as an autopilot for underwater vehicles to overcome model uncertainties while performing positioning and station keeping missions. Yuh [112] described the functional forms of vehicle dynamic equations of motion, the nature of loadings and the use of adaptive control via on line parameter identification. Tabaii *et al.* [103] designed a hybrid adaptive control systems in which plant system is simulated in the continuous domain while control and identification functions are performed in discrete

time. Choi and Yuh [13, 81, 115] developed and implemented a new multiple input multiple output (MIMO) adaptive controller using bound estimation for underwater robotic systems and experimented with the control system on an AUV named Omni Directional Intelligent Navigator (ODIN). Li and Lee [60] presented an adaptive nonlinear controller for diving control of an AUV without any restricting condition on the vehicle's pitch angle in the diving plane based on the backstepping method.

Yuh proposed a neural network control system using a recursive adaptation algorithm with a critic function (reinforced learning approach) in [113, 114]. The special feature of this controller is that the system adjusts itself directly and online without an explicit model of vehicle dynamics. In this approach, a feedforward neural network architecture with three layers of interconnection strengths is used. The experimental results to demonstrate the method in [113, 114] were presented by Lorenz and Yuh in [70]. Ishii *et al.* [47] proposed a neural network based control system called Self-Organizing Neural-Net-Controller System (SONCS), which executed identification of robot dynamics and controller adaptation in parallel with robot control. It examined its effectiveness through application to the heading control of an AUV.

DeBitetto [18] investigated a 14-rule fuzzy logic controller for the depth control of an AUV. Kato reported the implementation of a fuzzy algorithm to manage the guidance and control of an AUV for both attitude control and cable tracking [52]. Smith *et al.* [97] proposed a fuzzy logic controller for controlling and guiding a low-speed torpedo shaped vehicle. Heading, pitch, and depth are controlled simultaneously via three single-axis fuzzy logic controllers.

Wang and Lee presented a self-adaptive recurrent neuro-fuzzy controller as a feedforward controller and a proportional-derivative (PD) controller as a feedback controller for controlling an AUV in an unstructured environment in [109]. Guo *et al.* [41] proposed a sliding mode fuzzy controller to an AUV in shallow water in

order to perform line-of-sight guidance in the horizontal plane. Li and Lee [61] presented a semi-globally stable neural network adaptive control scheme for diving control of an AUV, where the unstructured uncertainties in pitch motion of the vehicle are assumed to be unbounded, although they still satisfy certain growth conditions characterized by bounding functions. Adaptation laws for the unknown but bounded uncertainties are derived from Lyapunov-based method as well as the update laws of the networks weights values. Fossen and Sagatun [32] derived a hybrid adaptive and sliding control scheme which compensates for the uncertainty in the input matrix by adding a discontinuous term to the existing adaptive control law. The hybrid controller is demonstrated in the horizontal motion control of the Norwegian Experimental Remotely Operated Vehicle (NEROV).

From previous literature review, we can see that divers control strategies have been developed for the AUV control problem for various applications. But the control problem of AUVs with wave disturbance has been studied by only a few authors. Riedel [91] showed that the knowledge of the wave disturbances can be used to improve the performance of controller for station keeping. Some states, which cannot be directly obtained such as fluid velocity, are related to the measurements which can be obtained directly. Riedel designed an Extended Kalman Filter for states and disturbances estimation using ground reference velocities measured by a Doppler Velocity Log (DVL) and relative velocities obtained by an Acoustic Doppler Velocimeter (ADV). Based on sliding mode control (SMC) technique, the station keeping controller for surge direction was designed with disturbance feed-forward compensation. This work was later extended to heave, pitch, yaw and sway motion in [21].

For the AUVs operating in shallow water, AUVs must be able to solve various complicated operational tasks where the control objectives differ depending on the particular kind of operation and outside circumstances. For instance, station keeping control is important for Mine Countermeasures (MCM) mission which concern precise control requirement. Due to the limited battery, we also need the

energy efficient control strategies for dynamic positioning and tracking missions. The goals of this research include the need to show that task assignments can be performed well if the characteristics of the operating environment are known. This is particularly important because of the need to operate in environmentally energetic areas and because of the unpredictable nature of the VSW/SZ region. The expensive ADV sensor is not economical for the low cost AUVs to obtain the wave disturbances information. Nonlinear observer is an alternative solution for this problem.

In this thesis the question of observer designs for AUVs operating shallow water is addressed. With this observer technique, we can filter out the wave frequency motions from the noisy measurements to avoid introducing the wave frequency motion into control loop for energy efficiency concern or estimated the wave velocities for station keeping control for precise control requirement. Based on the observers, output feedback controllers are derived to complete the various operation tasks and the stability proofs for the combination of observers and output feedback controllers are also investigated for various mission requirement of AUVs considering wave disturbances. Because wave disturbance is the main disturbance for AUVs in shallow water area, we assume that the dynamic model of AUV itself is known and won't consider the uncertainty of the dynamic model of AUV within this thesis.

1.3 Main Contributions

The objectives for my doctoral research have been the analysis of the different mission requirements and the controller designs for AUVs operating in shallow water environment with wave disturbances. The main contributions are as follows:

- Nonlinear observer designs for estimating wave disturbances

- Dynamic positioning control of AUVs with wave disturbance
- Station keeping control of AUVs in shallow water
- Output feedback controller design for high speed manoeuvering in shallow water environment

These contributions are elaborated in more details as follows.

1.3.1 Nonlinear Observer Designs

The goal of the present research is to develop nonlinear observers for AUVs to provide states and wave estimation in shallow water areas. Compared with traditional Kalman filter-based observer design, where the dynamic model of the vehicle is linearized around a set of operation points, the proposed nonlinear observer can guarantee the global convergence of the estimation. The observers are designed for AUVs manoeuvering in shallow water environment. Hence the coupled Coriolis and centripetal terms cannot be ignored in the model. To deal with the technical difficulty due to the Coriolis and centripetal terms, a coordinate transformation is introduced to remove these terms. Based on the transformed model, a nonlinear observer is firstly designed for tracking control of an AUV in shallow water area with known wave parameters. The low frequency (LF) positions and velocities of the vehicle, along with the wave frequency (WF) positions in the earth-fixed frame are well estimated. The global exponential stability (GES) of the observer is proved. An adaptive observer is then designed for tracking control of an AUV in shallow water area when the wave parameters are unknown. These estimation errors of the adaptive observer are globally asymptotically stable (GAS). Compared to the linear Kalman filter, the number of tuning parameters is significantly reduced. The main results have been published in [64, 66, 69].

1.3.2 Station Keeping Control Design

Station keeping requires the vehicle to be maintained at a desired pose relative to a world frame by counteracting external disturbances with its own thrusters or actuators. With new emphasis on naval mine countermeasure and reconnaissance in shallow water environment, station keeping capability becomes critical. Since small AUVs are sensitive to wave disturbance, AUVs operating in very shallow waters can perform better if wave information is available. By using our results in observer design, two output feedback control design strategies for station keeping of AUVs are proposed. The controllers are based on recently developed separation principle and observer backstepping technique. The results have been published in [65] and are being reviewed for journal publication.[68].

1.3.3 Dynamic Positioning Controller Design

Unlike the station keeping problem, dynamic positioning is concerned with minimizing the energy consumption by actuator. To the best of our knowledge, there has not been any work on DP for small AUVs in shallow water environment and existing results are obtained only for surface vessels. In most current implementation, wave perturbations are not measured. In order to avoid wear and tear on the actuators, it is necessary to filter out wave disturbances so as to reduce the action of actuators to counteract this wave motion. A control design strategy for dynamic positioning of AUVs is presented to solve this problem by using our developed observer results. The designed observer will provide the estimated states and filter out the wave frequency (WF) motion. Using the estimated signals from the observer, an observer backstepping controller is designed to maintain the AUV at a position without counteracting the wave disturbances.

1.3.4 Output Feedback Controller Design

Here we design an energy efficient output feedback controller for trajectory tracking mission of AUVs in shallow water. Based on our previously proposed observer, an observer backstepping controller is developed for tracking control of AUVs. To overcome the technical difficulties in stability proof due to coupling and nonlinearity effects, a coordinate transformation is introduced for the observer and controller designs. The nonlinear output feedback controller is developed to track the desired LF position in the earth-fixed frame without introducing WF disturbance into the feedback control loop. The complete system is proven to be globally exponentially stable (GES) by using Lyapunov stability analysis. The results have been published in [67, 69].

1.4 Thesis Organization

This thesis is organized as follows:

Chapter 2 derives the complete nonlinear equations of motion for a small underwater vehicle subject to shallow water waves. Kinematics, Newton's laws of angular and linear momentum, general hydrodynamics and external force modelling are discussed in detail.

Chapter 3 develops a nonlinear observer for general AUV model with known wave parameters and an adaptive observer for situations when the wave coefficients are unknown.

Chapter 4 proposes two strategies to design station keeping controllers by using separation principle and observer backstepping technique.

Chapter 5 discusses the dynamic positioning control of AUVs using the observer backstepping technique.

Chapter 6 presents a nonlinear output feedback tracking controller of AUVs by removing wave frequency disturbances.

Chapter 7 summarizes this thesis and provides recommendations for future research in this area.

Chapter 2

Mathematical Modelling of Underwater Vehicles

Control design of an underwater vehicle requires a mathematical model. In [22, 28, 45, 112], several models have been developed in various complexity and fidelity, but each model has vehicle specific simplifications and this makes it worthwhile to revisit a more generic and comprehensive model. To the best of our knowledge, there is not a single model that combines all aspects, such as external disturbances and their effects, into a generalized model for shallow water missions of small AUVs.

In this chapter, a generalized nonlinear dynamic model of AUVs without considering wave disturbance is first presented. Kinematics, Newton's law of linear and angular momentum, general hydrodynamics and external force modelling are discussed in details. By using linear wave theory, a generalized six-degree of freedom (6DOF) dynamic equations of motion for small underwater vehicles operating in shallow water is developed.

2.1 Coordinate Frame and Kinematics

2.1.1 Coordinate Frame

It is necessary to describe the positions/orientations and velocity/rotation rates of the vehicle by six independent coordinates or degrees of freedom (6 DOF) for underwater vehicles operating in three dimensional (3D) space. These coordinates are usually chosen corresponding to the position and orientation of vehicle and their time differentiation with respect to some set of mutually orthogonal coordinate axes fixed to an arbitrary origin which defines a coordinate frame. Hence, the forces/moments acting on or produced by actuators of underwater vehicles can be referenced to a set of coordinate axes. In this thesis, standard notation [83] is adopted to describe aforementioned 6 DOF quantities and is summarized in Table 2.1. This notation is also detailed in [28, 29].

To analyze the motion of AUVs in 6DOF, it is convenient to define 2 coordinate frames as indicated in Figure 2.1. The earth-fixed coordinate frame $OX_EY_EZ_E$ usually can be considered to be inertial. The moving coordinate frame $OX_GY_GZ_G$ is fixed to the vehicle which is described relative to the earth-fixed frame.

DOF	Motions	forces and moments	Linear and Angular Velocities	Positions and Euler Angles
1	Surge	$\boldsymbol{X}$	u	x
2	Sway	$\boldsymbol{Y}$	v	y
3	Heave	$\boldsymbol{Z}$	w	z
4	Roll	$\boldsymbol{K}$	p	ϕ
5	Pitch	$\boldsymbol{M}$	q	θ
6	Yaw	$\boldsymbol{N}$	r	ψ

Table 2.1: Notation of the 6DOF of AUVs

Based on this notation, the general motion of underwater vehicles in 6 DOF can be described by the following vectors:

$$\eta = \left[\eta_1^T, \ \eta_2^T \right]^T; \quad \eta_1 = \left[x, y, z \right]^T; \quad \eta_2 = \left[\phi, \theta, \psi \right]^T$$

$$\nu = \left[\nu_1^T, \ \nu_2^T \right]^T; \quad \nu_1 = \left[u, v, w \right]^T; \quad \nu_2 = \left[p, q, r \right]^T$$

$$\tau = \left[\tau_1^T, \ \tau_2^T \right]^T; \quad \tau_1 = \left[X, Y, Z \right]^T; \quad \tau_2 = \left[K, M, N \right]^T$$

Here η_1 and η_2 describe respectively the global positions and Euler angles vectors of vehicle in the earth-fixed frame, ν_1 and ν_2 denote respectively the linear and angular velocity vectors of vehicle in the body-fixed frame, τ_1 and τ_2 are the forces and moments vectors due to actuator action on the vehicle in the body-fixed frame.

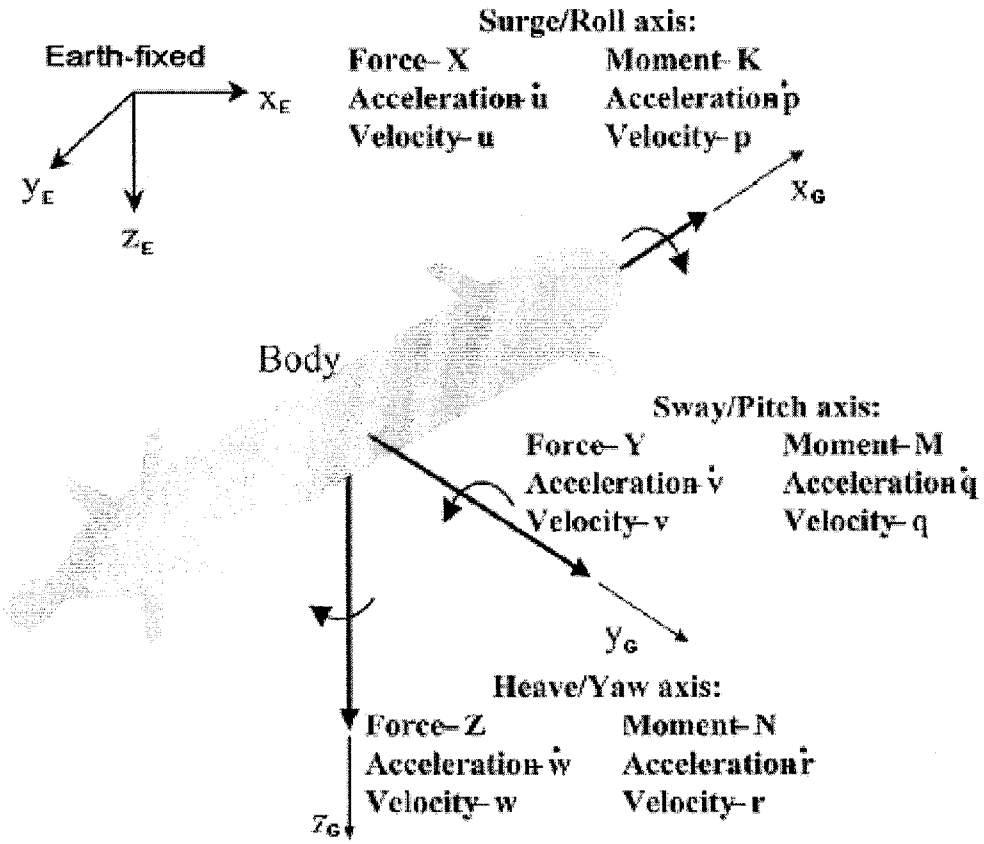

Figure 2.1: Earth-fixed frame and body-fixed frame

2.1.2 Kinematics

Kinematics deals with the relationships of motion quantities regardless of the forces induced by their prescribed motions.

The connection between translational velocity vector and the rate of change of translational position vector, $\dot{\eta}_1 = [\dot{x}, \dot{y}, \dot{z}]^T$, the linear components of the body-fixed velocity vector, $\nu_1 = [u, v, w]^T$, is described as follows [28, 91]

$$\begin{bmatrix} \dot{x} \\ \dot{y} \\ \dot{z} \end{bmatrix} = J_1(\eta) \begin{bmatrix} u \\ v \\ w \end{bmatrix} \tag{2.1}$$

where

$$J_1(\eta) = \begin{bmatrix} \cos\psi\cos\theta & \cos\psi\sin\theta\sin\phi - \sin\psi\cos\phi & \cos\psi\sin\theta\cos\phi + \sin\psi\sin\phi \\ \sin\psi\cos\theta & \sin\psi\sin\theta\sin\phi + \cos\psi\cos\phi & \sin\psi\sin\theta\cos\phi - \cos\psi\sin\phi \\ -\sin\theta & \cos\theta\sin\phi & \cos\theta\cos\phi \end{bmatrix}$$

with ϕ, θ and ψ being the Euler angles of the vehicle in roll, pitch and yaw, respectively.

It is noted that $J_1(\eta)$ is orthogonal:

$$J_1^{-1}(\eta) = J_1^T(\eta) \tag{2.3}$$

The body-fixed angular velocity vector $\nu_2 = [p, q, r]^T$ and the Euler rate vector $\dot{\eta}_2 = [\dot{\phi}, \dot{\theta}, \dot{\psi}]^T$ are related through a transformation matrix $J_2(\eta)$ according to:

$$\begin{bmatrix} \dot{\phi} \\ \dot{\theta} \\ \dot{\psi} \end{bmatrix} = J_2(\eta) \begin{bmatrix} p \\ q \\ r \end{bmatrix} \tag{2.4}$$

where

$$J_2(\eta) = \begin{bmatrix} 1 & \sin\phi\tan\theta & \cos\phi\tan\theta \\ 0 & \cos\phi & -\sin\phi \\ 0 & \sin\phi/\cos\theta & \cos\phi/\cos\theta \end{bmatrix} \tag{2.5}$$

Note that $J_2(\eta)$ has a singularity at pitch angle $\theta = \pm 90°$. In normal operations, this singularity is not a concern because the pitch angle is kept within $|\theta| < 90°$. If the vehicle has to operate at this singular configuration, we can use an alternate kinematic representation such as unit quaternions or Euler parameters [46] to avoid the singularity of Euler angles [29].

Equations (2.1) and (2.4) lead to the following compact form

$$\begin{bmatrix} \dot{\eta}_1 \\ \dot{\eta}_2 \end{bmatrix} = \begin{bmatrix} J_1(\eta) & 0 \\ 0 & J_2(\eta) \end{bmatrix} \begin{bmatrix} \nu_1 \\ \nu_2 \end{bmatrix} \tag{2.6}$$

The development so far has led to the kinematic relationships between translational and rotational velocities, as seen in the body-fixed frame, and the rates of change of global positions and Euler angles in earth-fixed frame.

2.2 Vehicle Rigid-Body Dynamics

The dynamic equations of underwater vehicles have been considered by many authors [22, 28, 44]. In this study, we briefly present a nonlinear six degrees of freedom (6 DOF) model based on Fossen [28]. The rigid body dynamic model of underwater vehicle in the body-fixed reference frame can be represented as

$$M_{RB}\dot{\nu} + C_{RB}(\nu)\nu = \tau_{RB} \tag{2.7}$$

$$\tau_{RB} = \underbrace{\tau}_{\substack{thruster \\ force}} - \underbrace{M_A\dot{\nu} - C_A(\nu)\nu}_{\substack{hydrodynamic \\ added\ mass}} - \underbrace{D(\nu)\nu}_{\substack{hydrodynamic \\ damping\ and\ lift}} - \underbrace{g(\eta)}_{\substack{restoring \\ forces}} \quad (2.8)$$

where

- M_{RB}—— Rigid body mass matrix including translational and rotational inertial elements;
- $C_{RB}(\nu)$—— State dependent matrix including rigid body Coriolis and centripetal elements;
- τ_{RB}——Generalized vector of external forces and moments;
- $M_A\dot{\nu} + C_A(\nu)\nu$——Total added mass forces and moments due to interaction of fluid particles surrounding submerged body;
- $D(\nu)\nu$——Hydrodynamic damping forces and moments;
- $g(\eta)$——Restoring forces and moments or hydrostatic forces and moments (weight and buoyancy);

Equation (2.7) is the most general form of Newton's laws for rigid body motion used today. Equation (2.8) express the external forces and moments resulting from hydrostatics, hydrodynamic lift and drag, added mass, and the control inputs of the vehicle propellers and fins. These forces are all defined in terms of vehicle coefficients.

In basic hydrodynamics, it is common to assume that the hydrodynamic forces and moments on a rigid body are obtained by linearly superposing [25]:

(1) *Radiation-Induced Forces*—— Forces on the body when the body is forced to oscillate with the wave excitation frequency and there are no incidental waves.

(2) *Froude-Kriloff and Diffraction Forces*— Forces on the body when the body is restrained from oscillating and there are incidental waves.

Radiation-induced forces and moments can be identified as the sum of added mass $M_A\dot{\nu} + C_A(\nu)\nu$, radiation-induced potential damping $D_P(\nu)$ and restoring forces $g(\eta)$.

Froude-Kriloff and diffraction forces will be treated separately in the next section where environmental forces are discussed in the context of waves. A more general discussion on marine hydrodynamics is found in Newman [79].

When an underwater vehicle is moving through a fluid, there is a certain amount of fluid which moves with it. The inertia and Coriolis matrices are related to the linear and angular accelerations and velocities of the rigid-body and to the force exerted on vehicles. In the same way, the added-mass and added-Coriolis matrices are related to the linear and angular accelerations and velocities due to the hydrodynamic force exerted by this amount of fluid.

Hydrodynamic damping for ocean vehicles is mainly caused by:

- $D_P(\nu)$— Radiation-induced potential damping due to forced body oscillations.
- $D_S(\nu)$— Linear skin friction due to laminar boundary layers and quadratic skin friction due to turbulent boundary layers.
- $D_W(\nu)$—Wave drift damping.
- $D_M(\nu)$— Damping due to vortex shedding (Morison's equation).

Consequently, the total hydrodynamic damping matrix can be written as a sum of these components, that is:

$$D(\nu) = D_P(\nu) + D_S(\nu) + D_W(\nu) + D_M(\nu) \tag{2.9}$$

In general, the damping matrix of underwater vehicles moving in 6 DOF at high speed will be highly nonlinear and coupled. Nevertheless, a rough approximation could be made by assuming that vehicle is performing a non-coupled motion, has three planes of symmetry and that terms higher than second order are negligible. Fossen [28] states that two main hydrodynamic damping forces have to be taken into account when dealing with underwater vehicles: (1) the quadratic drag and lift forces and (2) the linear skin friction. This suggests a diagonal structure of $D(\nu)$ with only linear and quadratic damping terms on the diagonal. So the equation can be expressed in the following form:

$$\begin{aligned} D(\nu) &= \text{diag}\{X_u, Y_v, Z_w, K_p, M_q, N_r\} \\ &\quad \text{diag}\{X_{u|u|}|u|, Y_{v|v|}|v|, Z_{w|w|}|w|, K_{p|p|}|p|, M_{q|q|}|q|, N_{r|r|}|r|\} \end{aligned} \tag{2.10}$$

The quadratic damping term can be neglected during station keeping or dynamic positioning but cannot be ignored in high speed maneuvering situations.

The vehicle experiences hydrostatic forces and moments as a result of the combined effects of the vehicle weight and buoyancy. The weight, W, and buoyant, B, forces that act at the centers of gravity and buoyancy must be defined from static analysis. For submerged bodies, the weight and buoyancy force vectors do not change with vehicle attitude. Since the weight and buoyancy terms in the applied forces act in the global vertical direction, they must be transformed into components in the body-fixed frame before they can be added into the dynamic equations of motion. Therefore, the net vertical force components can be expressed as

$$g_1(\eta) = \begin{bmatrix} (W-B)\sin\theta \\ -(W-B)\cos\theta\sin\phi \\ -(W-B)\cos\theta\cos\phi \end{bmatrix} \tag{2.11}$$

The weight portion of the vertical force acts at the center of gravity of the vehicle, while the buoyancy portion of the vertical force acts at the center of buoyancy. Because these forces act in locations away from the body center, they create a moment about the body center given by,

$$g_2(\eta) = \begin{bmatrix} -(y_G W - y_B B)\cos\theta c\phi + (z_G W - z_B B)\cos\theta\sin\phi \\ (z_G W - z_B B)\sin\theta + (x_G W - x_B B)\cos\theta c\phi \\ -(x_G W - x_B B)\cos\theta\sin\phi - (y_G W - y_B B)\sin\theta \end{bmatrix} \tag{2.12}$$

where W is the submerged weight of AUV, B is the buoyancy force of AUV, $r_G = [x_G, y_G, z_G]^T$ is the distance between the center of gravity of AUV and the origin of the body-fixed frame of AUV and $r_B = [x_B, y_B, z_B]^T$ is the distance between the center of buoyancy of AUV and the origin of the body-fixed frame of AUV.

So the total vertical hydrostatics force vector can be written as

$$g(\eta) = \begin{bmatrix} g_1(\eta) \\ g_2(\eta) \end{bmatrix} \tag{2.13}$$

By rearranging Equations (2.7) and (2.8), we get the following nonlinear model equation

$$M_{RB}\dot{\nu} + M_A\dot{\nu} = \tau - C_{RB}(\nu)\nu - C_A(\nu)\nu - D(\nu)\nu - g(\eta) \tag{2.14}$$

which can be rewritten as an equivalent form

$$M\dot{\nu} = \tau - C(\nu)\nu - D(\nu)\nu - g(\eta) \tag{2.15}$$

We should note that the dynamics equations of motion are not mathematically expressed in earth-fixed frame but in body-fixed frame. It means that interactions between a vehicle and the ocean environment are defined from the perspective of the vehicle, i.e. within the body coordinate system. This is because all actions and reactions between vehicle and environment are dependent on the orientation, shape, velocity and acceleration of the vehicle body, with the sole exceptions of gravity, waves and current. Also, moment of inertia terms in the mass matrix M can only be constant in a body-fixed frame, further making the body frame attractive for dynamics calculations. The following properties can be observed for the body coordinates vector representation [28]:

Property 1 *For a rigid body, the inertia matrix is strictly positive if and only if* $M_A > 0$. *That is:*

$$M = M_{RB} + M_A > 0 \tag{2.16}$$

If in addition we require that the body is at rest or low speed, under the assumption of an ideal fluid, the inertia matrix will also be symmetrical and positive definite. That is

$$M = M^T > 0 \tag{2.17}$$

Property 2 *For a rigid body moving through an ideal fluid, the Coriolis and centripetal matrix* $C(\nu)$ *can always be parameterized such that* $C(\nu)$ *is skew-symmetrical, that is:*

$$C(\nu) = -C^T(\nu) \quad \forall \quad \nu \in \mathbb{R}^6 \tag{2.18}$$

Property 3 *For a rigid body moving through an ideal fluid the hydrodynamic damping matrix will be real, non-symmetric and strictly positive:*

$$D(\nu) > 0 \quad \forall \quad \nu \in \mathbb{R}^6 \tag{2.19}$$

The dynamic model equation in earth-fixed frame can also be obtained by using following kinematic transformations:

$$\begin{aligned} \dot{\eta} &= J(\eta)\nu \quad &\Longleftrightarrow \quad \nu &= J^{-1}(\eta)\dot{\eta} \\ \ddot{\eta} &= \dot{J}(\eta)\nu + J(\eta)\dot{\nu} \quad &\Longleftrightarrow \quad \dot{\nu} &= J^{-1}(\eta)[\ddot{\eta} - \dot{J}(\eta)J^{-1}(\eta)\dot{\eta}] \end{aligned} \tag{2.20}$$

to eliminate ν and $\dot{\nu}$ in (2.15). Hence we can get the following earth-fixed vector expression of dynamic model:

$$M_\eta(\eta)\ddot{\eta} + C_\eta(\nu,\eta)\dot{\eta} + D_\eta(\nu,\eta)\dot{\eta} + g_\eta(\eta) = \tau_\eta \tag{2.21}$$

where

$$\begin{aligned} M_\eta(\eta) &= J^{-T}(\eta)MJ^{-1}(\eta) \\ C_\eta(\nu,\eta) &= J^{-T}(\eta)[C(\nu) - MJ^{-1}(\eta)\dot{\eta}]J^{-1}(\eta) \\ D_\eta(\nu,\eta) &= J^{-T}(\eta)D(\nu)J^{-1}(\eta) \\ g_\eta(\eta) &= J^{-T}(\eta)g(\eta) \\ \tau_\eta &= J^{-T}(\eta)\tau \end{aligned} \tag{2.22}$$

2.3 Wave Theory and Hydrodynamics

For AUVs to operate with a high degree of reliability, disturbances and their effects on the AUVs must be modelled mathematically with an adequate degree of accuracy. The main source of the dynamic disturbances encountered by underwater vehicles or submerged vessels are wave and current. These disturbance forces arise from buoyant and inertial effects due to ocean wave kinematics. The effects of incident waves on a submerged body can be divided up into several categories. The

largest part, first order forces act at the incident wave frequency. These forces move the vehicle, but usually result in oscillations about a mean state. Another part, second order forces which are the result of wave diffraction and wave interaction, have several different frequency components.

Wave diffraction of a single frequency wave results in a steady force and a varying force at twice the wave frequency. The double frequency force may be neglected, as the inertia of the underwater vehicle effectively filters it. Interaction of waves at different frequencies also results in forces. These forces consist of a component acting at the sum of the wave frequencies and a component acting at the difference of the wave frequencies. The force caused by the summation of the wave frequencies, again, may be neglected, as it is also filtered by the vehicle's inertia. The difference frequency component results in a slowly varying force on the AUVs. To best assess the performance of a vehicle in shallow water, it is necessary to generate a dynamic model comprising wave induced water velocity and acceleration to properly model the wave disturbance forces [28].

2.3.1 Linear Wave Theory

The information in this subsection is not new, except for the application to which this method is applied. The reader is referred to [12, 17, 55, 100] for more detailed descriptions of the mathematical formulations presented in this section.

As shown in Figure 2.2, the simplest free surface wave formation is plane progressive wave system where the water column is modelled as an inviscid, irrotational fluid in earth-fixed frame. From Figure 2.2, the motion of the wave is two dimensional, (x, z), sinusoidal in time with angular frequency ω, and propagates with a phase velocity c_p such that to an observer moving with this speed the wave appears to be stationary. A Cartesian coordinate system is adopted, see Figure 2.2, the plane of undisturbed free surface (still water level) as shown and the z-axis positive

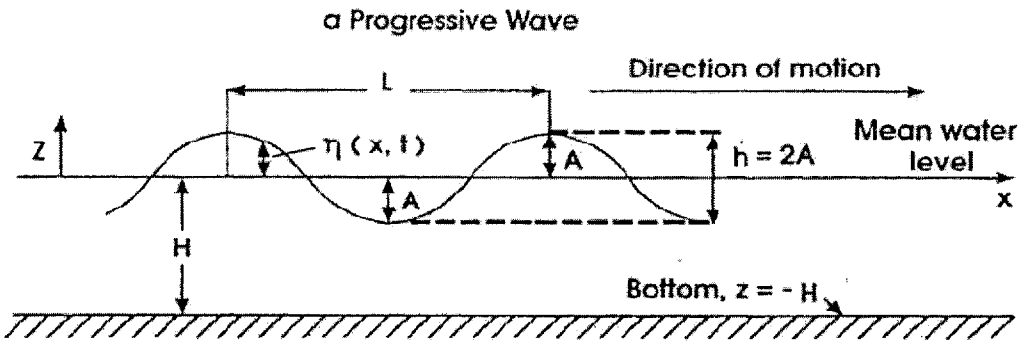

Figure 2.2: Monochromatic progressive surface gravity wave

upwards. So the vertical elevation of any point on the free surface may be defined by a function $z = \eta(x,t)$. With these requirements, the free surface elevation can be expressed in the following general form

$$\eta(x,t) = A\cos(kx - \omega t) \tag{2.23}$$

where the positive x-axis is chosen to coincide with the direction of wave propagation. A is the wave amplitude. $k = 2\pi/L$ is the wave number, where L is the distance between successive points on the wave with the same phase. $\omega = 2\pi/T$ is the angular frequency. The unit for k is rad/m and for $\omega is\ rad/s$. $c_p = \omega/k$ is called the phase velocity.

The waves on the surface set the rest of the water into motion. and at each point, (x,z), the fluid has a velocity

$$\mathbf{v}(x,z,t) = u(x,z,t)\mathbf{i} + w(x,z,t)\mathbf{k} \tag{2.24}$$

where z denotes the vertical coordinate measured upwards from the mean water level. We have now introduced unit vectors **i** and **k** pointing along the x-axis and the z-axis, respectively.

Because water is hard to compress, we will assume that this is incompressible for our convenient purpose. In an ***incompressible*** fluid, the velocity $\mathbf{v} = (u,v,w)$

at each point will satisfy the equation

$$\frac{\partial u}{\partial x} + \frac{\partial v}{\partial y} + \frac{\partial w}{\partial z} = 0 \tag{2.25}$$

called the ***equation of continuity***.

In our case the y-component of the velocity, v, is assumed to be zero. This means that we do not assume any variations across the channel. In addition, if the fluid is considered to be irrotational, the velocity may be expressed in terms of a so-called ***velocity potential*** Φ such that

$$u = \frac{\partial \Phi}{\partial x},\ v = \frac{\partial \Phi}{\partial y},\ w = \frac{\partial \Phi}{\partial z} \tag{2.26}$$

The concepts of "irrotationality" and "velocity potential" are treated in courses in fluid mechanics, and also in about every textbook about water waves. Most of the material stated in here may be found in standard textbooks on the topic, see the references [17, 12, 55, 100]. From Equations (2.25) and (2.26), We obtain

$$\frac{\partial^2 \Phi}{\partial x^2} + \frac{\partial^2 \Phi}{\partial y^2} + \frac{\partial^2 \Phi}{\partial z^2} = 0 \tag{2.27}$$

This equation is a very famous partial differential equation called the ***Laplace equation***.

The bottom of the channel is not permeable to the water, and therefore the vertical water velocity at the bottom ***must be zero at all times***:

$$w(x, z = -H, t) = \frac{\partial \Phi}{\partial z}(x, z = -H, t) = 0 \tag{2.28}$$

This constitutes a relation which must hold at the boundary, and it is therefore called a ***boundary condition***.

The conditions at the water surface are harder to obtain. It has been observed that the fluid near the surface remains near the surface during the wave motion as

long as the motion is smooth. That is, unless the waves break. The first boundary condition at the free surface consists of stating this property in mathematical terms. Consider a part of the surface at two neighboring times as indicated in Figure 2.3

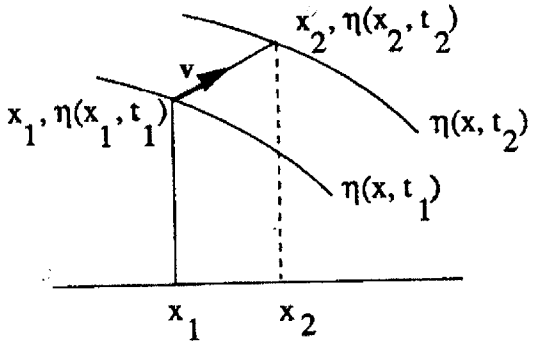

Figure 2.3: Motion of a fluid point on free surface

The point at $(x_1, \eta(x_1, t_1))$ moves with velocity $\mathbf{v}$ to $(x_2, \eta(x_2, t_2))$ during the time interval $\triangle t = t_2 - t_1$. Thus,

$$\eta(x_2, t_2) = \eta(x_1, t_1) + w \cdot (t_2 - t_1) \tag{2.29}$$

$$x_2 = x_1 + u \cdot (t_2 - t_1) \tag{2.30}$$

Let us also expand $\eta(x_2, t_2)$ in a Taylor series:

$$\eta(x_2, t_2) = \eta(x_1, t_2) + \frac{\partial \eta}{\partial x}(x_1, t_2)(x_2 - x_1) + \cdots \tag{2.31}$$

From Equations (2.29) and (2.31), we obtain

$$\eta(x_1, t_2) - \eta(x_1, t_1) + \frac{\partial \eta}{\partial x}(x_1, t_2)(x_2 - x_1) = w \cdot (t_2 - t_1) + \cdots \tag{2.32}$$

So we can rewrite the upper equation by letting $t_2 \rightarrow t_1$

$$\frac{\partial \eta}{\partial t} + u\frac{\partial \eta}{\partial x} = w \tag{2.33}$$

This is the mathematical formulation of the physical condition that a fluid particle at the surface should remain at the surface at all times. It tells you something about the motion of the surface and is therefore called the ***kinematic boundary condition.***

The other condition to be satisfied at the surface comes from the fact that the pressure p at the surface must be equal to the atmospheric pressure, which we assume is constant. This condition may be derived from Bernoulli's Equation which is also treated in basic courses on Fluid Mechanics. The equation states that for irrotational flow

$$\frac{p}{\rho} + \frac{\partial \Phi}{\partial t} + \frac{1}{2}(u^2 + w^2) + gz = C(t) \tag{2.34}$$

The function $C(t)$ is not important and may be set to an arbitrary convenient constant. If we let $C(t) = p_{atm}/\rho = 0$, Bernoulli's equation gives for the free surface:

$$\frac{\partial \Phi}{\partial t} + \frac{1}{2}(u^2 + w^2) + g\eta = 0 \qquad \text{(Has to hold at the surface } z = \eta(x,t)) \tag{2.35}$$

This condition, dealing with the force on the surface, is usually called the ***dynamic boundary condition.***

All together, we have now formulated the mathematical problems which must be solved in order to find the motion of the surface:

(1) Within the fluid, Laplace's equation must be satisfied

$$\frac{\partial^2 \Phi}{\partial x^2} + \frac{\partial^2 \Phi}{\partial z^2} = 0$$

(2) At the closed bottom, equation of continuity must be satisfied

$$w(x, z = -H, t) = \frac{\partial \Phi}{\partial z}(x, z = -H, t) = 0$$

(3) The surface is always made up of the same fluid particles:

$$\frac{\partial \eta}{\partial t} + u\frac{\partial \eta}{\partial x} = w \qquad \text{(Has to hold at the surface } z = \eta(x,t)\text{)}$$

(4) The pressure in the fluid at the free surface is equal to the atmospheric pressure:

$$\frac{\partial \Phi}{\partial t} + \frac{1}{2}(u^2 + w^2) + g\eta = 0 \qquad \text{(Has to hold at the surface } z = \eta(x,t)\text{)}$$

The mathematical problems stated in (1) to (4) are very difficult to solve. No complete solution is known, although we know a lot about special cases. one of the cases is that the magnitude of $\eta(x,t)$ is very small compared to the variations in the x-direction (For a wave we would say that the amplitude is small compared to the wavelength). So if we solve the above four Equations, we can get the ***velocity potential*** and then obtain the fluid particle velocity.

From the requirements of the problem, it is clear that the velocity potential Φ must be sinusoidal in the same sense as Equation (2.23); therefore a solution of the form

$$\Phi(x,z,t) = \sin(kx - \omega t)F(z) \tag{2.36}$$

Substituting Equation (2.36) into Equation (2.27),$F(z)$ must satisfy the ordinary differential equation

$$\frac{d^2F}{dt^2} - k^2F = 0 \tag{2.37}$$

throughout the domain of fluid. The solution to Equation (2.37) satisfying the bottom boundary condition Equation (2.28) is

$$F = C_1 \cosh(k(z+H)) \tag{2.38}$$

Equation (2.35) can be simplified to the next equation because the magnitude of u^2 and w^2 is very small when compared to the magnitude of the other two terms.

$$\frac{\partial \Phi(x,\eta,t)}{\partial t} + g\eta = 0 \tag{2.39}$$

By using the similar method, Equation (2.33) can be simplified as

$$\frac{\partial \eta}{\partial t} = \frac{\partial \Phi}{\partial z} = w \tag{2.40}$$

We can expand w in Taylor series as

$$w(x,\eta,t) = w(x,0,t) + \frac{\partial w}{\partial z}(x, z=0, t)\cdot \eta + O(\eta^2) \tag{2.41}$$

In accordance with the approximations we have already done, we may neglect the term $\partial w/\partial z\eta$, and simply use the Equation (2.41)

$$\frac{\partial \eta}{\partial t} = w(x,0,t) \tag{2.42}$$

A similar argument also linearizes the dynamic condition:

$$\frac{\partial \Phi(x,0,t)}{\partial t} = -g\eta(x,t) \tag{2.43}$$

Combining Equations (2.40) and (2.43) we obtain

$$\frac{\partial^2 \Phi}{\partial t^2} + g\frac{\partial \Phi}{\partial z} = 0, \text{on } z = 0 \tag{2.44}$$

Substituting Equations (2.36) and (2.38) into the surface boundary condition, Equation (2.44) yields an important relationship between the wavenumber k and the frequency ω

$$\omega^2 = gk\tanh(kH) \tag{2.45}$$

which is called the ***dispersion relationship***. The dispersion relationship tells us how the frequency and the wavenumber are connected. By solving Equation (2.39) and (2.23),We can get the parameter C_1

$$\frac{\omega}{g}C_1\cosh(kh) = A \tag{2.46}$$

Substitution of Equations (2.38) and (2.46) into the velocity potential function, Equation (2.36), yields

$$\Phi(x,z,t) = \frac{Ag}{\omega}\frac{\cosh(k(z+H))}{\cosh(kH)}\sin(kx-\omega t) \tag{2.47}$$

By using the Equations (2.26), (2.34) and (2.47), we can get the expression of the fluid particle velocity and pressure fields:

$$\begin{aligned} u(x,z,t) &= A\frac{gk}{\omega}\frac{\cosh(k(z+H))}{\cosh(kH)}\cos(kx-\omega t) \\ w(x,z,t) &= A\frac{gk}{\omega}\frac{\sinh(k(z+H))}{\cosh(kH)}\sin(kx-\omega t) \\ p(x,z,t) &= \rho gA\frac{\cosh(k(z+H))}{\cosh(kH)}\cos(kx-\omega t) - \rho gz + p_{atm} \end{aligned} \tag{2.48}$$

There are several simplifications that mey be made to the above-derived expression for the case of shallow and deep water. The shallow and deep water ranges correspond to $H/L < 1/20$ and $H/L > 1/2$ respectively. It can be seen from Equation (2.48) that the trajectories of the fluid particles are elliptical as shown in Figure (2.4), and the fluid particle velocity is related to the wave number k, angle frequency ω and the depth of the water H. The left illustration in Figure (2.4) is for shallow water, and the right one is for deep water. We can see that shallow water waves are non-dispersive, i.e., the vertical component of wave particle velocity is linear in depth. The horizontal velocity at the bottom for shallow water wave is non-zero, but for deep water is zero.

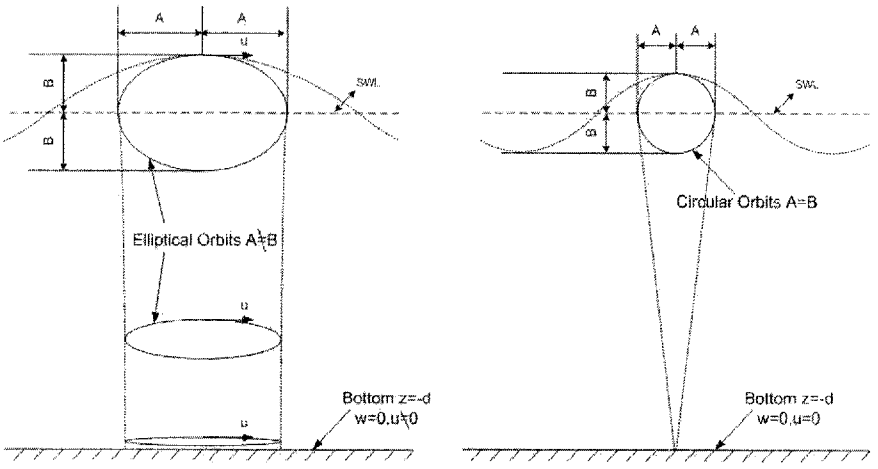

Figure 2.4: Water particle displacement for shallow and deep water wave

2.3.2 Hydrodynamics

Hydrodynamic forces and moments are the result of interactions between body and fluid. The forces and moments on the body arise from the modification to the pressure distribution summed around surface area of the body. This modification to the pressure field can only arise from relative velocity and acceleration between the body and fluid. Therefore, it is necessary to redefine the body-fixed velocity vector ν in terms of a relative velocity vector of the AUV to the wave in the body-fixed frame, $\nu_r = \nu - u_f$, where $\nu_r = [u_r, v_r, w_r, p, q, r]^T$ and u_f is defined as the body-fixed fluid velocity. Also at this time it is also convenient to define an earth-fixed fluid velocity vector $\mathbf{U}_f$, where $\mathbf{U}_f = [U_f, V_f, W_f, 0, 0, 0]^T$. Since it is assumed that the fluid velocity is irrotational, no changes to the angular rate terms are necessary in the earth-fixed fluid velocity vector, and no angular rates are present in the body-fixed fluid velocity vector. The body-fixed fluid velocity can be expressed as

$$u_f = \begin{bmatrix} J_1(\eta) & 0 \\ 0 & J_2(\eta) \end{bmatrix} \mathbf{U}_f = J(\eta)\mathbf{U}_f \tag{2.49}$$

Using the linear wave theory [28], we propose a wave model for the first-order wave induced motion vector, $\mathbf{U}_f$, in this thesis. The state-space expression of the wave model in three degrees of freedom is:

$$\dot{\xi} = \begin{bmatrix} \dot{\xi}_1 \\ \dot{\xi}_2 \end{bmatrix} = \begin{bmatrix} 0 & I \\ \Omega_{21} & \Omega_{22} \end{bmatrix} \begin{bmatrix} \xi_1 \\ \xi_2 \end{bmatrix} + \begin{bmatrix} 0 \\ \Psi_1 \end{bmatrix} n_1 \tag{2.50}$$

$$U_f = \begin{bmatrix} 0 & I \\ 0 & 0 \end{bmatrix} \begin{bmatrix} \xi_1 \\ \xi_2 \end{bmatrix} = \Gamma\xi \tag{2.51}$$

where $\xi_1, \xi_2 \in \mathcal{R}^3$ are water particle position and velocity vectors. $\Omega_{21} = -\text{diag}\{\omega_{o1}^2, \omega_{o2}^2, \omega_{o3}^2\}$, $\Omega_{22} = -\text{diag}\{2\zeta_1\omega_{o1}, 2\zeta_2\omega_{o2}, 2\zeta_3\omega_{o3}\}$, $\omega_{oi}(i = 1, 2, 3)$ are the dominant wave frequencies and $\zeta_i(i = 1, 2, 3)$ are the damping ratios of the wave in surge, sway and heave direction respectively. $\Psi_1 = \text{diag}\{\sigma_1, \sigma_2, \sigma_3\}$ is a constant matrix with $\sigma_i(i = 1, 2, 3)$ as parameters related to wave intensity. Because we assume that the wave is irrotational, the velocity of the wave in the earth-fixed frame is denoted by $\mathbf{U}_f = \begin{bmatrix} U_f & V_f & W_f & 0 & 0 & 0 \end{bmatrix}^T$. n_1 in (2.50) is the zero-mean Gaussian white noise vector that excites the wave model.

This model (2.50) and (2.51) can be rewritten as (for the wave velocities in surge, sway and heave directions, respectively):

$$h_w^i(s) = \frac{U_f^i}{n_1^i}(s) = \frac{\sigma_i s}{s^2 + 2\zeta_i\omega_{oi}s + \omega_{oi}^2} \ (i = 1, 2, 3) \tag{2.52}$$

Referring to Equations (2.7), (2.8) and (2.14), it can be seen that the only parts related to the hydrodynamics are total added mass forces and moments and hydrodynamic damping. When we discuss the hydrodynamics in previous section, we assume that the vehicle is operated in the ideal fluid. But in reality, the vehicle must be operated in real fluid environment with incident wave. So we must consider the Froude-Kriloff forces and moments term into the hydrodynamics model for underwater vehicles operating in shallow water environment. Using potential

flow theory [17, 79], the Froude-Kriloff forces and moments vector can be expressed as

$$f_{FK} = M_{FK}\dot{u}_f \tag{2.53}$$

where $\dot{u}_f$ is the fluid particle acceleration in body-fixed frame, which can be measured by Acoustic Doppler Velocimeter (ADV) such as SonTek's ADVOcean and Nortek Vector Velocimeter, and M_{FK} is the Froude-Kriloff mass matrix. The expression of this mass matrix for a small volume completely submerged body is

$$M_{FK} = \begin{bmatrix} \overline{m} & 0 & 0 & 0 & \overline{m}z_B & -\overline{m}y_B \\ 0 & \overline{m} & 0 & -\overline{m}z_B & 0 & \overline{m}x_B \\ 0 & 0 & \overline{m} & \overline{m}y_B & -\overline{m}x_B & 0 \\ 0 & -\overline{m}z_B & \overline{m}y_B & \overline{I}_{xx} & \overline{I}_{xy} & \overline{I}_{xz} \\ \overline{m}z_B & 0 & -\overline{m}x_B & \overline{I}_{yx} & \overline{I}_{yy} & \overline{I}_{yz} \\ -\overline{m}y_B & \overline{m}x_B & 0 & \overline{I}_{zx} & \overline{I}_{zy} & \overline{I}_{zz} \end{bmatrix} \tag{2.54}$$

where $\overline{m} = B/g, \overline{I}_{xx} = \sum_{i=1}^{N} d\overline{m}_i(y^2 + z^2)$ and $\overline{I}_{xy} = \overline{I}_{yx} = -\sum_{i=1}^{N} d\overline{m}_i(xy)$.

2.4 Nonlinear Model of AUVs Operating in Shallow Water Environment

Recent developments in AUV technology have mainly focused on the electronics, sensors and navigation aspects which render the vehicle autonomous, and somewhat less on the classical aspects such as vehicle dynamics and hydrodynamics [88]. The preciously developed hydrodynamic models used in the AUVs are mainly used for underwater vehicles operating in deep oceans and empirical methods. Aided by sophisticated controllers and with application mainly focused on deep waters, the hydrodynamic models have performed satisfactorily. The need of accurate

hydrodynamics models for shallow-water or near-surface missions is becoming increasingly important for mine countermeasure and surveillance missions in coastal or littoral water.

There was no suitable onboard sensors for small AUVs to measure the shape of sea surface until 1999. Since then, only a few researches have been conducted on the small AUVs by using this technology. By using an ADV Ocean (Acoustic Doppler Velocimeter Ocean) probe, Riedel [91] proposed a method to measure the spectrum and direction of shallow water wave, which is related to the magnitude of force acting on the vehicles. Riedel then designed a sliding model control (SMC) for station keeping control [92]. But he only considered the kinematic and dynamic part of models in surge direction.

2.4.1 Dynamic Model for Station Keeping

Station keeping requires maintaining the vehicle in a fixed position or pose in the earth-fixed frame. To achieve mission, an AUV needs to counteract all external disturbances. Hence, it is convenient to express the wave disturbances in the dynamic model of AUVs.

When the fluid motion is present, Froude-Kriloff forces and moments vector (2.53) must be added in (2.14). Then Equation (2.14) can be modified to:

$$M_{RB}\dot{\nu} + M_A\dot{\nu}_r = \tau - C_{RB}(\nu)\nu - C_A(\nu_r)\nu_r - D(\nu_r)\nu_r - g(\eta) + M_{FK}\dot{u}_f \quad (2.55)$$

This equation is a mixture of various coordinate frame variables; body-fixed, body-fixed relative, earth-fixed and fluid. To solve this system of equations, the equations must be expressed in variables that can be related to each other. Since the vehicle is considered to be in an unsteady fluid referenced to the earth-fixed frame, logical choice for variables is body-fixed relative ν_r and earth-fixed frame.

So Equation (2.55) can be modified as

$$\begin{aligned}(M_{RB}+M_A)\dot{\nu}_r &= \tau - C_{RB}(\nu_r)\nu_r - C_A(\nu_r)\nu_r - D(\nu_r)\nu_r - g(\eta) \\ &\quad -M_{RB}\frac{d(u_f)}{dt} - C_{RB}(u_f)u_f + M_{FK}\frac{d(u_f)}{dt}\end{aligned} \tag{2.56}$$

From Equation (2.56) and recalling that the fluid is defined as irrotational, we can conclude that the $C_{RB}(u_f)$ term on the right hand side of Equation (2.56) is zero. The Froude-Kriloff excitation forces and moments are functions of the weight and buoyancy mismatch $(W-B)$, the fluid velocities and fluid accelerations expressed in body-fixed frame. So Equation (2.56) can be simplified as

$$\begin{aligned}(M_{RB}+M_A)\dot{\nu}_r &= \tau - C_{RB}(\nu_r)\nu_r - C_A(\nu_r)\nu_r - D(\nu_r)\nu_r - g(\eta) \\ &\quad -M_{RB}\frac{d(u_f)}{dt} + M_{FK}\frac{d(u_f)}{dt}\end{aligned} \tag{2.57}$$

When the vehicle is neutrally buoyant, from the definition of M_{RB} and M_{FK}, we can see that M_{RB} is equal to M_{FK}. So Equation (2.57) can be simplified as

$$\begin{aligned}M\dot{\nu}_r &= \tau - C_{RB}(\nu_r)\nu_r - C_A(\nu_r)\nu_r - D(\nu_r)\nu_r - g(\eta) \\ &= \tau - C(\nu_r)\nu_r - D(\nu_r)\nu_r - g(\eta)\end{aligned} \tag{2.58}$$

So at this point the 6DOF equation of motion of underwater vehicles has been modified to Equation (2.57) to account for a moving fluid by representing the body-fixed velocities in relative terms.

However, because the system of Equation (2.6) is for the case of no fluid motion, it must be augmented to provide the necessary link between the global and body-fixed velocities. In order to account for the fluid motion, either wave induced or

steady current, Equation (2.6) must be modified to

$$\begin{bmatrix} \dot{x} \\ \dot{y} \\ \dot{z} \end{bmatrix} = J_1(\eta)(\phi,\theta,\psi) \begin{bmatrix} u_r \\ v_r \\ w_r \end{bmatrix} + \begin{bmatrix} U_f \\ V_f \\ W_f \end{bmatrix} \tag{2.59}$$

$$\begin{bmatrix} \dot{\phi} \\ \dot{\theta} \\ \dot{\psi} \end{bmatrix} = \begin{bmatrix} 1 & \sin\phi\tan\theta & \cos\phi\tan\theta \\ 0 & \cos\phi & -\sin\phi \\ 0 & \sin\phi/\cos\theta & \cos\phi/\cos\theta \end{bmatrix} \begin{bmatrix} p \\ q \\ r \end{bmatrix} = J_2(\eta)\nu_2 \tag{2.60}$$

Equations (2.59) and (2.60) can be combined as

$$\dot{\eta} = J(\eta)\nu_r + \mathbf{U}_f \tag{2.61}$$

Based on Equations (2.50), (2.51), (2.58) and (2.61), a compact form of the nonlinear model of underwater vehicles in shallow water environment can be expressed as

$$\begin{aligned} \begin{bmatrix} \dot{\xi}_1 \\ \dot{\xi}_2 \end{bmatrix} &= \begin{bmatrix} 0 & I \\ \Omega_{21} & \Omega_{22} \end{bmatrix} \begin{bmatrix} \xi_1 \\ \xi_2 \end{bmatrix} + \begin{bmatrix} 0 \\ \Psi_1 \end{bmatrix} n_1 \\ U_f &= \begin{bmatrix} 0 & I \\ 0 & 0 \end{bmatrix} \begin{bmatrix} \xi_1 \\ \xi_2 \end{bmatrix} = \Gamma\xi \\ \dot{\eta} &= J(\eta)\nu_r + \mathbf{U}_f \\ y &= \eta \\ M\dot{\nu}_r &= \tau - C(\nu_r)\nu_r - D(\nu_r)\nu_r - g(\eta) \end{aligned} \tag{2.62}$$

Although the precious compact form of nonlinear model of underwater vehicles describe the complete model considering the wave disturbance, Equation (2.62) is

suitable for controller design in station keeping mission, which is fulfilled by counteracting all external disturbances through actuators. For other missions requiring actuator energy efficiency, such as dynamic positioning and output tracking, Equation (2.62) is not the appropriate choice.

2.4.2 Model for Dynamic Positioning and Output Tracking

When considering the actuator energy efficiency, only the slow varying disturbances should be counteracted by propulsion system, whereas the oscillatory motion due to the waves (first-order wave disturbances) should not enter the feedback control loop [33]. It has been shown that linear treatment of wave disturbance is effective for control system design in marine vehicle motions with waves during course keeping [23, 36, 89]. The controller design is based on the so-called wave filtering techniques, which separate the position and heading measurements into a low-frequency (LF) and wave frequency (WF) position and heading estimate [29].

In mathematical modelling of the AUVs dynamics in shallow water area for actuator energy efficiency, it is common to separate AUV model into a low-frequency (LF) model and a wave-frequency (WF) model. Hence the total AUV motion is a superposition of the corresponding LF and the WF components as shown in Figure 2.5.

Similar to Equations (2.50) and (2.51), the wave motion can be expressed in the following form.

$$\dot{\xi} = \begin{bmatrix} \dot{\xi}_1 \\ \dot{\xi}_2 \end{bmatrix} = \begin{bmatrix} 0 & I \\ \Omega_{21} & \Omega_{22} \end{bmatrix} \begin{bmatrix} \xi_1 \\ \xi_2 \end{bmatrix} + \begin{bmatrix} 0 \\ \Psi_1 \end{bmatrix} n_1 \tag{2.63}$$

$$\eta_f = \begin{bmatrix} 0 & I \\ 0 & 0 \end{bmatrix} \begin{bmatrix} \xi_1 \\ \xi_2 \end{bmatrix} = \Gamma\xi \tag{2.64}$$

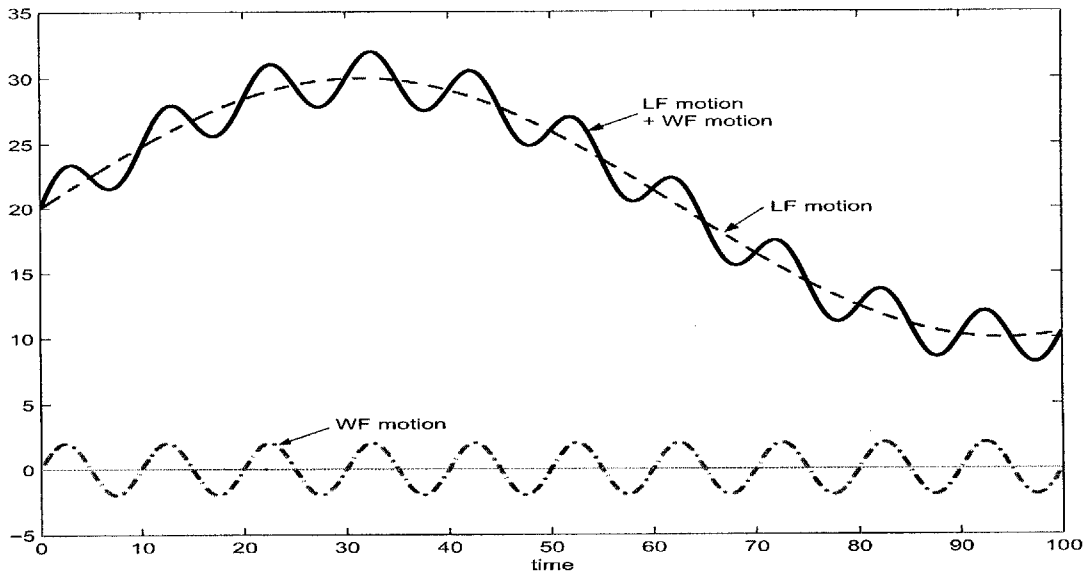

Figure 2.5: Superposition of low-frequency (LF) vessel position and wave frequency (WF) position. Only the total position is measurable

where $\xi_2 \in \mathcal{R}^3$ is the irrotational wave-induced WF position component in earth-fixed frame, $\Omega_{21} = -\text{diag}\{\omega_{o1}^2, \omega_{o2}^2, \omega_{o3}^2\}$, $\Omega_{22} = -\text{diag}\{2\zeta_1\omega_{o1}, 2\zeta_2\omega_{o2}, 2\zeta_3\omega_{o3}\}$, here ζ_i (i=1,2,3) are the damping ratios sand ω_{oi1}(i=1,2,3) are the dominant frequencies of the wave-induced WF motion component in surge, sway and heave direction respectively. Ψ_1=diag$\{\sigma_1, \sigma_2, \sigma_3\}$ is a constant matrix related to the wave intensity. We assume that the wave is irrotational, so the wave particle in the earth-fixed frame is denoted by $\eta_f = \begin{bmatrix} x_f & y_f & z_f & 0 & 0 & 0 \end{bmatrix}^T$. n_1 in (2.63) is the zero-mean Gaussian white noise vector that excites the second-order wave model [33]. Here we assume that the WF disturbance on rotational motion of AUVs is very small and will be ignored in the following analysis [29]. However, the performance of the closed-loop system will be verified with WF disturbance in the rotational motion in simulations.

The kinematic model of an AUV in shallow water still is described by the following

equations:

$$\begin{bmatrix} \dot{\eta}_1 \\ \dot{\eta}_2 \end{bmatrix} = \begin{bmatrix} J_1(\eta) & 0 \\ 0 & J_2(\eta) \end{bmatrix} \begin{bmatrix} \nu_1 \\ \nu_2 \end{bmatrix} \tag{2.65}$$

The position and orientation measurements of AUV can be written as:

$$y = \eta + \eta_f + d \tag{2.66}$$

where $d \in \mathcal{R}^6$ is the zero mean Gaussian white measurement noise and unmodeled disturbance vector. This disturbance term is negligible compared to the WF motion component. However, it will be shown through simulation that this measurement noise has no significant effect on the performance of the observer.

So the compact nonlinear model of underwater vehicles for the energy efficiency consideration can be written as the following forms:

$$\begin{aligned} \begin{bmatrix} \dot{\xi}_1 \\ \dot{\xi}_2 \end{bmatrix} &= \begin{bmatrix} 0 & I \\ \Omega_{21} & \Omega_{22} \end{bmatrix} \begin{bmatrix} \xi_1 \\ \xi_2 \end{bmatrix} + \begin{bmatrix} 0 \\ \Psi_1 \end{bmatrix} n_1 \\ \eta_f &= \begin{bmatrix} 0 & I \\ 0 & 0 \end{bmatrix} \begin{bmatrix} \xi_1 \\ \xi_2 \end{bmatrix} = \Gamma\xi \\ y &= J(\eta)\nu + \eta_f = \eta + \eta_f \\ M\dot{\nu} &= \tau - C(\nu)\nu - D(\nu)\nu - g(\eta) \end{aligned} \tag{2.67}$$

2.5 Conclusion

The structure and properties of nonlinear dynamic model of AUVs are very important to take into consideration when we designing control systems for AUVs operating shallow water environment for various tasks. In this chapter, the kinematic

and dynamic relationships are presented for a small AUV operating in shallow water areas. We discussed the inertia of ambient water-vehicle system, Coriolis and centripetal forces and damping are formulated in a vectorial form with emphasis on the matrix properties of the model. Based on linear wave theory, we obtained the model of shallow water wave and then identified the hydrodynamic forces arising from wave disturbances. Subsequently, a generalized six-degree of freedom (6DOF) equations of motion for small AUVs operating in shallow water is developed. The wave disturbance is introduced into the dynamic model as wave velocities and relative velocities. We can design a control strategy for station keeping control by contracting the wave forces through actuators.

A simplified model for energy efficiency purpose is presented based on the linear treatment of wave disturbances. The wave disturbances are only introduced into the kinematic model of AUVs. The results presented are useful for control engineer who want to design energy efficient control systems for AUVs exploiting the structural properties of the AUV model in the stability analysis.

Chapter 3

Nonlinear Observer Designs

3.1 Introduction

In marine vehicle systems, linear translational velocities such as surge, sway and heave velocities usually are difficult to be derived from available position measurements. These typical sensors include Doppler Velocity Log (DVL), Ultra-Short Baseline (USBL), Inertia Navigation System (INS) and Global Positioning System (GPS) which yield only absolute vehicular position and velocity [48, 73]. The typical approach is to use GPS to calibrate the dead-reckoning sensors and DVL prior to the AUV's initial dive and then used only dead reckoning throughout the mission. As GPS signals cannot travel through water, AUVs need to surface at periodic interval to obtain precise position to perform sensor calibrations, and then dive back down to continue its missions using the position fix in subsequent real-time navigation [38, 58]. As the position measurements are usually corrupted by noise, numerical differentiation of position measurements to obtain relative velocity is not advantageous due to severe noise [33]. So estimation of the translational velocities must be determined from noisy measurements by using the state observers with a wave model. These estimated signals will be used for the controller

design. In this chapter, we design a nonlinear adaptive observer for high speed tracking control of an AUV with wave filtering in shallow water environments.

When the mission purpose is considering energy efficiency, it is not desirable to counteract the high frequency oscillatory movement due to wave. So it is critical to design the controller to avoid wear and tear on thrusters and to save energy. This is achieved by using wave filtering method, which separates the position and heading measurements into low-frequency (LF) and wave frequency (WF) position and heading estimates. These techniques are mostly used in dynamic positioning (DP) and position mooring (PM) systems for ships operating in horizontal plan.

In the traditional DP systems, the wave filtering and state estimation problems are solved by using linear Kalman filters. When the Kalman filter is used in the observer design, the ship kinematics and dynamics model are linearized about a set of pre-defined constant yaw angles, typically 36 operation points in steps of 10 degrees, to cover the whole heading envelope between 0 and 360 degrees [9, 93, 34, 98]. This problem is also solved by using H_∞ technique by Katebi *et al.* [51, 90]. The liberalization of kinematic equations will degrade the performance, moreover, the global stability of the whole system cannot be guaranteed when the observer is used in conjunction with a linear controller. However, if the nonlinearities of the systems satisfy a global Lipschitz condition, a modification of the extended Kalman filter can ensure global exponential stability [90]. Another approach with comparable performance is to utilize the model structure and let the observer "linearize" itself about the measured compass heading. Compared to traditional extended Kalman-filters, the on-line explicit linearization is avoided, and global stability properties are more easily established since the nonlinear kinematics can be treated as a known time-varying block. The number of tuning parameters is significantly reduced and the tuning parameters are coupled more directly to the physics of the system. Examples of this method are the passivation designs [33, 102], further extensions to higher order monotonic damping terms [1], incorporation of position, velocity and partial acceleration feedback [63] and using

of contraction theory [50].

New methods in nonlinear system theory have also been applied not only to the control problem, but also to the observer design problem. Slotine *et al.* [95, 110], Canudas de Wit and Slotine [110] present a sliding mode observer using the similar concept to the sliding mode control. Passivity and observer designs for mechanical systems are treated in Ortega *et al.* [84]. An overview of some different methods on nonlinear observer design can be found in [82].

For tracking control problem, the velocities of the marine vehicle cannot be assumed to be near zero. Hence, Coriolis and centripetal forces and moments must be included into the vehicle model, as opposed to dynamic positioning or position mooring systems. To facility stability proof of our observer design, a coordinate transformation is firstly made to remove the Coriolis and centripetal terms. The observer design is carried out using the transformed model by assuming the constant known wave model. The global exponential stability (GES) of the closed observer system is proved by Lyapunov stability theory. When considering the unknown wave model, we design an adaptive observer by using the augment observer technique [24]. Based on the Lasalle's lemma, the global asymptotic stability (GAS) of the system can be guaranteed.

3.2 Model Description

The mathematical model of an AUV with 6DOF under the influence of wave disturbances, Equation (2.67), can be rewritten as [29], [20]

$$\dot{\eta}_1 = J_1(\eta_2)\nu_1 \tag{3.1}$$

$$\dot{\eta}_2 = J_2(\eta_2)\nu_2 \tag{3.2}$$

$$M_1\dot{\nu}_1 = -C_1(\nu_1)\nu_2 - D_1(\nu_1)\nu_1 - g_1(\eta_2) + \tau_1 \tag{3.3}$$

$$M_2\dot{\nu}_2 = -C_1(\nu_1)\nu_1 - C_2(\nu_2)\nu_2 - D_2(\nu_2)\nu_2 - g_2(\eta_2) + \tau_2 \tag{3.4}$$

$$\dot{\xi} = \begin{bmatrix} \dot{\xi}_1 \\ \dot{\xi}_2 \end{bmatrix} = \begin{bmatrix} 0 & I \\ \Omega_{21} & \Omega_{22} \end{bmatrix} \begin{bmatrix} \xi_1 \\ \xi_2 \end{bmatrix} + \begin{bmatrix} 0 \\ \Psi_1 \end{bmatrix} n_1 \tag{3.5}$$

$$y = \begin{bmatrix} \eta_1 \\ \eta_2 \end{bmatrix} + \begin{bmatrix} \eta_w \\ 0 \end{bmatrix} = \begin{bmatrix} \eta_1 \\ \eta_2 \end{bmatrix} + \begin{bmatrix} 0 & I_{3\times3} \\ 0 & 0 \end{bmatrix} \begin{bmatrix} \xi_1 \\ \xi_2 \end{bmatrix} = \eta + \Gamma\xi \tag{3.6}$$

where $\eta_1 = \begin{bmatrix} x & y & z \end{bmatrix}^T$ denotes the LF motion position vector in the earth-fixed frame, $\eta_2 = \begin{bmatrix} \phi & \theta & \psi \end{bmatrix}^T$ is the heading angle vector in the earth-fixed frame, $\nu_1 = \begin{bmatrix} u & v & w \end{bmatrix}^T$ is the vehicle's LF velocity vector in surge, sway and heave directions in the body-fixed frame, $\nu_2 = \begin{bmatrix} p & q & r \end{bmatrix}^T$ is the vector of vehicle's roll, pitch and yaw velocities expressed in the body-fixed frame. $\xi_2 \in \mathcal{R}^3$ is the high frequency wave-induced WF motion component to AUVs in the earth-fixed frame. Ω_{21}=-diag$\{\omega_{o1}^2, \omega_{o2}^2, \omega_{o3}^2\}$, Ω_{22}=-diag$\{2\zeta_1\omega_{o1}, 2\zeta_2\omega_{o2}, 2\zeta_3\omega_{o3}\}$, here ζ_i (i=1,2,3) is the relative damping ratio and ω_{oi}(i=1,2,3) is the dominant frequency of the wave-induced AUVs motion in surge, sway and heave direction, respectively. Ψ_1 is a constant matrix related to the wave intensity. n_1 is the zero mean white noise vector to drive the wave model. The WF motion component $\eta_w = \xi_2 = \begin{bmatrix} x_w & y_w & z_w \end{bmatrix}^T$ is added to η_1, the low-frequency position components of the AUV.

The inertia matrices of AUV are given as follows:

$$M_1 = \text{diag}(m_{11}, m_{22}, m_{33}),\ M_2 = \text{diag}(m_{44}, m_{55}, m_{66}) \tag{3.7}$$

where $m_{jj}(0 \le j \le 6)$ denote the positive constant inertia terms including added mass in surge, sway, heave, roll, pitch and yaw, respectively.

The Coriolis and centripetal matrices are given by

$$C_1(\nu_1) = \begin{bmatrix} 0 & m_{33}w & -m_{22}v \\ -m_{33}w & 0 & m_{11}u \\ m_{22}v & -m_{11}u & 0 \end{bmatrix}$$
$$C_2(\nu_2) = \begin{bmatrix} 0 & m_{66}r & -m_{55}q \\ -m_{66}r & 0 & m_{44}p \\ m_{55}q & -m_{44}p & 0 \end{bmatrix} \tag{3.8}$$

The damping matrices are

$$\begin{aligned} D_1(\nu_1) &= D_1 + D_{1q}(\nu_1) \\ &= \text{diag}\{d_u, d_v, d_w\} + \text{diag}\{\sum_{i=2}^{3} d_{ui}|u|^{i-1}, \sum_{i=2}^{3} d_{vi}|v|^{i-1}, \sum_{i=2}^{3} d_{wi}|w|^{i-1})\} \\ D_2(\nu_2) &= D_2 + D_{2q}(\nu_2) \\ &= \text{diag}\{d_p, d_q, d_r\} + \text{diag}\{\sum_{i=2}^{3} d_{pi}|p|^{i-1}, \sum_{i=2}^{3} d_{qi}|q|^{i-1}, \sum_{i=2}^{3} d_{ri}|r|^{i-1})\} \end{aligned} \tag{3.9}$$

where the positive constant terms $d_u, d_v, d_w, d_p, d_q\ d_r,\ d_{ui}, d_{vi}, d_{wi}, d_{pi}, d_{qi}$ and d_{ri} $(i = 1, 2, 3)$ denote the hydrodynamic damping in surge, sway, heave, roll, pitch and yaw. The damping matrices can be viewed as sum of a constant term, D_1 or D_2, and a quadratic damping term, $D_{1q}(\nu_1)$ or $D_{2q}(\nu_2)$.

The restoring force vectors $g_1(\eta_2)$ and $g_2(\eta_2)$ are given by Equations (2.11) and (2.12). $\tau_1 = [\tau_u, \tau_v, \tau_w]$ and $\tau_2 = [\tau_p, \tau_q, \tau_r]$ are the control forces and moments vectors.

3.3 Observer Design With Constant Wave Model

As irrotational wave disturbances affect only the translational motion of AUVs in surge, sway and heave directions, the main objectives of the observer design are to estimate the vehicle's low-frequency (LF) velocities in surge, sway and heave directions and to filter out the wave frequency (WF) motion components from positioning measurements to avoid wear and tear on thrusters and excessive energy depletion. The proposed approach to design an observer for AUVs is to construct an auxiliary dynamic system that reconstructs the estimation of the vehicle's LF velocities and WF motion components from input-output measurements. Fossen and Strand [33] proposed a nonlinear observer that was proven to be passive and globally exponentially stable (GES) for dynamic positioning control of surface ships. This work was extended to six degrees of freedom for station keeping of AUVs in shallow water by Liu *et al.* [64]. But these two papers used only simplified models for low speed condition which do not include the Coriolis and centripetal forces and moments.

In this study, the nonlinear observers proposed in [33, 64] are extended to tracking control of AUVs which encompasses the Coriolis and centripetal forces and moments. Here we first introduce a coordinate transformation to solve the observer design problem due to the presence of the Coriolis and centripetal terms. A nonlinear observer design is then designed and shown to be globally exponentially stable (GES) based on the transformed model.

3.3.1 Coordinate Transformation

To facilities stability proof of the observer design, we introduce the following coordinate transformation

$$\begin{aligned} \alpha_1 &= \eta_1 \\ \alpha_2 &= Q(\eta_2)\nu_1 \end{aligned} \tag{3.10}$$

where $Q(\eta_2) \in \mathcal{R}^{3\times 3}$ is a non-singular matrix to be determined. A similar coordinate transformation has been introduced by Do and Jiang in [19, 49]. But there are significant differences in dimensions and kinematic transformation matrix properties between the coordinate transformation designed in here and in [19, 49]. Using Equations (3.1) and (3.3), we get the differentiation of (α_1, α_2) as follows:

$$\dot{\alpha}_1 = J_1(\eta_2)Q^{-1}(\eta_2)\alpha_2 \tag{3.11}$$

$$\begin{aligned} \dot{\alpha}_2 &= \dot{Q}(\eta_2)\nu_1 + Q(\eta_2)\dot{\nu}_1 \\ &= [\dot{Q}(\eta_2)\nu_1 - Q(\eta_2)M_1^{-1}C_1(\nu_1)\nu_2] \\ &\quad +Q(\eta_2)M_1^{-1}(-D_1(\nu_1)\nu_1 - g_1(\eta_2) + \tau_1) \end{aligned} \tag{3.12}$$

Notice that the differential Equation (2.2), the Jacobin transformation matrix, leads to:

$$\dot{J}_1(\eta_2) = J_1(\eta_2)S(\eta_2) \tag{3.13}$$

where

$$S(\eta_2) = \begin{bmatrix} 0 & -r & q \\ r & 0 & -p \\ -q & p & 0 \end{bmatrix} \tag{3.14}$$

Hence, choosing $Q(\eta_2) = J_1(\eta_2)M_1$ leads to:

$$\begin{aligned} & \dot{Q}(\eta_2)\nu_1 - Q(\eta_2)M_1^{-1}C_1(\nu_1)\nu_2 \\ = \; & \dot{J}_1(\eta_2)M_1\nu_1 - J_1(\eta_2)M_1M_1^{-1}C_1(\nu_1)\nu_2 \\ = \; & J_1(\eta_2)S(\eta_2)M_1\nu_1 - J_1(\eta_2)C_1(\nu_1)\nu_2 \\ = \; & 0 \end{aligned} \tag{3.15}$$

Using the coordinate transformation Equation (3.10) and results in Equation (3.14), Equations (3.11) and (3.12) can be reduced to:

$$\dot{\alpha}_1 = J_1(\eta_2)M_1^{-1}J_1^{-1}(\eta_2)\alpha_2 \tag{3.16}$$

$$\dot{\alpha}_2 = J_1(\eta_2)(-D_1(\nu_1)\nu_1 - g_1(\eta_2) + \tau_1) \tag{3.17}$$

where $\alpha_1 = \eta_1$ and $\alpha_2 = J_1(\eta_2)M_1\nu_1$.

So the complete model of the vehicle system can be expressed as follows

$$\dot{\alpha}_1 = J_1(\eta_2)M_1^{-1}J_1^{-1}(\eta_2)\alpha_2 \tag{3.18}$$

$$\dot{\eta}_2 = J_2(\eta_2)\nu_2 \tag{3.19}$$

$$\dot{\xi} = \begin{bmatrix} 0 & I \\ \Omega_{21} & \Omega_{22} \end{bmatrix} \xi \tag{3.20}$$

$$\dot{\alpha}_2 = J_1(\eta_2)(-D_1(\nu_1)\nu_1 - g_1(\eta_2) + \tau_1) \tag{3.21}$$

$$\dot{\nu}_2 = M_2^{-1}(-C_1(\nu_1)\nu_1 - C_2(\nu_2)\nu_2 - D_2(\nu_2)\nu_2 - g_2(\eta_2) + \tau_2) \tag{3.22}$$

$$\begin{bmatrix} y_1 \\ y_2 \end{bmatrix} = \begin{bmatrix} \eta_1 \\ \eta_2 \end{bmatrix} + \begin{bmatrix} \eta_w \\ 0 \end{bmatrix} = \eta + \Gamma\xi = \begin{bmatrix} \alpha_1 \\ \eta_2 \end{bmatrix} + \Gamma\xi \tag{3.23}$$

The compact forms are for translational motion

$$\dot{\eta}_0 = A_0\eta_0 + B_0 J_1(\eta_2) M_1^{-1} J_1^{-1}(\eta_2)\alpha_2 \tag{3.24}$$

$$\dot{\alpha}_2 = J_1(\eta_2)(-D_1(\nu_1)\nu_1 - g_1(\eta_2) + \tau_1) \tag{3.25}$$

$$y_1 = C_0\eta_0 \tag{3.26}$$

and for rotational motion

$$\dot{\eta}_2 = J_2(\eta_2)\nu_2 \tag{3.27}$$

$$\dot{\nu}_2 = M_2^{-1}(-C_1(\nu_1)\nu_1 - C_2(\nu_2)\nu_2 - D_2(\nu_2)\nu_2 - g_2(\eta_2) + \tau_2) \tag{3.28}$$

$$y_2 = \eta_2 \tag{3.29}$$

where $\eta_0 = \left[\xi_1^T, \xi_2^T, \alpha_1^T\right]^T$, $A_0 = \begin{bmatrix} 0 & I & 0 \\ \Omega_{21} & \Omega_{21} & 0 \\ 0 & 0 & 0 \end{bmatrix}$, $B_0 = \begin{bmatrix} 0 \\ 0 \\ I \end{bmatrix}$, $C_0 = \begin{bmatrix} 0 & I & I \end{bmatrix}$.

Here we already get the transformed dynamic model of the AUV system. By using coordinate transformation, the Coriolis and centripetal term in Equation (3.3) is cancelled as shown in Equation (3.25). This will bring great convenience for stability proof of the following observer design.

3.3.2 Observer Structure

As the wave disturbances only affect translational motions of the vehicle and the heading angles and rotational velocities can be measured accurately by using the gyro compass and IMU [10, 80], the objective of the observer design is to generate the LF position estimations, estimations of LF translational velocities and to filter out the WF motion from the position measurements. The observer has the property of a notch filter in the frequency range of the wave disturbances when the dominant wave frequency is known. Here the observer structure design is motivated by the work of Strand and Fossen [33]. We have extended their work in two areas: (i) We introduce a coordinate transformation to prove the GES in the presence of Coriolis and centripetal forces. (ii) The wave disturbances affect the motion of the vehicle in surge, sway and heave directions in 3D space.

The observer for dynamics Equations (3.24)-(3.26) is proposed as

$$\dot{\hat{\eta}}_0 = A_0\hat{\eta}_0 + B_0 J_1(\eta_2)M_1^{-1}J_1^{-1}(\eta_2)\hat{\alpha}_2 + K\tilde{y}_1 \tag{3.30}$$

$$\dot{\hat{\alpha}}_2 = J_1(\eta_2)(-D_1(\hat{\nu}_1)\hat{\nu}_1 - g_1(\eta_2) + \tau_1 + M_1^{-1}J_1^{-1}(\eta_2)K_4\tilde{y}_1) \tag{3.31}$$

$$\hat{y}_1 = C_0\hat{\eta}_0 \tag{3.32}$$

where $\tilde{y}_1 = y_1 - \hat{y}_1$ is the estimation error of position and $K = \left[K_1^T, K_2^T, K_3^T\right]^T$ with K_1, K_2, K_3 and $K_4 \in \mathcal{R}^{3\times 3}$ are the observer gain matrices to be determined later. $\hat{\eta}_0 = \left[\hat{\xi}_1^T, \hat{\xi}_2^T, \hat{\alpha}_1^T\right]^T$ comprises the WF position estimate $\hat{\xi}_2$ and LF position estimate $\hat{\alpha}_1$. $\hat{\alpha}_2$ is the LF velocity estimation.

Position error dynamics can be obtained by subtracting (3.24)-(3.26) from (3.30)-(3.32), respectively.

$$\dot{\tilde{\eta}}_0 = (A_0 - KC_0)\tilde{\eta}_0 + B_0 J_1(\eta_2)M_1^{-1}J_1^{-1}(\eta_2)\tilde{\alpha}_2 \tag{3.33}$$

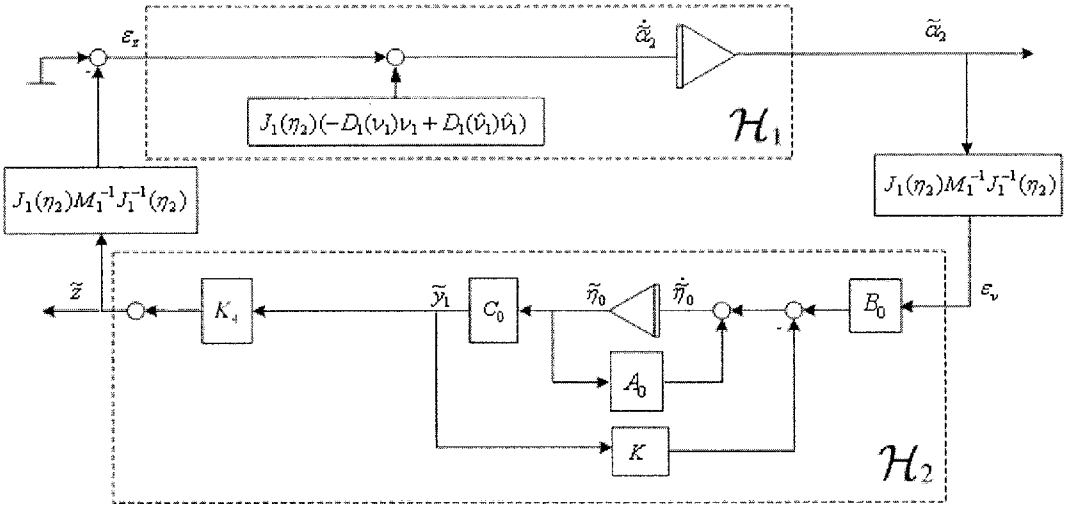

Figure 3.1: Dynamics of the LF position and velocity estimation errors.

$$\dot{\tilde{\alpha}}_2 = J_1(\eta_2)(-D_1(\nu_1)\nu_1 + D_1(\hat{\nu}_1)\hat{\nu}_1 - M_1^{-1}J_1^{-1}(\eta_2)K_4\tilde{y}_1) \tag{3.34}$$

$$\tilde{y}_1 = C_0\tilde{\eta}_0 \tag{3.35}$$

where $\tilde{\eta}_0 = \eta_0 - \hat{\eta}_0$ and $\tilde{\alpha}_2 = \alpha_2 - \hat{\alpha}_2$.

In Equation (3.34), we use $D_1(\nu_1)\nu_1$ and $D_1(\hat{\nu}_1)\hat{\nu}_1$ instead of the form of α_2 and $\hat{\alpha}_2$ for notational clarity in stability proof in the next section. The position error dynamics is illustrated using block diagram in Figure 4.1 where two new error terms, $\varepsilon_z = -J_1(\eta_2)M_1^{-1}J_1^{-1}(\eta_2)\tilde{z}$ and $\varepsilon_\nu = -J_1(\eta_2)M_1^{-1}J_1^{-1}(\eta_2)\tilde{\alpha}_2$, are defined. The observer error dynamic model can be rewritten as

$$\dot{\tilde{\eta}}_0 = A\tilde{\eta}_0 + BJ_1(\eta_2)M_1^{-1}J_1^{-1}(\eta_2)\tilde{\alpha}_2 \tag{3.36}$$

$$\tilde{z} = C\tilde{\eta}_0 \tag{3.37}$$

$$\dot{\tilde{\alpha}}_2 = J_1(\eta_2)(-D_1(\nu_1)\nu_1 + D_1(\hat{\nu}_1)\hat{\nu}_1) - J_1(\eta_2)M_1^{-1}J_1^{-1}(\eta_2)\tilde{z} \tag{3.38}$$

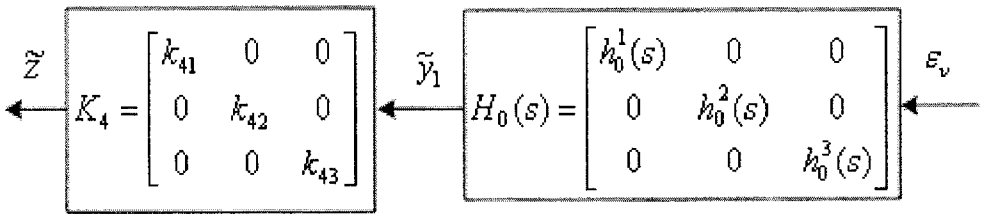

Figure 3.2: Decoupled transfer functions of LF position observer error dynamics.

where $\tilde{z} = K_4\tilde{y}_1$, $A = (A_0 - KC_0) = \begin{bmatrix} 0 & I - K_1 & -K_1 \\ \Omega_{21} & \Omega_{22} - K_2 & -K_2 \\ 0 & -K_3 & -K_3 \end{bmatrix}$, $B = B_0 = \begin{bmatrix} 0 \\ 0 \\ I \end{bmatrix}$

and $C = K_4C_0 = \begin{bmatrix} 0 & K_4 & K_4 \end{bmatrix}$.

3.3.3 Pole-Placement Algorithm

The gain matrices in the observer Equations (3.30) and (3.31) are chosen with the following structures:

$$\begin{aligned} K_1 &= \text{diag}\{k_{11}, k_{12}, k_{13}\} \\ K_2 &= \text{diag}\{k_{21}, k_{22}, k_{23}\} \\ K_3 &= \text{diag}\{k_{31}, k_{32}, k_{33}\} \\ K_4 &= \text{diag}\{k_{41}, k_{42}, k_{43}\} \end{aligned} \tag{3.39}$$

For the observer error dynamics, the mapping $\varepsilon_\nu \mapsto \tilde{z}$ in Figure 4.1 can be described by three decoupled transfer functions $\tilde{z}(s) = H(s)\varepsilon_\nu = K_4H_0(s)\varepsilon_\nu$, with $H_0(s) = C_0(sI - A_0 + KC_0)^{-1}B_0$.

The diagonal structure of $H(s)$ is shown in Figure 3.2 and the three decoupled

transfer functions $h^i(s)$ (i=1,2,3) of $H(s)$ are

$$\begin{aligned} h^i(s) &= \frac{\tilde{z}}{\varepsilon_\nu}(s) \\ &= \frac{k_{4i}(s^2 + 2\zeta_i\omega_{oi}s + \omega_{oi}^2)}{s^3 + (k_{3i} + k_{2i} + 2\zeta_i\omega_{oi})s^2 + (\omega_{oi}^2 + 2k_{3i}\zeta_i\omega_{oi} - k_{1i}\omega_{oi}^2)s + k_{3i}\omega_{oi}^2} \end{aligned} \tag{3.40}$$

Next, we will find the observer gain matrices to obtain the desired notch effect and low-pass effect (wave filtering) of the observer error dynamics Equation (3.40). The desired $h_{0d}^i(s)$ (for i=1,2,3) are specified as

$$h_{0d}^i(s) = \frac{s^2 + 2\zeta_i\omega_{oi}s + \omega_{oi}^2}{(s^2 + 2\zeta_{ni}\omega_{oi}s + \omega_{oi}^2)(s + \omega_{ci})} \tag{3.41}$$

where $\omega_{ci} > \omega_{oi}$ is the filter cut-off frequency and $\zeta_{ni} > \zeta_i$ determines the notch effect. Comparing Equations (3.40) and (3.41) yields the following formulas for the filter gains in K_1, K_2 and K_3:

$$\begin{aligned} k_{1i} &= -2\omega_{ci}(\zeta_{ni} - \zeta_i)\frac{1}{\omega_{oi}} \\ k_{2i} &= 2\omega_{oi}(\zeta_{ni} - \zeta_i) \\ k_{3i} &= \omega_{ci} \end{aligned} \tag{3.42}$$

We can notice that the filter gains can be calculated with respect to the dominant wave frequencies ω_{oi} if desired. The parameters for the observer gain matrix K_4 only affects the magnitude of transfer function of $h^i(s)$. So $h^i(s)$ have the same phase plots with $h_{0d}^i(s)$ and parameters for the observer gain matrix K_4 is not strictly constrained.

For illustration, one set of $h_0^i(s)$ (for i=1,2,3) is chosen as

$$h_0^i(s) = \frac{s^2 + 2 \times 0.1 \times 0.7s + 0.7^2}{(s^2 + 2 \times 1.1 \times 0.7s + 0.7^2)(s + 1.5)} \tag{3.43}$$

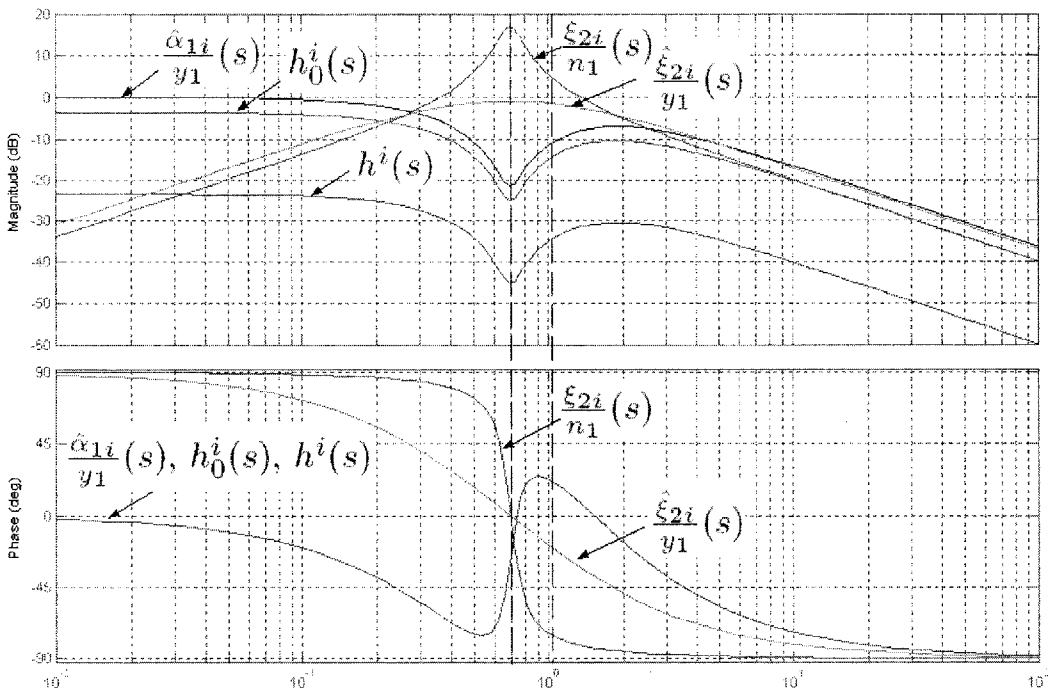

Figure 3.3: Bode plots of the transfer function $\frac{\hat{\alpha}_{1i}}{y_1}(s)$, $h_0^i(s)$, $h^i(s)$, $\frac{\hat{\xi}_{2i}}{y_1}(s)$ and $\frac{\xi_{2i}}{n_1}(s)$ (i=1,2,3)

where the dominant frequency of wave is $\omega_{oi} = 0.7$, the damping ratio of the wave is $\zeta_i = 0.1$, the cut-off frequency is chosen as $\omega_{ci} = 1.5$ and the notch effect parameters is chosen as $\zeta_{ni} = 1.1$. In Figure 3.3, the functions $h^i(s) = h_B^i(s)h_0^i(s)$ (i=1,2,3) are illustrated for a set of filter gains for the three decoupled transfer functions showing that all have phase greater than $-90°$, if the observer gain matrices are chosen as (3.42). In the Bode plots diagram, the transfer function of $h_0^i(s)$ is also illustrated.

Remark 1 Here we briefly analyze the property of observer dynamics. The observer Equations (3.30)-(3.32) can be rewritten as the following state-space model:

$$\begin{bmatrix} \dot{\hat{\xi}}_1 \\ \dot{\hat{\xi}}_2 \\ \dot{\hat{\alpha}}_1 \end{bmatrix} = \begin{bmatrix} 0 & I - K_1 & -K_1 \\ \Omega_{21} & \Omega_{22} - K_2 & -K_2 \\ 0 & -K_3 & -K_3 \end{bmatrix} \begin{bmatrix} \hat{\xi}_1 \\ \hat{\xi}_2 \\ \hat{\alpha}_1 \end{bmatrix}$$

$$+\begin{bmatrix} 0 \\ 0 \\ I \end{bmatrix} J_1(\eta_2) M_1^{-1} J_1^{-1}(\eta_2) \hat{\alpha}_2 + \begin{bmatrix} K_1 \\ K_2 \\ K_3 \end{bmatrix} y_1. \tag{3.44}$$

From Equation (3.44), the transfer functions from measurements, y_1, to the LF positions, $\hat{\alpha}_{1i}$ (i=1,2,3), of the AUV is expressed as:

$$\frac{\hat{\alpha}_{1i}}{y_1}(s) = \frac{k_{3i}(s^2 + 2\zeta_i\omega_{oi}s + \omega_{oi}^2)}{s^3 + (k_{3i} + k_{2i} + 2\zeta_i\omega_{oi})s^2 + (\omega_{oi}^2 + 2k_{3i}\zeta_i\omega_{oi} - k_{1i}\omega_{oi}^2)s + k_{3i}\omega_{oi}^2} \tag{3.45}$$

The Equation (3.45) has the property of notch filer, , as shown in Equation (3.41). Hence it can filter out the WF position component and estimate the LF position of the AUV from the output measurements.

We also can identify the transfer function of the estimated WF motion as here:

$$\frac{\hat{\xi}_{2i}}{y_1}(s) = \frac{k_{2i}s^2 + k_{1i}\omega_{oi}^2 s}{s^3 + (k_{3i} + k_{2i} + 2\zeta_i\omega_{oi})s^2 + (\omega_{oi}^2 + 2k_{3i}\zeta_i\omega_{oi} - k_{1i}\omega_{oi}^2)s + k_{3i}\omega_{oi}^2} \tag{3.46}$$

which estimate the WF disturbance in surge, sway and heave direction. From Figure 3.3, we can see the Bode plot of transfer function of $\frac{\hat{\xi}_{2i}}{y_1}(s)$, and the Bode plot of original wave model $\frac{\xi_{2i}}{n_1}(s)$ which is driven by the white noise n_1.

Remark 2 Equations (3.45) and (3.40) are similar in the structure except for the gains in (3.40). But the physical meaning of these two equations are totally different. Equation (3.45) describes the observer transfer function of the estimated states $\hat{\alpha}_{1i}$ which is LF positions component. Equation (3.40) is the error dynamic transfer function of $\tilde{z}(s)$ with input of the error term ε_ν. Only the Equation (3.40), which will be used for the stability proof of the observer error dynamic system.

3.3.4 Stability Analysis

Lemma 3.1 (Kalman-Yakubovich-Popov(KYP) lemma) [54] *Let* $Z(s) = \mathcal{C}(sI - \mathcal{A})^{-1}\mathcal{B}$ *be a* $n \times n$ *transfer function matrix, where* $\mathcal{A}$ *is Hurwitz,* $(\mathcal{A}, \mathcal{B})$ *is controllable, and* $(\mathcal{A}, \mathcal{C})$ *is observable. Then,* $Z(s)$ *is strictly positive real (SPR) if and only if there exist positive-definite matrices* $\mathcal{P} = \mathcal{P}^T$ *and* $\mathcal{Q} = \mathcal{Q}^T$ *such that*

$$\mathcal{P}\mathcal{A} + \mathcal{A}^T\mathcal{P} = -\mathcal{Q}, \tag{3.47}$$

$$\mathcal{B}^T\mathcal{P} = \mathcal{C} \tag{3.48}$$

Proposition 3.1 (SPR of velocity estimation error). *If the gain matrices in the observer Equations (3.30)- (3.32) are chosen with the structures as (3.39) then we can choose appropriate values of* K_1, K_2 *and* K_3 *such that the triple* (A, B, C) *in Equations (3.36) and (3.37) is strictly positive real (SPR).*

Proof From Figure 3.3, we can see that all three decoupled transfer functions have phase greater then $-90°$. Base on the SPR properties [54], the SPR requirement is satisfied.

Theorem 3.1 (Globally exponentially stable nonlinear observer) *For the AUV translational dynamic model described by Equations (3.24)- (3.26), the nonlinear observer Equations (3.30)-(3.32) is globally exponentially stable if* K_1, K_2, K_3 *and* K_4 *are chosen such that the triple* (A, B, C) *in (3.36) and (3.37) is strictly positive real (SPR).*

Proof We propose the following Lyapunov function candidate:

$$V_{obs} = \tilde{\alpha}_2^T\tilde{\alpha}_2 + \tilde{\eta}_0^T P\tilde{\eta}_0 \tag{3.49}$$

Differentiation of V along the trajectories of $\tilde{\alpha}_2$ and $\tilde{\eta}_0$ in Equations (3.36) and (3.38) yields

$$\begin{aligned}
\dot{V}_{obs} &= 2\tilde{\alpha}_2^T(J_1(\eta_2)(-D_1(\nu_1)\nu_1 + D_1(\hat{\nu}_1)\hat{\nu}_1) - J_1(\eta_2)M_1^{-1}J_1^{-1}(\eta_2)\tilde{z}) \\
&\quad +\tilde{\eta}_0^T(PA + A^TP)\tilde{\eta}_0 \\
&\quad +2\tilde{\alpha}_2 J_1(\eta_2)M_1^{-1}J_1^{-1}(\eta_2)B^TP\tilde{\eta}_0 \qquad (3.50) \\
&= 2\tilde{\alpha}_2^T J_1(\eta_2)(-D_1(\nu_1)\nu_1 + D_1(\hat{\nu}_1)\hat{\nu}_1) - 2\tilde{\alpha}_2^T J_1(\eta_2)M_1^{-1}J_1^{-1}(\eta_2)C\tilde{\eta}_0 \\
&\quad -\tilde{\eta}_0^T Q\tilde{\eta}_0 + 2\tilde{\alpha}_2 J_1(\eta_2)M_1^{-1}J_1^{-1}(\eta_2)B^TP\tilde{\eta}_0
\end{aligned}$$

Based on the definitions $B^TP = C$ and Equation (3.37), we have $B^TP\tilde{\eta}_0 = C\tilde{\eta}_0 = \tilde{z}$. Since $\alpha_2 = J_1(\eta_2)M_1\nu_1$ and $J_1^{-1}(\eta_2) = J_1^T(\eta_2)$, we will get

$$\begin{aligned}
\dot{V}_{obs} &= 2\tilde{\nu}_1^T M_1^T J_1^T(\eta_2)J_1(\eta_2)(-D_1(\nu_1)\nu_1 + D_1(\hat{\nu}_1)\hat{\nu}_1) - \tilde{\eta}_0^T Q\tilde{\eta}_0 \\
&= 2\tilde{\nu}_1^T M_1^T(-D_1(\nu_1)\nu_1 + D_1(\hat{\nu}_1)\hat{\nu}_1) - \tilde{\eta}_0^T Q\tilde{\eta}_0 \qquad (3.51) \\
&\leq -2\tilde{\nu}_1^T M_1^T D_1\tilde{\nu}_1 - \tilde{\eta}_0^T Q\tilde{\eta}_0 \qquad (3.52) \\
&< 0 \quad \forall\tilde{\nu}_1, \tilde{\eta}_0 \neq 0
\end{aligned}$$

Here we use the property that $D(\nu_1)\nu_1$ is a nondecreasing function.

So $\tilde{\alpha}_2$ and $\tilde{\eta}_0 = \left[\tilde{\xi}_1^T, \tilde{\xi}_2^T, \tilde{\alpha}_1^T\right]^T$ converge exponentially to zero. As $J_1(\eta_2)$ is a nonsingular transformation matrix, $\tilde{\nu}_1 = M_1^{-1}J_1^{-1}(\eta_2)\tilde{\alpha}_2$ will also converge to zero exponentially.

3.4 Adaptive Observer Design

In the previous section, we assume the wave frequency and damping ratio of wave disturbance are measurable and known. Here we address the problem when the wave disturbance frequency is unknown.

To solve this problem, we use the adaptive observer technique through augmented observer technique.

3.4.1 Observer Structure

Since the wave models are assumed to be decoupled, Ω_{21} and Ω_{22} in Ω are diagonal matrices, and we have:

$$\Omega = \begin{bmatrix} 0 & I \\ \Omega_{21} & \Omega_{22} \end{bmatrix} = \begin{bmatrix} 0 & I \\ -\text{diag}(\theta_{w1}) & -\text{diag}(\theta_{w2}) \end{bmatrix} \tag{3.53}$$

where $\theta_w = [\theta_{w1}^T, \theta_{w2}^T]^T$, and $\theta_{w1}, \theta_{w2} \in \mathcal{R}^3$ contain the unknown wave model parameters to be estimated. Here we assume that these unknown parameters are slowly varying and are treated as constants in the analysis, such that

$$\dot{\theta}_w = 0 \tag{3.54}$$

Here is the complete dynamic model of the AUV after the coordinate transformation.

$$\dot{\alpha}_1 = J_1(\eta_2) M_1^{-1} J_1^{-1}(\eta_2) \alpha_2 \tag{3.55}$$

$$\dot{\eta}_2 = J_2(\eta_2) \nu_2 \tag{3.56}$$

$$\dot{\xi} = \Omega \xi \tag{3.57}$$

$$\dot{\alpha}_2 = J_1(\eta_2)(-D_1(\nu_1)\nu_1 - g_1(\eta_2) + \tau_1) \tag{3.58}$$

$$\dot{\nu}_2 = M_2^{-1}(-C_1(\nu_1)\nu_1 - C_2(\nu_2)\nu_2 - D_2(\nu_2)\nu_2 - g_2(\eta_2) + \tau_2) \tag{3.59}$$

$$\begin{bmatrix} y_1 \\ y_2 \end{bmatrix} = \begin{bmatrix} \eta_1 \\ \eta_2 \end{bmatrix} + \begin{bmatrix} \eta_w \\ 0 \end{bmatrix} = \eta + \Gamma\xi = \begin{bmatrix} \alpha_1 \\ \eta_2 \end{bmatrix} + \Gamma\xi \tag{3.60}$$

To design the adaptive observer, we firstly introduce the following additional states as augmented states.

$$\dot{x}_f = -T_f^{-1}x_f + \tilde{y}_1 \tag{3.61}$$

$$\tilde{y}_f = -T_f^{-1}x_f + \tilde{y}_1 \tag{3.62}$$

where $x_f, \tilde{y}_f \in \mathcal{R}^3$ are the low-pass and high pass filtered innovation signals respectively. Moreover,

$$x_f^i(s) = \frac{T_{fi}}{1 + T_{fi}s}\tilde{y}_1^i(s) \quad (i = 1, 2, 3) \tag{3.63}$$

$$\tilde{y}_f^i(s) = \frac{T_{fi}s}{1 + T_{fi}s}\tilde{y}_1^i(s) \quad (i = 1, 2, 3) \tag{3.64}$$

The cutoff frequency in the filters should be below the frequencies of the dominant waves in the wave model (3.5). $\tilde{y}_1^i$, x_f^i and $\tilde{y}_f^i$ (i=1,2,3) are the respective components of vectors $\tilde{y}_1$, x_f and $\tilde{y}_f$.

The augmented observer is formulated as:

$$\dot{\hat{\xi}} = \Omega(\hat{\theta}_w)\hat{\xi} + K_a\tilde{y}_f \tag{3.65}$$

$$\dot{\hat{\alpha}}_1 = J_1(\eta_2)M_1^{-1}J_1^{-1}(\eta_2)\hat{\alpha}_2 + K_{3a}\tilde{y}_f \tag{3.66}$$

$$\dot{\hat{\alpha}}_2 = J_1(\eta_2)(-D_1(\hat{\nu}_1)\hat{\nu}_1 - g_1(\eta_2) + \tau_1 + M_1^{-1}J_1^{-1}(\eta_2)K_{4a}\tilde{y}_f) \tag{3.67}$$

where $D_1(\hat{\nu}_1)\hat{\nu}_1$ instead of the form of $\hat{\alpha}_2$ for notational clarity in stability proof in the next section, $\hat{\theta}_w$ is the estimated wave model parameters which will be determined through adaptive law, $\tilde{y}_f$ is the high pass filtered innovation signals and $K_a = \left[K_{1a}^T, K_{2a}^T\right]^T$ with K_{1a}, K_{2a}, K_{3a} and $K_{4a} \in \mathcal{R}^{3\times 3}$ are the adaptive observer gain matrices to be determined later.

The observer estimation errors are defined as $\tilde{\xi} = \xi - \hat{\xi}$, $\tilde{\alpha}_1 = \alpha_1 - \hat{\alpha}_1$ and $\tilde{\alpha}_2 = \alpha_2 - \hat{\alpha}_2$. So the observer error dynamics of wave model is

$$\begin{aligned}
\dot{\tilde{\xi}} &= \Omega\xi - \Omega(\hat{\theta}_w)\hat{\xi} - K_a\tilde{y}_f \\
&= \Omega\tilde{\xi} + \begin{bmatrix} 0 \\ I \end{bmatrix}\begin{bmatrix} 0 & 0 \\ \hat{\xi}_1 & \hat{\xi}_2 \end{bmatrix}\begin{bmatrix} \tilde{\theta}_{w1} \\ \tilde{\theta}_{w2} \end{bmatrix} - K_a\tilde{y}_f \\
&= \Omega\tilde{\xi} + B_{w0}\gamma_w^T(\hat{\xi})\tilde{\theta}_w - K_a(\tilde{\xi}_2 + \tilde{\alpha}_1 - T_f^{-1}x_f)
\end{aligned} \tag{3.68}$$

where $B_{w0} = \begin{bmatrix} 0 \\ I \end{bmatrix}$, $\gamma_w^T(\hat{\xi}) = \begin{bmatrix} 0 & 0 \\ \hat{\xi}_1 & \hat{\xi}_2 \end{bmatrix}$ and $\tilde{\theta}_w = \begin{bmatrix} \tilde{\theta}_{w1} \\ \tilde{\theta}_{w2} \end{bmatrix}$. $\tilde{\theta}_w = \hat{\theta}_w - \theta_w$ denotes the estimation error.

The other observer error dynamics are:

$$\dot{\tilde{\alpha}}_1 = J_1(\eta_2)M_1^{-1}J_1^{-1}(\eta_2)\tilde{\alpha}_2 - K_{3a}\tilde{y}_f \tag{3.69}$$

$$\dot{\tilde{\alpha}}_2 = J_1(\eta_2)(-D_1(\nu_1)\nu_1 + D_1(\hat{\nu}_1)\hat{\nu}_1 - M_1^{-1}J_1^{-1}(\eta_2)K_{4a}\tilde{y}_f) \tag{3.70}$$

So the compact form of the error dynamics can be written as:

$$\dot{\tilde{x}}_a = A_a\tilde{x}_a + B_aJ_1(\eta_2)M_1^{-1}J_1^{-1}(\eta_2)\tilde{\alpha}_2 + B_w\gamma_w^T(\hat{\xi})\tilde{\theta}_w \tag{3.71}$$

$$\dot{\tilde{\alpha}}_2 = J_1(\eta_2)(-D_1(\nu_1)\nu_1 + D_1(\hat{\nu}_1)\hat{\nu}_1 - M_1^{-1}J_1^{-1}(\eta_2)C_a\tilde{x}_a) \tag{3.72}$$

$$\tilde{y}_f = C_w \tilde{x}_a \tag{3.73}$$

where $\tilde{x}_a = \begin{bmatrix} \tilde{\xi}_1^T & \tilde{\xi}_2^T & \tilde{\alpha}_1^T & x_f^T \end{bmatrix}$ and

$$A_a = \begin{bmatrix} 0 & I - K_{1a} & -K_{1a} & K_{1a}T_f^{-1} \\ \Omega_{21} & \Omega_{22} - K_{2a} & -K_{2a} & K_{2a}T_f^{-1} \\ 0 & -K_{3a} & -K_{3a} & K_{3a}T_f^{-1} \\ 0 & I & I & -T_f^{-1} \end{bmatrix}, \; B_a = \begin{bmatrix} 0 \\ 0 \\ 1 \\ 0 \end{bmatrix}, \; B_w = \begin{bmatrix} 0 \\ 1 \\ 0 \\ 0 \end{bmatrix}, \; C_a = \begin{bmatrix} 0 & K_{4a} & K_{4a} & -K_{4a}T_f^{-1} \end{bmatrix} \text{ and } C_w = \begin{bmatrix} 0 & I & I & -T_f^{-1} \end{bmatrix}.$$

We also can make the following definition

$$A = A_a, \quad B = \begin{bmatrix} B_a & B_w \end{bmatrix} \text{ and } \quad C = \begin{bmatrix} C_a \\ C_w \end{bmatrix} \tag{3.74}$$

Next, we will derive the observer gain matrices and the adaptive law for the observer.

3.4.2 Pole-Placement Algorithm

The gain matrices in the observer (3.65)- (3.67) are chosen with the following structures:

$$\begin{aligned} K_{1a} &= \text{diag}\{k_{1a1}, k_{1a2}, k_{1a3}\} \\ K_{2a} &= \text{diag}\{k_{2a1}, k_{2a2}, k_{2a3}\} \\ K_{3a} &= \text{diag}\{k_{3a1}, k_{3a2}, k_{3a3}\} \\ K_{4a} &= \text{diag}\{k_{4a1}, k_{4a2}, k_{4a3}\} \end{aligned} \tag{3.75}$$

We can obtain the transfer function of the observer error dynamics. Here we define $J_1(\eta_2)M_1^{-1}J_1^{-1}(\eta_2)\tilde{\alpha}_2$ and $C_a\tilde{x}_a$ as $\varepsilon_{\nu a}$ and $\tilde{z}_a$ respectively. Here the mapping from

$\varepsilon_{va} \rightarrow \tilde{z}_a$ can be described by three decoupled transfer functions $z_a(s) = H_a(s)\varepsilon_{va}$.

The transfer functions $h_a^i(s)$ $(i = 1, 2, 3)$ of $H_a(s)$ are:

$$h_a^i(s) = \frac{(s^2 + 2\zeta_i\omega_{oi}s + \omega_{oi}^2)k_{4ai}s}{(s^2 + (T_{fi}^{-1} + k_{3ai})s)(s^2 + 2\zeta_i\omega_{oi}s + \omega_{oi}^2) + k_{2ai}s^3 - k_{1ai}\omega_{oi}^2 s^2} \tag{3.76}$$

The transfer functions of the mapping from $\gamma_w^T(\hat{\xi})\tilde{\theta}_w \rightarrow \tilde{y}_f$ can be described by the following three decoupled transfer functions $H_w(s) = h_w^i(s)$ $(i = 1, 2, 3)$

$$h_w^i(s) = \frac{s^3}{(s^2 + (T_{fi}^{-1} + k_{3ai})s)(s^2 + 2\zeta_i\omega_{oi}s + \omega_{oi}^2) + k_{2ai}s^3 - k_{1ai}\omega_{oi}^2 s^2} \tag{3.77}$$

To get the desired transfer function specified in (3.41), we choose the observer gains as here,

$$k_{1ai} = -2\omega_{ci}(\zeta_{ni} - \zeta_i)\frac{1}{\omega_{oi}}, \tag{3.78}$$

$$k_{2ai} = 2\omega_{oi}(\zeta_{ni} - \zeta_i) \tag{3.79}$$

$$k_{3ai} = \omega_{ci} - T_{fi}^{-1} \tag{3.80}$$

$$k_{4ai} = \omega_{ci} - T_{fi}^{-1} \tag{3.81}$$

These observer gain can guarantee that all the decoupled transfer functions, $H_a(s)$ and $H_w(s)$, all have phase greater than $-90°$, if the observer gain matricies are chosen as (3.78)-(3.81).

3.4.3 Stability Analysis

Proposition 3.2 (SPR velocity estimation error). *If the gain matrices in the observer Equations (3.65)- (3.67) are chosen with the structures as Equation (3.75) then we can choose appropriate values of K_{1a}, K_{2a}, K_{3a}, and K_{4a} such that the triple (A, B, C) in (3.71)-(3.73) satisfies the KYP lemma.*

Proof From Figure 3.3, we can see that all three decoupled transfer functions have phase greater then $-90°$. Base on the SPR properties [54], the SPR requirement and thus the KYP lemma are satisfied.

Theorem 3.2 (Globally asymptotically stable nonlinear observer) *Considering the AUV motion described by (3.55)- (3.60), The nonlinear observer (3.65)-(3.67) is globally asymptotically stable.*

Proof Consider the following Lyapunov function candidate:

$$V_{aobs} = \tilde{\alpha}_2^T \tilde{\alpha}_2 + \tilde{x}_a^T P_a \tilde{x}_a + \tilde{\theta}_w^T \Gamma_w^{-1} \tilde{\theta}_w \tag{3.82}$$

Differentiation of V along the trajectories of $\tilde{x}_a$ and $\tilde{\alpha}_2$ in (3.71) and (3.72) yields

$$\begin{aligned} \dot{V}_{obs} = \; & 2\tilde{\alpha}_2^T (J_1(\eta_2)(-D_1(\nu_1)\nu_1 + D_1(\hat{\nu}_1)\hat{\nu}_1) - J_1(\eta_2) M_1^{-1} J_1^{-1}(\eta_2) C_a \tilde{x}_a) \\ & + \tilde{x}_a^T (P_a A_a + A_a^T P_a)\tilde{x}_a + 2\tilde{\alpha}_2 J_1(\eta_2) M_1^{-1} J_1^{-1}(\eta_2) B_a^T P_a \tilde{x}_a \\ & + 2\tilde{\theta}_w^T \gamma_w(\hat{\xi}) B_w^T P_a \tilde{x}_a + 2\tilde{\theta}_w^T \Gamma_w^{-1} \dot{\tilde{\theta}}_w \end{aligned} \tag{3.83}$$

In the adaptive case, we want the wave-frequency adaptive law to be updated by the high-pass filtered innovations signals. Hence, it is required that:

$$P_a A_a + A_a^T P_a = -Q_a \tag{3.84}$$

$$B_a^T P_a = C_a \tag{3.85}$$

$$B_w^T P_a = C_w \tag{3.86}$$

Here $C_w = \begin{bmatrix} 0 & 1 & 1 & -T_f^{-1} \end{bmatrix}$ and $C_w \tilde{x}_a = \tilde{y}_f$.

By using the frequency theorem, we can guarantee the existence of P_a with $\mathcal{P} = P_a$, $\mathcal{A} = A_a$, $u = \begin{bmatrix} \varepsilon_\nu^T, & \tilde{\theta}_w^T \gamma_w \end{bmatrix}^T$ and $B = \begin{bmatrix} B_a & B_w \end{bmatrix}$, $C = \begin{bmatrix} C_a \\ C_w \end{bmatrix}$.

Here we choose the adaptive law as:

$$\dot{\tilde{\theta}}_w \overset{\dot{\theta}_w = 0}{=\!=} -\Gamma_w \gamma_w(\hat{\xi}) C_w \tilde{x}_a = -\Gamma_w \gamma_w(\hat{\xi}) \tilde{y}_f \tag{3.87}$$

Based on the definitions $B^T P = C$ and (3.71), we have $B^T P \tilde{x}_a = C \tilde{x}_a$. And we use the definition of $\tilde{\alpha}_2 = J_1(\eta_2) M_1 \tilde{\nu}_1$ and the property of transfer matrix, $J_1^{-1}(\eta_2) = J_1^T(\eta_2)$, we will get

$$\begin{aligned}
\dot{V}_{aobs} &= 2\tilde{\nu}_1^T M_1^T J_1^T(\eta_2) J_1(\eta_2)(-D_1(\nu_1)\nu_1 + D_1(\hat{\nu}_1)\hat{\nu}_1) - \tilde{x}^T Q \tilde{x} \\
&= 2\tilde{\nu}_1^T M_1^T (-D_1(\nu_1)\nu_1 + D_1(\hat{\nu}_1)\hat{\nu}_1) - \tilde{x}_a^T Q_a \tilde{x}_a \qquad (3.88) \\
&\leq -2\tilde{\nu}_1^T M_1^T D_1 \tilde{\nu}_1 - \tilde{x}_a^T Q \tilde{x}_a \qquad (3.89) \\
&< 0 \quad \forall \tilde{\nu}_1, \tilde{x}_a \neq 0
\end{aligned}$$

Here we use the property of $D(\nu_1)\nu_1$ is a nondecreasing function.

Based on the Lasallw's lemma, the global asymptotic convergence of the estimation error can be guaranteed. So the $\tilde{\alpha}_2$, $\tilde{\nu}_1$ and $\tilde{x}_a = \left[\tilde{\xi}_1^T, \tilde{\xi}_2^T, \tilde{\alpha}_1^T, \tilde{x}_f^T\right]^T$ converge asymptotically to zero.

3.5 Simulation Results

To demonstrate the performance of the proposed nonlinear observer and adaptive observer, simulation study is carried out using the AUV model of the vehicle KAMBARA [94]. The AUV dynamics is described by Equations (3.3) and (3.4) with the parameter values given in Appendix A.

Here we propose the adaptive observer simulation results. In the observer design, the simulation is performed in four phase.

- The wave disturbance is in pure sinusoid form and the observer gain is derived according to the given wave model from 0s to 100s.
- The wave disturbance is in pure sinusoid form and the adaptive observer gain is derived from the adaptive observer algorism from 100s to 200s.
- The wave disturbance is in white noise driven form and the observer gain is derived according to the given wave model from 200s to 300s.
- The wave disturbance is in white noise driven form and the adaptive observer gain is derived from the adaptive observer algorism from 300s to 400s.

The wave model parameters in Equation (3.5) are chosen as $\zeta_i = 0.1$ and $\omega_{oi} = 0.6283$ (i=1-3) corresponding to a wave period of 10s in surge, sway and heave. The desired notch filter parameters are chosen as $\zeta_{ni} = 5$ and $\omega_{ci} = 5$. The parameter for the filtered innovation vectors is $T_f = 0.71 I_{3\times3}$. In the observer design, the given parameters for the wave model are $\zeta_i = 0.3$ and $\omega_{oi} = 0.4$ (i=1-3). From Equations (3.78)-(3.81), we choose the adaptive obsever gain matrices as $K_{1a} = -117.5 I_{3\times3}$, $K_{2a} = 3.76 I_{3\times3}$, $K_{3a} = 3.5915 I_{3\times3}$ and $K_{4a} = 3.5915 I_{3\times3}$. The parameter for the adaptive observer law is $\Gamma_w = 0.01 I_{6\times6}$.

In the simulation study, we use three coupled PI controllers to control the velocity of the vehicle in surge, sway and heave direction. The desired velocities

are settled as $u_{d0} = 2m/s$, $v_{d0} = 0m/s$ is $w_{d0} = 0m/s$ firstly and then are $u_{d1} = 3m/s$, $v_{d1} = 2m/s$ is $w_{d1} = 0.5m/s$. The initial condition of the KAMBARA is $(\nu_1, \eta_1) = (0.1, 0.1, 0.1, 0, 0, 5)$. The initial condition of the observer is $(\hat{\alpha}_1, \hat{\alpha}_2) = (0.5, 0.5, 5.5, 0, 0, 0)$. The amplitude of the pure sinusoid wave-induced motion in surge, sway and heave are limited to $1m, 1m$ and $0.2m$, respectively. The amplitude of the wave-induced motion driven by white noise in surge, sway and heave are limited to $1m, 1m$ and $0.1m$, respectively. The simulation results are shown in Figures 3.4-3.10.

We can see that excellent tracking of LF velocities of the AUV in surge, sway and heave directions is obtained in Figures 3.4, 3.6 and 3.8. In simulation the wave model is driven by the zero-mean Gaussian white noise although it was assumed to be zero in the stability analysis. This is to demonstrate the good performance of the observer in the presence of stochastic noise. The WF position in surge, sway and heave directions and their estimates are shown in Figures 3.5, 3.7 and 3.9 respectively. From the simulation results for the observed wave error in Figure 3.10, we can see that the adaptive observer in second and fourth phases has better performances then the ordinate observer in estimating both the pure wave and white-noise driven wave. In the first 2 phases of simulation, the estimation error for sinusoid wave cannot converge to zero. This is due to the phase delay of the observer error dynamic. The lase 2 phased of simulation, the estimation error also doesn't converge to zero. This is due to the phase delay and random noise which drive the wave model.

3.6 Conclusion

In this chapter, we have solved the nonlinear observer design for AUVs operating shallow water environment concerning energy efficient problems. The LF positions and velocities of the vehicle, along with the WF positions in the earth-fixed frame

are well estimated. The GES of the observer is proved. Compared with traditional linear observer designs, such as Kalman filter, the turning method are very straightforward and coupled more directly with the physics of the system. The global stability of the observer are guaranteed. The turning parameters are significant reduced. This will facilitate the implementation of the software algorithm in the computer.

Based on the augmented observer technique, an adaptive observer is then designed for tracking control of an AUV in shallow water area concerning unknown wave parameters. Traditionally wave filtering has been obtained by gain-scheduling techniques, where the WF model is known or estimated on-line using a wave frequency tracker. Here, the adaptive wave filtering is directly introduced into the observer design with simplified implementation. These estimation errors of the adaptive observer are globally asymptotically stable (GAS). Case study and simulation results show that the nonlinear adaptive observer performs better then the ordinary observer concerning the unknown wave frequency and damping ratio. All the estimation errors converge asymptotically to zero. Although the proposed observers in this chapter are for filtering the WF wave disturbances and estimation LF positions and velocities for energy efficient condition, the observer design technique also can be used for station keeping control which concerns precise motion requirement.

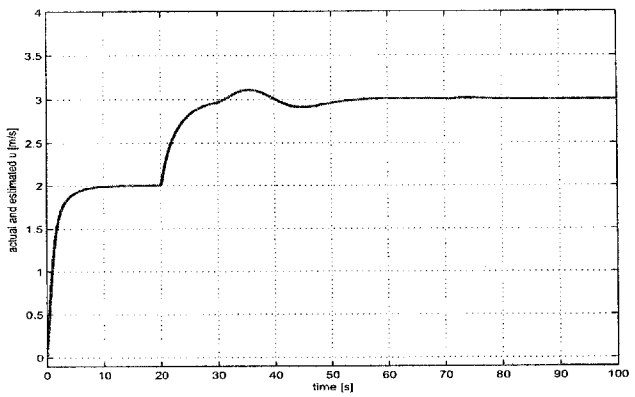

Figure 3.4: The actual LF velocity and its estimate by using the adaptive observer in surge direction

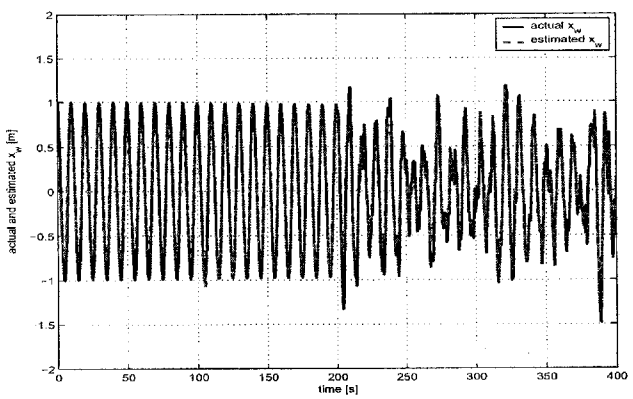

Figure 3.5: The actual WF disturbance and its estimates by using the adaptive observer in surge direction

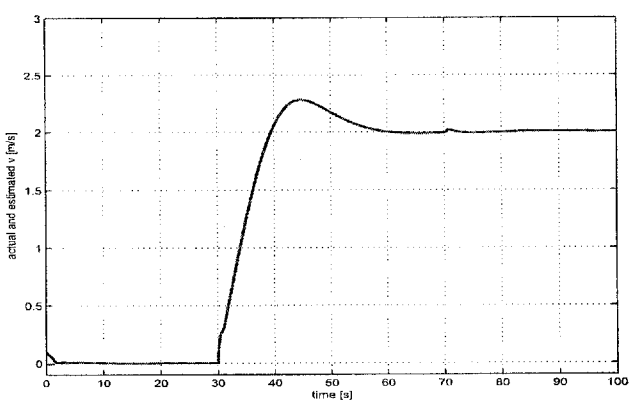

Figure 3.6: The actual LF velocity and its estimate by using the adaptive observer in sway direction

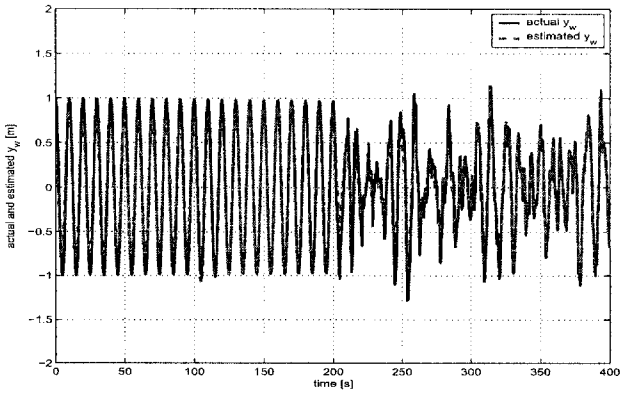

Figure 3.7: The actual WF disturbance and its estimates by using the adaptive observer in sway direction

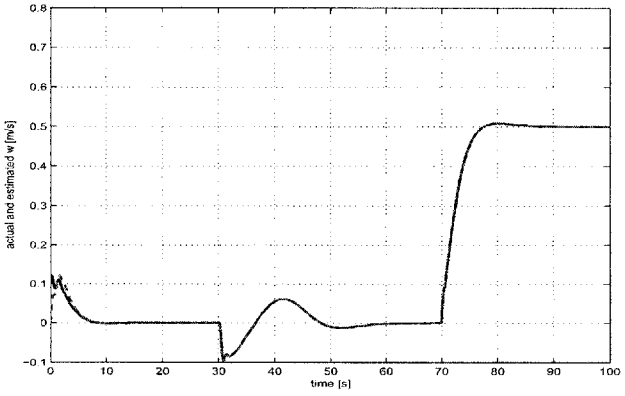

Figure 3.8: The actual LF velocity and its estimate by using the adaptive observer in heave direction

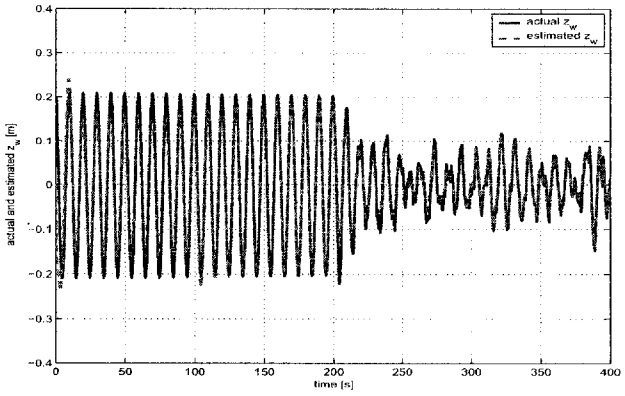

Figure 3.9: The actual WF disturbance and its estimates by using the adaptive observer in heave direction

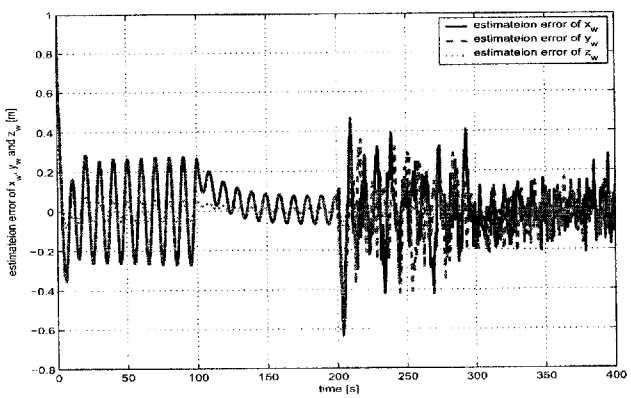

Figure 3.10: The estimation errors of WF disturbance by using the adaptive observer in surge, sway and heave directions

Chapter 4

Station Keeping Control Designs

4.1 Introduction

There is a significant meaning for autonomous underwater vehicles(AUVs) to have the capability of station keeping. Station keeping is the ability to maintain position and orientation with regard to a fixed point in a 3-dimensional (3D) environment by counteracting all the external disturbances. This capability is requested by various vehicles, such as, satellites, ships, remotely operated vehicles (ROVs) and AUVs. The vehicles use different control algorithms to counteract any motion or external disturbances by using thruster controls.

Station keeping is typically applied to ROVs and AUVs in a variety of missions, including inspection and repair of undersea structures, data collection, mine countermeasures, and surveillance. Many recent developments have been reported:

Cunha *et al.* [15] designed an adaptive position controller for an ROV, based on an output feedback variable structure model reference adaptive control (VS-MRAC) algorithm. The performance of the technique is evaluated by initially using simulation models and then full-scale sea trials utilizing an actual ROV. Results show

that this technique of position control consistently outperforms the conventional proportional-proportional integral (P-PI) control technique, by providing more accurate position tracking and parametric uncertainties and remarkable disturbance rejection. The structure of the P-PI controller for a generic degree of freedom consists of an inner velocity proportional integral control loop and an outer position proportional control.

Lots *et al.* [72] demonstrated the applicability of the 2D visual servoing to underwater vehicle station keeping in horizontal plane. Zwaan *et al.* [107] addressed the use of vision technology for automatic station keeping control of underwater vehicles relative to some naturally textured environmental region in 3D space. For a camera moving in 3D space, the observed deformations of the tracked image region are according to planar projective transformations and reveal information about the robot relative position and orientation with respect to the landmark. This information is then used in a visual feedback loop so as to realize station keeping. By using a direct motion vision algorithm that employs simple moments of the readily available spatiotemporal derivatives of the image function over selected image regions, Negahdaripour *et al.* [78] estimated the displacement and yaw angle relative to the desired station position and orientation and exploited this information to generate appropriate feedback signals to the thrusters to maintain station.

Only few research studies have been conducted for the station keeping control of underwater vehicles in shallow water environment. In [91], Riedel showed that the knowledge of the wave disturbances can be used to improve the controller's performance for station keeping. Some states, which cannot be directly obtained such as fluid velocity, are related to the measurements which can be obtained directly. Here the relative velocity of the AUV to wave in the body-fixed from is measured by an Acoustic Doppler Velocimeter Ocean Probe (ADVOcean), the ground-reference velocity is obtained from Navigator Doppler Velocity Log (DVL). Riedel used an Extended Kalman Filter for state and disturbance estimation to

compensate for the wave induced disturbance. The surge controller was a station keeping controller based on sliding mode control technology with disturbance feed-forward compensation. The work of Riedel was later extended to more degrees of freedom; heave, pitch, yaw and sway in [21].

In this chapter, we first present the dynamic model of AUVs for station keeping (SK) in shallow water environment. Then based on the observer design method in previous chapter, we design a similar nonlinear observer to estimate the shallow water wave velocities, relative velocities and noise-free positions and rotation angles which are used in the output feedback controller. We propose two different kinds of control methods for station keeping of AUVs in shallow water environment. Motivated by the output feedback controllers for dynamic positioning of ships [71], we will present a globally asymptotically stabilizing (GAS) output feedback controller for station keeping of AUVs operating in shallow water area. First, we design a state feedback control law assuming full state information are measurable. Then we modify the control law using estimated states. The stability proof of this approach for the closed-loop system requires that the nonlinear system satisfy the separation principle. The separation principle is based on recent results of cascaded nonlinear systems and Lyapunov stability theory. The second control method is based on observer backstepping technique in [56]. Simulation results for both methods that illustrate the performance of the control laws derived are also included. Finally, this chapter closes with some concluding remarks.

4.2 Output Feedback Control via Backstepping Design

4.2.1 Model Description

The model described by Equation (2.62) can be rewritten as follows:

$$\dot{\xi} = \begin{bmatrix} \dot{\xi}_1 \\ \dot{\xi}_2 \end{bmatrix} = \begin{bmatrix} 0 & I \\ \Omega_{21} & \Omega_{22} \end{bmatrix} \begin{bmatrix} \xi_1 \\ \xi_2 \end{bmatrix} + \begin{bmatrix} 0 \\ \sum_2 \end{bmatrix} n_1 \tag{4.1}$$

$$\mathbf{U}_f = \begin{bmatrix} 0 & I \end{bmatrix} \begin{bmatrix} \xi_1 \\ \xi_2 \end{bmatrix} = \Gamma\xi \tag{4.2}$$

$$\dot{\eta}_1 = J_1(\eta_2)\nu_{1r} + \mathbf{U}_f \tag{4.3}$$

$$\dot{\eta}_2 = J_2(\eta_2)\nu_2 \tag{4.4}$$

$$M_1\dot{\nu}_{1r} = -C_1(\nu_{1r})\nu_2 - D_1(\nu_{1r})\nu_{1r} - g_1(\eta_2) + \tau_1 \tag{4.5}$$

$$M_2\dot{\nu}_2 = -C_1(\nu_{1r})\nu_{1r} - C_2(\nu_2)\nu_2 - D_2(\nu_2)\nu_2 - g_2(\eta_2) + \tau_2 \tag{4.6}$$

The inertia matrices of AUV are given as follows:

$$M_1 = \text{diag}(m_{11}, m_{22}, m_{33}), \quad M_2 = \text{diag}(m_{44}, m_{55}, m_{66}) \tag{4.7}$$

where m_{jj}, $1 \leq j \leq 6$, denote the positive constant inertia terms including added mass in surge, sway, heave, roll, pitch and yaw, respectively.

The Coriolis and centripetal matrices are given by

$$C_1(\nu_{1r}) = \begin{bmatrix} 0 & m_{33}w_r & -m_{22}v_r \\ -m_{33}w_r & 0 & m_{11}u_r \\ m_{22}v_r & -m_{11}u_r & 0 \end{bmatrix}$$

$$C_2(\nu_2) = \begin{bmatrix} 0 & m_{66}r & -m_{55}q \\ -m_{66}r & 0 & m_{44}p \\ m_{55}q & -m_{44}p & 0 \end{bmatrix} \tag{4.8}$$

The damping matrices are

$$\begin{aligned} D_1(\nu_{1r}) &= D_1 + D_{1q}(\nu_{1r}) \\ &= \text{diag}\{d_u, d_v, d_w\} + \text{diag}\{\sum_{i=2}^{3} d_{ui}|u_r|^{i-1}, \sum_{i=2}^{3} d_{vi}|v_r|^{i-1}, \sum_{i=2}^{3} d_{wi}|w_r|^{i-1}\} \\ D_2(\nu_2) &= D_2 + D_{2q}(\nu_2) \\ &= \text{diag}\{d_p, d_q, d_r\} + \text{diag}\{\sum_{i=2}^{3} d_{pi}|p|^{i-1}, \sum_{i=2}^{3} d_{qi}|q|^{i-1}, \sum_{i=2}^{3} d_{ri}|r|^{i-1}\} \end{aligned} \tag{4.9}$$

where the positive constant terms $d_u, d_v, d_w, d_p, d_q\ d_r,\ d_{ui}, d_{vi}, d_{wi}, d_{pi}, d_{qi}$ and d_{ri} $(i = 2, 3)$ denote the hydrodynamic damping in surge, sway, heave, roll, pitch and yaw. The damping matrices can be viewed as a sum of a constant term, D_1 or D_2, and a quadratic damping term, $D_{1q}(\nu_{1r})$ or $D_{2q}(\nu_2)$.

The restoring force vectors $g_1(\eta_2)$ and $g_2(\eta_2)$ are given by

$$g_1(\eta_2) = \begin{bmatrix} (W-B)sin\theta \\ -(W-B)cos\theta sin\phi \\ -(W-B)cos\theta cos\phi \end{bmatrix} \tag{4.10}$$

and

$$g_2(\eta_2) = \begin{bmatrix} -(y_G W - y_B B)cos\theta cos\phi + (z_G W - z_B B)cos\theta sin\phi \\ (z_G W - z_B B)sin\theta + (x_G W - x_B B)cos\theta cos\phi \\ -(x_G W - x_B B)cos\theta sin\phi - (y_G W - y_B B)sin\theta \end{bmatrix} \tag{4.11}$$

where W is the submerged weight of AUV, B is buoyancy force of AUV, $r_G = [x_G, y_G, z_G]^T$ is the distance between center of gravity of AUV and origin of the body-fixed frame of AUV and $r_B = [x_B, y_B, z_B]^T$ is the distance between center of buoyancy of AUV and origin of the body-fixed frame of AUV [91, 29].

The AUV is fully actuated and available control inputs are

$$\tau_1 = [\tau_u, \tau_v, \tau_w], \qquad \tau_2 = [\tau_p, \tau_q, \tau_r] \tag{4.12}$$

where $\tau_u, \tau_v, \tau_w, \tau_p, \tau_q$ and τ_r are the control forces and torques in surge, sway, heave, roll, pitch and yaw, respectively.

4.2.2 Nonlinear Observer Design

In real application, not all the states are measurable and thus observers are needed for control purpose. For station keeping control, we need the information on wave disturbance. Using measurement obtained from the AUV's Acoustic Doppler Velocimeter (ADV), Doppler and motion package, Riedel [91] designed an Extended Kalman Filter for states and wave disturbances estimation which is used for station keeping controller design to compensate the wave induced disturbance. But for low cost AUV, it is not desirable to use the expensive ADV sensor to derive the wave disturbance. As irrotational wave disturbances only affect translational motion of AUVs explicitly in surge, sway and heave directions [91], the main objectives of the observer design are to estimate the wave velocities and relative velocities of AUV in Equations (4.2) and (4.5). Fossen and Strand [33] proposed a nonlinear

observer for dynamic positioning control of surface ships, which was proven to be passive and globally exponentially stable. This work was extended to six degrees of freedom (DOF) for station keeping of AUVs in shallow water by Liu *et al.* [64]. But these two papers only used simplified models for low speed condition, which did not consider the Coriolis and centripetal forces and moments.

Inspired by the previous nonlinear observers in Chapter 3, we will design a nonlinear observer by using available position and attitude measurement for station keeping control taking into account the Coriolis and centripetal forces and moments. The main difference is that the precious nonlinear observer in Chapter 3 is used to filter out high frequency wave disturbance and to estimate the low frequency motion of ships in surge, sway and yaw directions for dynamic positioning in horizontal plane to achieve energy efficiency. Here, the nonlinear observer is used to estimate the wave velocities and relative velocities of AUVs in translational motion for station keeping control in which AUVs will need to use their actuators to counteract the high frequency wave disturbances. The models used in these two situations are also quite different. In our observer design, we first introduce a coordinate transformation to simplify the observer design problem due to the presence of the Coriolis and centripetal terms. Based on the transformed model, a nonlinear observer is then designed and shown to be globally exponentially stable (GES).

Coordinate transformation

To facilitate stability proof of our observer design, we first introduce the following coordinate transformation to remove the Coriolis and centripetal term $C_1(\nu_{1r})\nu_2$ in (4.5)

$$\begin{aligned} \alpha_1 &= \eta_1 \\ \alpha_2 &= Q(\eta_2)\nu_{1r} \end{aligned} \tag{4.13}$$

where $Q(\eta_2) \in \mathcal{R}^{3\times 3}$ is a non-singular matrix to be determined. Using Equations (4.3) and (4.5), we get the differentiation of (α_1, α_2) as follows:

$$\dot{\alpha}_1 = \dot{\eta}_1 = J_1(\eta_2)\nu_{1r} + \mathbf{U}_f \tag{4.14}$$

$$\begin{aligned}\dot{\alpha}_2 &= \dot{Q}(\eta_2)\nu_{1r} + Q(\eta_2)\dot{\nu}_{1r} \\ &= [\dot{Q}(\eta_2)\nu_{1r} - Q(\eta_2)M_1^{-1}C_1(\nu_{1r})\nu_2] \\ &\quad + Q(\eta_2)M_1^{-1}(-D_1(\nu_{1r})\nu_{1r} - g_1(\eta_2) + \tau_1)\end{aligned} \tag{4.15}$$

Note that

$$\dot{J}_1(\eta_2) = J_1(\eta_2)S(\eta_2) \tag{4.16}$$

where

$$S(\eta_2) = \begin{bmatrix} 0 & -r & q \\ r & 0 & -p \\ -q & p & 0 \end{bmatrix} \tag{4.17}$$

Hence, choosing $Q(\eta_2) = J_1(\eta_2)M_1$ leads to:

$$\begin{aligned}\dot{Q}(\eta_2)\nu_{1r} - Q(\eta_2)M_1^{-1}C_1(\nu_{1r})\nu_2 &= \dot{J}_1(\eta_2)M_1\nu_{1r} - J_1(\eta_2)M_1M_1^{-1}C_1(\nu_{1r})\nu_2 \\ &= J_1(\eta_2)S(\eta_2)M_1\nu_{1r} - J_1(\eta_2)C_1(\nu_{1r})\nu_2 \\ &= 0\end{aligned} \tag{4.18}$$

Using the coordinate transformation in (4.13) and result in (4.18), Equations (4.14) and (4.15) can be reduced to:

$$\dot{\alpha}_1 = J_1(\eta_2)M_1^{-1}J_1^{-1}(\eta_2)\alpha_2 + \mathbf{U}_f \tag{4.19}$$

$$\dot{\alpha}_2 = J_1(\eta_2)(-D_1(\nu_{1r})\nu_{1r} - g_1(\eta_2) + \tau_1) \tag{4.20}$$

where $\alpha_1 = \eta_1$ and $\alpha_2 = J_1(\eta_2)M_1\nu_{1r}$.

So the complete model of AUVs in shallow water areas can be expressed in new coordinate frame as follows

$$\dot{\alpha}_1 = J_1(\eta_2)M_1^{-1}J_1^{-1}(\eta_2)\alpha_2 + \mathbf{U}_f \tag{4.21}$$

$$\dot{\xi} = \begin{bmatrix} 0 & I \\ \Omega_{21} & \Omega_{22} \end{bmatrix} \xi \tag{4.22}$$

$$\dot{\alpha}_2 = J_1(\eta_2)(-D_1(\nu_{1r})\nu_{1r} - g_1(\eta_2) + \tau_1) \tag{4.23}$$

$$\dot{\eta}_2 = J_2(\eta_2)\nu_2 \tag{4.24}$$

$$\dot{\nu}_2 = M_2^{-1}(-C_1(\nu_{1r})\nu_{1r} - C_2(\nu_2)\nu_2 - D_2(\nu_2)\nu_2 - g_2(\eta_2) + \tau_2) \tag{4.25}$$

$$y = \begin{bmatrix} y_1 \\ y_2 \end{bmatrix} = \begin{bmatrix} \eta_1 \\ \eta_2 \end{bmatrix} \tag{4.26}$$

The compact forms for translational motion are expressed as:

$$\dot{\eta}_0 = A_0\eta_0 + B_0J_1(\eta_2)M_1^{-1}J_1^{-1}(\eta_2)\alpha_2 \tag{4.27}$$

$$\dot{\alpha}_2 = J_1(\eta_2)(-D_1(\nu_{1r})\nu_{1r} - g_1(\eta_2) + \tau_1) \tag{4.28}$$

$$y_1 = C_0\eta_0 \tag{4.29}$$

and for rotational motion

$$\dot{\eta}_2 = J_2(\eta_2)\nu_2 \tag{4.30}$$

$$\dot{\nu}_2 = M_2^{-1}(-C_1(\nu_{1r})\nu_{1r} - C_2(\nu_2)\nu_2 - D_2(\nu_2)\nu_2 - g_2(\eta_2) + \tau_2) \tag{4.31}$$

$$y_2 = \eta_2 \tag{4.32}$$

where $\eta_0 = \left[\xi_1^T, \xi_2^T, \alpha_1^T\right]^T$, $A_0 = \begin{bmatrix} 0 & I & 0 \\ \Omega_{21} & \Omega_{21} & 0 \\ 0 & I & 0 \end{bmatrix}$, $B_0 = \begin{bmatrix} 0 \\ 0 \\ I \end{bmatrix}$, $C_0 = \begin{bmatrix} 0 & 0 & I \end{bmatrix}$.

By using the coordinate transformation in (4.13), the Coriolis and centripetal term in Equation (4.5) has been removed as shown in Equation (4.28). Based on the transformed dynamic model, a nonlinear observer will be designed in the following part.

Observer structure

Similar to previous observer design in Chapter 3, we propose the following observer for translational motion dynamics. The observer for dynamics (4.27)-(4.29) is proposed as

$$\dot{\hat{\eta}}_0 = A_0\hat{\eta}_0 + B_0 J_1(\eta_2) M_1^{-1} J_1^{-1}(\eta_2)\hat{\alpha}_2 + K\tilde{y}_1 \tag{4.33}$$

$$\dot{\hat{\alpha}}_2 = J_1(\eta_2)(-D_1(\hat{\nu}_{1r})\hat{\nu}_{1r} - g_1(\eta_2) + \tau_1 + M_1^{-1} J_1^{-1}(\eta_2) K_4 \tilde{y}_1) \tag{4.34}$$

$$\hat{y}_1 = C_0\hat{\eta}_0 \tag{4.35}$$

where $\tilde{y}_1 = y_1 - \hat{y}_1$ is the estimation error vector of position and $K = \begin{bmatrix} K_1 \\ K_2 \\ K_3 \end{bmatrix}$ with K_1, K_2, K_3 and $K_4 \in \mathcal{R}^{3\times 3}$ are the observer gain matrices to be determined later. $\hat{\eta}_0 = \begin{bmatrix} \hat{\xi}_1 \\ \hat{\xi}_2 \\ \hat{\alpha}_1 \end{bmatrix}$ comprises the wave velocities estimation $\hat{\xi}_2$ and the position estimation $\hat{\alpha}_1$. $\hat{\nu}_{1r} = M_1^{-1} J_1^{-1}(\eta_2)\hat{\alpha}_2$ is the relative velocity estimation.

Position error dynamics can be obtained by subtracting (4.33)-(4.35) from (4.27)-(4.29), respectively,

$$\dot{\tilde{\eta}}_0 = (A_0 - KC_0)\tilde{\eta}_0 + B_0 J_1(\eta_2) M_1^{-1} J_1^{-1}(\eta_2)\tilde{\alpha}_2 \tag{4.36}$$

$$\dot{\tilde{\alpha}}_2 = J_1(\eta_2)(-D_1(\nu_{1r})\nu_{1r} + D_1(\hat{\nu}_{1r})\hat{\nu}_{1r} - M_1^{-1} J_1^{-1}(\eta_2) K_4 \tilde{y}_1) \tag{4.37}$$

$$\tilde{y}_1 = C_0 \tilde{\eta}_0 \tag{4.38}$$

where $\tilde{\eta}_0 = \eta_0 - \hat{\eta}_0$ and $\tilde{\alpha}_2 = \alpha_2 - \hat{\alpha}_2$.

In (4.28), (4.34) and (4.37), we use $D(\nu_{1r})\nu_{1r}$ and $D(\hat{\nu}_{1r})\hat{\nu}_{1r}$ instead of the form of α_2 and $\hat{\alpha}_2$ for notational clarity in subsequent stability proof. The observer error dynamics in (4.36)-(4.38) is illustrated using a block diagram in Figure 4.1 where two new error terms, $\varepsilon_z = -J_1(\eta_2)M_1^{-1}J_1^{-1}(\eta_2)K_4\tilde{y}_1$ and $\varepsilon_\nu = J_1(\eta_2)M_1^{-1}J_1^{-1}(\eta_2)\tilde{\alpha}_2$, are defined.

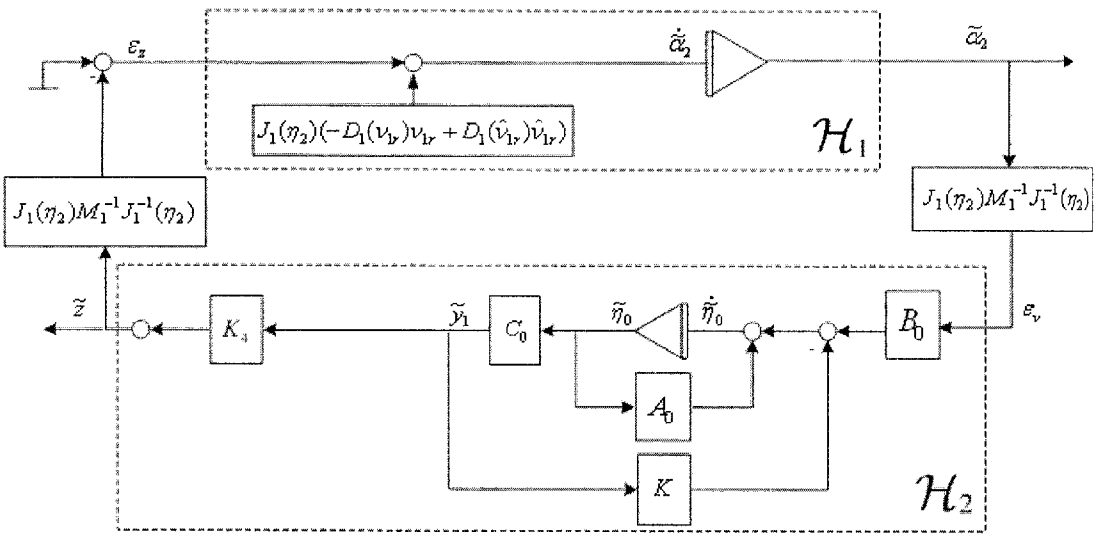

Figure 4.1: Dynamics of the position and relative velocity estimation errors.

The observer error dynamic model can be rewritten as

$$\dot{\tilde{\eta}}_0 = A\tilde{\eta}_0 + B\varepsilon_\nu \tag{4.39}$$

$$\tilde{z} = C\tilde{\eta}_0 \tag{4.40}$$

$$\dot{\bar{\alpha}}_2 = J_1(\eta_2)(-D_1(\nu_{1r})\nu_{1r} + D_1(\hat{\nu}_{1r})\hat{\nu}_{1r}) - J_1(\eta_2)M_1^{-1}J_1^{-1}(\eta_2)\tilde{z} \tag{4.41}$$

where $\tilde{z} = K_4\tilde{y}_1$,

$$A = (A_0 - KC_0) = \begin{bmatrix} 0 & I & -K_1 \\ \Omega_{21} & \Omega_{22}0 & -K_2 \\ 0 & I & -K_3 \end{bmatrix}, B = B_0 = \begin{bmatrix} 0 \\ 0 \\ I \end{bmatrix} \text{ and}$$

$$C = K_4C_0 = \begin{bmatrix} 0 & 0 & K_4 \end{bmatrix}.$$

Using the observer design technique in Chapter 3, the gain matrices in the observer (4.33) and (4.34) are chosen with the following structures:

$$\begin{aligned} K_1 &= \text{diag}\{k_{11}, k_{12}, k_{13}\} \\ K_2 &= \text{diag}\{k_{21}, k_{22}, k_{23}\} \\ K_3 &= \text{diag}\{k_{31}, k_{32}, k_{33}\} \\ K_4 &= \text{diag}\{k_{41}, k_{42}, k_{43}\} \end{aligned} \tag{4.42}$$

where

$$\begin{aligned} k_{1i} &= 2\omega_{oi}(\zeta_{ni} - \zeta_i) \\ k_{2i} &= 2\omega_{oi}(\zeta_{ni}\omega_{ci} - \zeta_i k_{3i}) \\ k_{3i} &= 2\omega_{oi}(\zeta_{ni} - \zeta_i) + \omega_{ci} \end{aligned} \tag{4.43}$$

Stability analysis

Theorem 4.1 (Globally exponentially stable nonlinear observer) *For the AUV translational dynamic model described by (4.27)- (4.29), the nonlinear observer (4.33)-(4.35) is globally exponentially stable if K_1, K_2 and K_3 are chosen according to the structure in (4.42) with parameters in (4.43) such that the triple (A, B, C) in (4.39) and (4.40) is strictly positive real (SPR).*

Proof With these observer gains, we can guarantee that all three decoupled observer error dynamics transfer functions can be designed to have phase greater then $-90°$. And thus the SPR requirement is satisfied. According to the Kalman-Yakubovich-Popov (KYP) lemma [54], there exist positive-definite matrices $P = P^T$ and $Q = Q^T$ such that

$$PA + A^T P = -Q, \tag{4.44}$$

$$B^T P = C \tag{4.45}$$

We propose the following Lyapunov function candidate:

$$V_{obs} = \tilde{\alpha}_2^T \tilde{\alpha}_2 + \tilde{\eta}_0^T P \tilde{\eta}_0 \tag{4.46}$$

Differentiation of V along the trajectories of $\tilde{\alpha}_2$ and $\tilde{\eta}_0$ in (4.39) and (4.41) yields

$$\begin{aligned} \dot{V}_{obs} &= 2\tilde{\alpha}_2^T (J_1(\eta_2)(-D_1(\nu_{1r})\nu_{1r} + D_1(\hat{\nu}_{1r})\hat{\nu}_{1r}) - J_1(\eta_2) M_1^{-1} J_1^{-1}(\eta_2)\tilde{z}) \\ &\quad + \tilde{\eta}_0^T (PA + A^T P)\tilde{\eta}_0 \\ &\quad + 2\tilde{\alpha}_2 J_1(\eta_2) M_1^{-1} J_1^{-1}(\eta_2) B^T P \tilde{\eta}_0 \qquad (4.47) \\ &= 2\tilde{\alpha}_2^T J_1(\eta_2)(-D_1(\nu_{1r})\nu_{1r} + D_1(\hat{\nu}_{1r})\hat{\nu}_{1r}) - 2\tilde{\alpha}_2^T J_1(\eta_2) M_1^{-1} J_1^{-1}(\eta_2) C \tilde{\eta}_0 \\ &\quad - \tilde{\eta}_0^T Q \tilde{\eta}_0 + 2\tilde{\alpha}_2 J_1(\eta_2) M_1^{-1} J_1^{-1}(\eta_2) B^T P \tilde{\eta}_0 \end{aligned}$$

Based on the definition $B^T P = C$ and using (4.40), we have $B^T P\tilde{\eta}_0 = C\tilde{\eta}_0 = \tilde{z}$. Since $\alpha_2 = J_1(\eta_2)M_1\nu_{1r}$ and $J_1^{-1}(\eta_2) = J_1^T(\eta_2)$, we get

$$\begin{aligned}
\dot{V}_{obs} &= 2\tilde{\nu}_{1r}^T M_1^T J_1^T(\eta_2)J_1(\eta_2)(-D_1(\nu_{1r})\nu_{1r} + D_1(\hat{\nu}_{1r})\hat{\nu}_{1r}) - \tilde{\eta}_0^T Q\tilde{\eta}_0 \\
&= 2\tilde{\nu}_{1r}^T M_1^T(-D_1(\nu_{1r})\nu_{1r} + D_1(\hat{\nu}_{1r})\hat{\nu}_{1r}) - \tilde{\eta}_0^T Q\tilde{\eta}_0 \qquad (4.48) \\
&\leq -2\tilde{\nu}_{1r}^T M_1^T D_1\tilde{\nu}_{1r} - \tilde{\eta}_0^T Q\tilde{\eta}_0 \qquad (4.49) \\
&< 0 \quad \forall\tilde{\nu}_{1r}, \tilde{\eta}_0 \neq 0
\end{aligned}$$

Here we use the property that $D_1(\nu_{1r})$ is a nondecreasing function.

So $\tilde{\alpha}_2$ and $\tilde{\eta}_0 = \left[\tilde{\xi}_1^T, \tilde{\xi}_2^T, \tilde{\alpha}_1^T\right]^T$ converge exponentially to zero. As $J_1(\eta_2)$ is a nonsingular transformation matrix, the relative velocity of AUVs, $\tilde{\nu}_{1r} = M_1^{-1}J_1^{-1}(\eta_2)\tilde{\alpha}_2$, will also converge to zero exponentially.

4.2.3 Nonlinear Controller Design

To keep the AUVs at a fixed point, we need counteract the external disturbance by using the thrusters. By using the nonlinear observer developed in the previous section, we can estimate the wave velocities and relative velocities of AUVs in translational motion. Then we can design an output feedback controller to keep the AUVs at a fixed position by counteracting the high frequency wave disturbance due to waves. Here we present an output feedback controller for translational motion of AUVs using observer backstepping technique in [56]. For rotational motion, we present a backstepping controller by directly using the attitude measurement. Backstepping makes use of a recursive procedure that breaks down the control problem of the full system into a sequence of designs for lower order systems [56, 54]. The observer backstepping method in this section is based on the work of Aarset *et al.* [2], which is an extension of the results in Fossen and Grøvlen [30].

The results in [30, 2] focused on dynamic positioning control of ships to achieve energy efficiency for actuators. In this section, the backstepping control technique is used for station keeping of AUVs to meet precision requirement.

Observer backstepping controller design for translational motion

Step 1 Since $\alpha_1 = \eta_1$ is combined with the wave motion and corrupted by the measurement noise, the tracking error $\hat{\alpha}_1 - \alpha_d$ is used for observer backstepping design because the observer guarantees $\hat{\alpha}_1$ converge to α_1 exponentially,.

We first define the error variable z_1 as

$$z_1 = \hat{\alpha}_1 - \alpha_d + K_I \int_0^t (\hat{\alpha}_1 - \alpha_d) d\tau = \dot{e}_{1I} + K_I e_{1I} \tag{4.50}$$

where $K_I > 0$ is a diagonal integration gain matrix used to eliminate steady state errors and $\dot{e}_{1I} = \hat{\alpha}_1 - \alpha_d$.

Differentiating (4.50) with respect to time and using Equation (4.33) yields

$$\dot{z}_1 = \hat{\xi}_2 + J_1(\eta_2) M_1^{-1} J_1^{-1}(\eta_2) \hat{\alpha}_2 + K_3 \tilde{y}_1 - \dot{\alpha}_d + K_I(\hat{\alpha}_1 - \alpha_d) \tag{4.51}$$

The virtual control vector is chosen as $\gamma_1 = \hat{\xi}_2 + J_1(\eta_2) M_1^{-1} J_1^{-1}(\eta_2) \hat{\alpha}_2 = z_2 + \beta_1$ with a stabilizing function $\beta_1 = -(E_1 + F_1) z_1 + \dot{\alpha}_d - K_I(\hat{\alpha}_1 - \alpha_d)$. So Equation (4.51) results in

$$\dot{z}_1 = -(E_1 + F_1) z_1 + z_2 + K_3 \tilde{y}_1 \tag{4.52}$$

E_1 is a strictly positive diagonal feedback design matrix expressed as $E_1 = \text{diag}\{e_1, e_2, e_3\}$ where e_i (i=1,2,3) are positive and F_1 is a strictly positive diagonal damping matrix

defined as:

$$F_1 = \begin{bmatrix} e_1 k_{31}^2 & 0 & 0 \\ 0 & e_2 k_{32}^2 & 0 \\ 0 & 0 & e_3 k_{33}^2 \end{bmatrix} \tag{4.53}$$

Where k_{3i} (i=1,2,3) are the observer gain elements in K_3. The damping term $-F_1 z_1$ is used to compensate the disturbance like term $K_3 \tilde{y}_1$.

Step 2 From the definition of γ_1 and z_2, we get $z_2 = \hat{\xi}_2 + J_1(\eta_2) M_1^{-1} J_1^{-1}(\eta_2) \hat{\alpha}_2 + (E_1 + F_1) z_1 - \dot{\alpha}_d + K_I(\hat{\alpha}_1 - \alpha_d)$.

Time differentiation of z_2 is:

$$\begin{aligned} \dot{z}_2 &= \dot{\gamma}_1 - \dot{\beta}_1 \\ &= \dot{\hat{\xi}}_2 + J_1(\eta_2) S(\eta_2) M_1^{-1} J_1^T(\eta_2) \hat{\alpha}_2 + J_1(\eta_2) M_1^{-1} S^T(\eta_2) J_1^T(\eta_2) \hat{\alpha}_2 \\ &\quad + J_1(\eta_2) M_1^{-1} J_1^T(\eta_2) J_1(\eta_2) (-D_1(\hat{\nu}_{1r}) \hat{\nu}_{1r} - g_1(\eta_2) + \tau_1 + M_1^{-1} J_1^{-1}(\eta_2) K_4 \tilde{y}_1) \\ &\quad + (E_1 + F_1) \dot{z}_1 - \ddot{\alpha}_d + K_I(\dot{\hat{\alpha}}_1 - \dot{\alpha}_d) \qquad (4.5 \\ &= \Omega_{21} \hat{\xi}_1 + \Omega_{22} \hat{\xi}_2 + K_2 \tilde{y}_1 + J_1(\eta_2) S(\eta_2) M_1^{-1} J_1^T(\eta_2) \hat{\alpha}_2 + J_1(\eta_2) M_1^{-1} S^T(\eta_2) J_1^T(\eta_2) \\ &\quad + J_1(\eta_2) M_1^{-1} J_1^T(\eta_2) J_1(\eta_2) (-D_1(\hat{\nu}_{1r}) \hat{\nu}_{1r} - g_1(\eta_2) + \tau_1 + M_1^{-1} J_1^{-1}(\eta_2) K_4 \tilde{y}_1) \\ &\quad + (E_1 + F_1)(-(E_1 + F_1) z_1 + z_2 + K_3 \tilde{y}_1) - \ddot{\alpha}_d \\ &\quad + K_I(\hat{\xi}_2 + J_1(\eta_2) M_1^{-1} J_1^T(\eta_2) \hat{\alpha}_2 + K_3 \tilde{y}_1 - \dot{\alpha}_d) \end{aligned}$$

By defining Λ_1 as

$$\begin{aligned} \Lambda_1 &= \Omega_{21} \hat{\xi}_1 + \Omega_{22} \hat{\xi}_2 + J_1(\eta_2) S(\eta_2) M_1^{-1} J_1^T(\eta_2) \hat{\alpha}_2 + J_1(\eta_2) M_1^{-1} S^T(\eta_2) J_1^T(\eta_2) \hat{\alpha}_2 \\ &\quad + J_1(\eta_2) M_1^{-1} (-D_1(\hat{\nu}_{1r}) \hat{\nu}_{1r} - g_1(\eta_2) + M_1^{-1} J_1^{-1}(\eta_2) K_4 \tilde{y}_1) \qquad (4.55) \\ &\quad + (E_1 + F_1)(-(E_1 + F_1) z_1 + z_2) - \ddot{\alpha}_d \\ &\quad + K_I(J_1(\eta_2) M_1^{-1} J_1^T(\eta_2) \hat{\alpha}_2 - \dot{\alpha}_d) \end{aligned}$$

Equation (4.54) can be written as

$$\begin{aligned}\dot{z}_2 &= J_1(\eta_2)M_1^{-1}\tau_1 + \Lambda_1 \\ &\quad +(K_2 + (E_1 + F_1)K_3 + K_I K_3)\tilde{y}_1\end{aligned} \tag{4.56}$$

Because all the terms in $K_2 + (E_1 + F_1)K_3 + K_I K_3$ are diagonal matrix, we define a term $\Theta = K_2 + (E_1 + F_1)K_3 + K_I K_3$ as

$$\Theta = \begin{bmatrix} \theta_1 & 0 & 0 \\ 0 & \theta_2 & 0 \\ 0 & 0 & \theta_3 \end{bmatrix}. \tag{4.57}$$

The following choice of feedback controller is made

$$\tau_1 = -M_1 J_1^{-1}(\eta_1)(\Lambda_1 + (E_2 + F_2)z_2 + z_1) \tag{4.58}$$

E_2 is a strictly positive diagonal feedback design matrix expressed as $E_2 = \text{diag}\{e_3, e_4, e_5\}$ where e_i (i=4,5,6) are positive constants. The F_2 is chosen as a strictly positive diagonal damping matrix. The damping term $-F_2 z_2$ is used to compensate the disturbance like term $\Theta\tilde{y}_1$. So the resulting z_2-error dynamics is

$$\dot{z}_2 = -(E_2 + F_2)z_2 - z_1 + \Theta\tilde{y}_1. \tag{4.59}$$

The strictly positive diagonal damping matrix F_2 is defined as

$$F_2 = \begin{bmatrix} e_4\theta_1^2 & 0 & 0 \\ 0 & e_5\theta_2^2 & 0 \\ 0 & 0 & e_6\theta_3^2 \end{bmatrix} \tag{4.60}$$

By combining Equations (4.39)-(4.41) and (4.59), the resulting error dynamics of the whole system can be written as

$$\dot{z} = -(E_z + F_z)z + Ez + \Upsilon\tilde{y}_1 \tag{4.61}$$

$$\dot{\tilde{\eta}}_0 = A\tilde{\eta}_0 + BJ_1(\eta_2)M_1^{-1}J_1^{-1}(\eta_2)\tilde{\alpha}_2 \tag{4.62}$$

$$\dot{\tilde{\alpha}}_2 = J_1(\eta_2)(-D_1(\nu_{1r})\nu_{1r} + D_1(\hat{\nu}_{1r})\hat{\nu}_{1r}) - J_1(\eta_2)M_1^{-1}J_1^{-1}(\eta_2)C\tilde{\eta}_0 \tag{4.63}$$

where $z = [z_1^T, z_2^T]^T$ and $E_z = \begin{bmatrix} E_1 & 0 \\ 0 & E_2 \end{bmatrix}$, $F_z = \begin{bmatrix} F_1 & 0 \\ 0 & F_2 \end{bmatrix}$, $E = \begin{bmatrix} 0 & 1 \\ -1 & 0 \end{bmatrix}$, $\Upsilon = \begin{bmatrix} K_3 \\ \Theta \end{bmatrix}$.

A Lyapunov function candidate for the control law is

$$V_{con} = \frac{1}{2}z^T z + e_{1I}^T K_I E_1 e_{1I}. \tag{4.64}$$

So the Lyapunov function candidate for the whole observer-controller system is

$$\begin{aligned} V_1 &= V_{con} + V_{obs} \\ &= \frac{1}{2}z^T z + e_{1I}^T K_I E_1 e_{1I} + \tilde{\alpha}_2^T\tilde{\alpha}_2 + \tilde{\eta}_0^T P\tilde{\eta}_0. \end{aligned} \tag{4.65}$$

The time differentiation of Equation (4.65) is

$$\begin{aligned} \dot{V}_1 &= \dot{V}_{con} + \dot{V}_{obs} \\ &= z^T\dot{z} + 2e_{1I}^T K_I E_1\dot{e}_{1I} + 2\tilde{\nu}_{1r}^T M_1^T(-D_1(\nu_{1r})\nu_{1r} + D_1(\hat{\nu}_{1r})\hat{\nu}_{1r}) - \tilde{\eta}_0^T Q\tilde{\eta}_0 \\ &= -z_1^T E_1 z_1 - z_1^T F_1 z_1 + z_1^T K_3\tilde{y}_1 \\ &\quad -z_2^T E_2 z_2 - z_2^T F_2 z_2 + z_2^T\Theta\tilde{y}_1 \\ &\quad +2e_{1I}^T K_I E_1\dot{e}_{1I} + 2\tilde{\nu}_{1r}^T M_1^T(-D_1(\nu_{1r})\nu_{1r} + D_1(\hat{\nu}_{1r})\hat{\nu}_{1r}) - \tilde{\eta}_0^T Q\tilde{\eta}_0 \end{aligned} \tag{4.66}$$

Adding the following zero terms

$$\frac{1}{4}(\tilde{\eta}_0^T C_0^T G_2 C_0 \tilde{\eta}_0 - \tilde{\eta}_0^T C_0^T G_2 C_0 \tilde{\eta}_0) = 0 \tag{4.67}$$

with $G_1 = \begin{bmatrix} \frac{1}{e_1} & 0 & 0 \\ 0 & \frac{1}{e_2} & 0 \\ 0 & 0 & \frac{1}{e_3} \end{bmatrix}$, $G_2 = \begin{bmatrix} \frac{1}{e_4} & 0 & 0 \\ 0 & \frac{1}{e_5} & 0 \\ 0 & 0 & \frac{1}{e_6} \end{bmatrix}$, $C_0 = \begin{bmatrix} 0 & 0 & I \end{bmatrix}$ and $C_0\tilde{\eta}_0 = \tilde{y}_1$ into (4.66), and considering the relation [2]

$$\begin{aligned} -z_1^T F_1 z_1 + z_1^T K_3 \tilde{y}_1 - \frac{1}{4}\tilde{\eta}_0^T C_0^T G_1 C_0 \tilde{\eta}_0 \leq 0 \\ -z_2^T F_2 z_2 + z_2^T \Theta \tilde{y}_1 - \frac{1}{4}\tilde{\eta}_0^T C_0^T G_2 C_0 \tilde{\eta}_0 \leq 0, \end{aligned} \tag{4.68}$$

Equation (4.66) can be written as

$$\begin{aligned} \dot{V}_1 \leq & -z_1^T E_1 z_1 + \frac{1}{4}\tilde{\eta}_0^T C_0^T G_1 C_0 \tilde{\eta}_0 \\ & -z_2^T E_2 z_2 + \frac{1}{4}\tilde{\eta}_0^T C_0^T G_2 C_0 \tilde{\eta}_0 \\ & +2e_{1I}^T K_I E_1 \dot{e}_{1I} - 2\tilde{\nu}_{1r}^T M_1^T D_1 \tilde{\nu}_{1r} - \tilde{\eta}_0^T Q \tilde{\eta}_0 \\ \leq & -(\dot{e}_{1I} + K_I e_I)^T E_1 (\dot{e}_{1I} + K_I e_{1I}) + 2e_{1I}^T K_I E_1 \dot{e}_{1I} \\ & -z_2^T E_2 z_2 - 2\tilde{\nu}_{1r}^T M_1^T D_1 \tilde{\nu}_{1r} \\ & -\tilde{\eta}_0^T (Q - \frac{1}{4}C_0^T G_1 C_0 - \frac{1}{4}C_0^T G_2 C_0)\tilde{\eta}_0 \\ \leq & -\dot{e}_{1I}^T E_1 \dot{e}_{1I} - e_{1I}^T K_I^T E_1 K_I e_{1I} - z_2^T E_2 z_2 \\ & -2\tilde{\nu}_{1r}^T M_1^T D_1 \tilde{\nu}_{1r} \\ & -\tilde{\eta}_0^T (Q - \frac{1}{4}C_0^T G_1 C_0 - \frac{1}{4}C_0^T G_2 C_0)\tilde{\eta}_0 \\ < & \ 0 \qquad \forall \tilde{\eta}_0 \neq 0, \tilde{\nu}_{1r} \neq 0. \end{aligned} \tag{4.69}$$

$\dot{V}_1$ can be made negative definite by choosing the positive definite matrix $Q > \frac{1}{4}C_0^T G_1 C_0 + \frac{1}{4}C_0^T G_2 C_0$. So according to Lyapunov stability theory, the AUV system

with observer (4.33)-(4.35) and controller law (4.58) is GES.

Backstepping controller design for rotational motion

The dynamics of the rotational motion is

$$\dot{\eta}_2 = J_2(\eta_2)\nu_2 \tag{4.70}$$

$$\dot{\nu}_2 = M_2^{-1}(-C_1(\nu_{1r})\nu_{1r} - C_2(\nu_2)\nu_2 - D_2(\nu_2)\nu_2 - g_2(\eta_2) + \tau_2) \tag{4.71}$$

$$y_2 = \eta_2 \tag{4.72}$$

where $J_2(\eta_2)$ is the kinematic transformation matrix and both η_2 and ν_2 are measurable.

Because we can measure the attitude and Euler angle rate with great accuracy, we present a backstepping controller by directly using the attitude measurement for rotational motion.

Step 1 Similar to previous design, we first define the error variable z_3 as

$$z_3 = \eta_2 - \eta_{2d} + K_I \int_0^t (\eta_2 - \eta_{2d})d\tau = \dot{e}_{2I} + K_I e_{2I} \tag{4.73}$$

where $K_I > 0$ still has the same definition as in the previous section in (4.50) and $\dot{e}_{2I} = \eta_2 - \eta_{2d}$. Based on (6.21), we obtain the following by differentiating (6.24)

$$\dot{z}_3 = J_2(\eta_2)\nu_2 - \dot{\eta}_{2d} + K_I(\eta_2 - \eta_{2d}) \tag{4.74}$$

The virtual control vector is chosen as $\gamma_2 = J_2(\eta_2)\nu_2 = z_4 + \beta_2$ with the stabilizing function $\beta_2 = -E_3 z_3 + \dot{\eta}_{2d} - K_I(\eta_2 - \eta_{2d})$. So Equation (6.25) becomes

$$\dot{z}_3 = -E_3 z_3 + z_4 \tag{4.75}$$

where E_3 is a strictly positive diagonal feedback design matrix.

Step 2 Differentiating z_4, we get

$$\begin{aligned}\dot{z}_4 &= \dot{\gamma}_2 - \dot{\beta}_2 \\ &= \dot{J}_2(\eta_2)\nu_2 + J_2(\eta_2)\dot{\nu}_2 + E_3\dot{z}_3 - \ddot{\eta}_{2d} + K_I(\dot{\eta}_2 - \dot{\eta}_{2d}) \\ &= \dot{J}_2(\eta_2)\nu_2 + J_2(\eta_2)M_2^{-1}(\tau_2 - C_1(\nu_{1r})\nu_{1r} - C_2(\nu_2)\nu_2 - D_2(\nu_2)\nu_2 - g_2(\eta_2)) \\ &\quad + E_3(-E_3z_3 + z_4) - \ddot{\eta}_{2d} + K_I(J_2(\eta_2)\nu_2 - \dot{\eta}_{2d})\end{aligned} \tag{4.76}$$

By defining Λ_2 as

$$\begin{aligned}\Lambda_2 &= \dot{J}_2(\eta_2)\nu_2 + J_2(\eta_2)M_2^{-1}(-C_2(\nu_2)\nu_2 - D_2(\nu_2)\nu_2 - g_2(\eta_2)) \\ &\quad + E_3(-E_3z_3 + z_4) - \ddot{\eta}_{2d} + K_I(J_2(\eta_2)\nu_2 - \dot{\eta}_{2d})\end{aligned} \tag{4.77}$$

Equation (6.27) can be rewritten as

$$\dot{z}_4 = J_2(\eta_2)M_2^{-1}\tau_2 - J_2(\eta_2)M_2^{-1}C_1(\nu_{1r})\nu_{1r} + \Lambda_2 \tag{4.78}$$

We can easily choose the following controller

$$\tau_2 = -M_2J_2^{-1}(\eta_2)(\Lambda_2 + E_4z_4 + z_3) + C_1(\hat{\nu}_{1r})\hat{\nu}_{1r} \tag{4.79}$$

So the resulting z_4 error dynamics is

$$\dot{z}_4 = -E_4z_4 - z_3 - J_2(\eta_2)M_2^{-1}(C_1(\nu_{1r})\nu_{1r} - C_1(\hat{\nu}_{1r})\hat{\nu}_{1r}) \tag{4.80}$$

where F_4 is a strictly positive feedback matrix usually chosen to be diagonal form.

Defining the following Lyapunov function candidate

$$V_2 = \frac{1}{2} z_3^T z_3 + \frac{1}{2} z_4^T z_4 \tag{4.81}$$

So the time differentiation of Equation (6.33) is

$$\dot{V}_2 = -z_3^T E_3 z_3 - z_4^T E_4 z_4 - z_4^T J_2(\eta_2) M_2^{-1} (C_1(\nu_{1r})\nu_{1r} - C_1(\hat{\nu}_{1r})\hat{\nu}_{1r}) < 0 \tag{4.82}$$

Based on the previous GES property of observer design, so the GES of this orientational controller is guaranteed.

4.2.4 Simulation Results

To demonstrate the performance of the proposed observer and controller, simulation study is carried out by using the AUV model of the vehicle KAMBARA [94]. The AUV dynamics is described by (4.5) and (4.6) with the parameter values given in Appendix A.

The wave model parameters are chosen as $\zeta_i = 0.1$ and $\omega_i = 0.7854$ (i=1-3) corresponding to a wave period of 8s in surge, sway and heave. The amplitude of wave velocity relative to the earth-fixed frame in surge, sway and heave are limited to 0.4m/s, 0.4m/s and 0.1m/s, respectively. The notch filter parameters are chosen as $\zeta_{ni} = 10$ and $\omega_{ci} = 10$. From (4.43) , we choose

$$K_1 = 15.5509 I_{3\times 3}, \quad K_2 = 153.0665 I_{3\times 3}, \quad K_3 = 25.5509 I_{3\times 3} \tag{4.83}$$

as numerical values for the observer gain matrices. In simulation, the wave model is driven by the zero mean Gaussian white noise although it was assumed to be zero in the stability analysis. This is to demonstrate the good performance of the observer in the presence of stochastic noise.

In the simulation study, the initial condition of the KAMBARA is $\nu_1 = [0,0,0]^T$, $\nu_2 = [0,0,0]^T$, $\eta_1 = [1.5,2.5,4]^T$ and $\eta_2 = [0.3,0.3,0.3]^T$. The initial condition of the observer is $\hat{\alpha}_1 = [1.3,2.3,3.9]^T$ and $\hat{\alpha}_2 = [0.1,0.1,0.1]^T$. The desired position and orientational angles are $\eta_{1d} = [1,2,3.5]^T$, $\eta_{2d} = [0,0.1,0.2]^T$.

Using (4.53) and (4.60), we select $E_1 = E_2 = 1I_{3\times3}$, $F_1 = 0.005K_3^2 = 3.2642I_{3\times3}$, $F_2 = 0.005\Theta^2 = 90.4598I_{3\times3}$, $E_3 = 0.6I_{3\times3}$, $E_4 = 2I_{3\times3}$. To test the robustness of the observer and controller, we include the position measurement noises in our simulation.

The simulation results are shown in Figures 4.2-4.16. Figures 4.2, 4.3 and 4.4 show the desired, actual and estimated position in surge, sway and heave directions. WAs shown in these figures, AUV can maintain its position with great accuracy by counteracting the wave disturbances. Figures 4.5, 4.6 and 4.7 show the actual and desired attitude angles in roll, pitch and yaw. We can see that position and attitude angle converge to the desired one exponentially. The actual and estimated relative velocities in surge, sway and heave directions are shown in 4.8, 4.9 and 4.10. The first-order wave velocities in surge, sway and heave directions and their estimates are shown in 4.11, 4.12 and 4.13. The control input forces and moments are shown in 4.14 and 4.15. The exponential convergence of the wave disturbance estimation errors can be seen from Figure 4.16. It can be recognized that the stochastic behavior of the wave disturbance is estimated well even though it is assumed that there is no white noise in the original wave model.

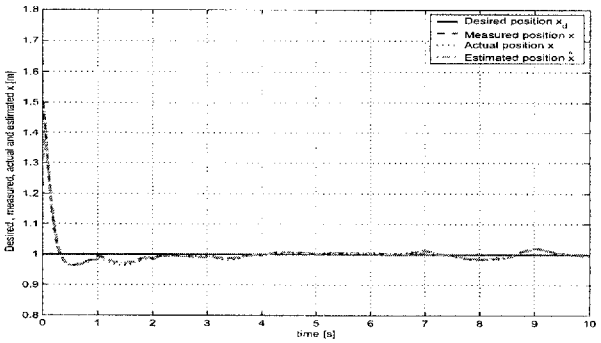

Figure 4.2: The desired, actual, and estimated position in surge

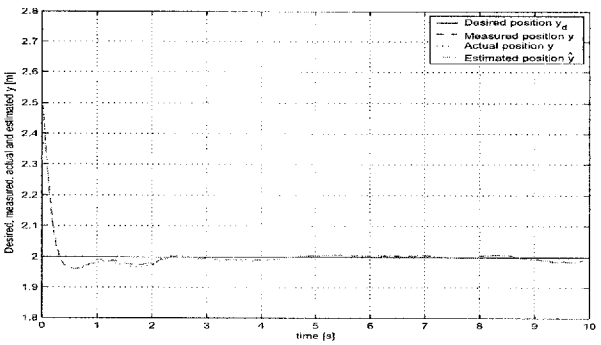

Figure 4.3: The desired, actual, and estimated position in sway

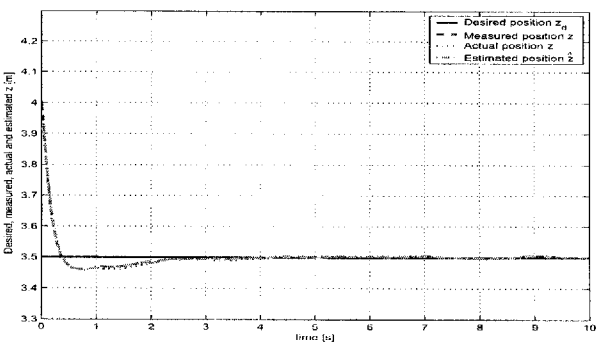

Figure 4.4: The desired, actual, and estimated position in heave

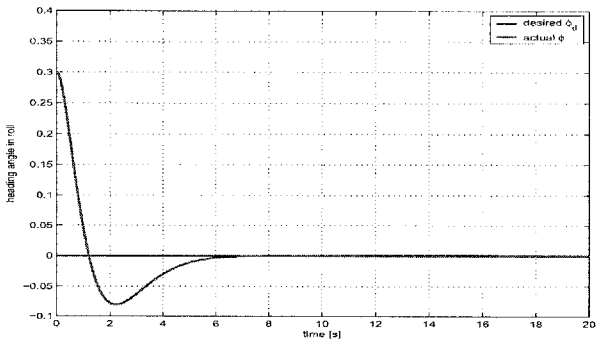

Figure 4.5: The desired and actual attitude in roll

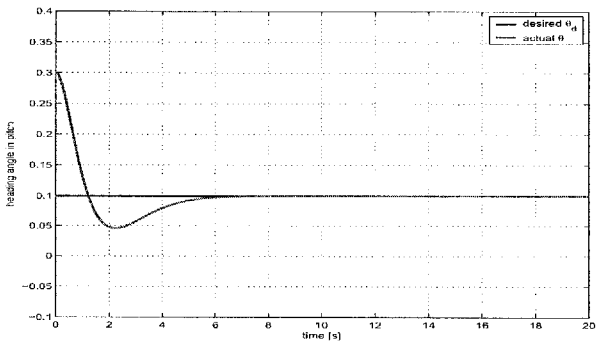

Figure 4.6: The desired and actual attitude in pitch

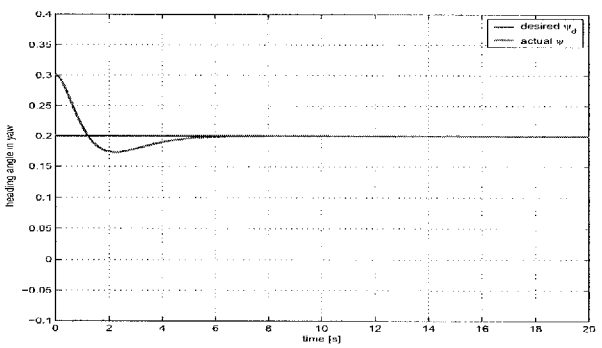

Figure 4.7: The desired and actual attitude in yaw

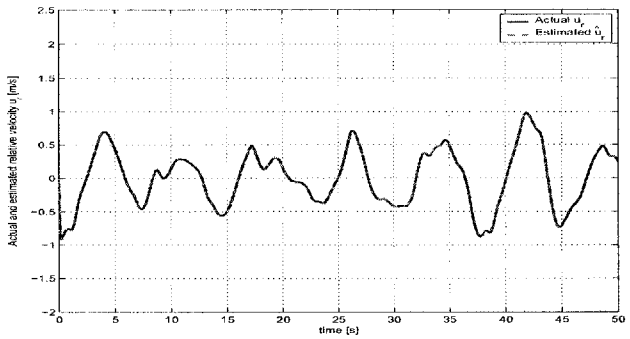

Figure 4.8: The actual relative velocity and its estimate in surge

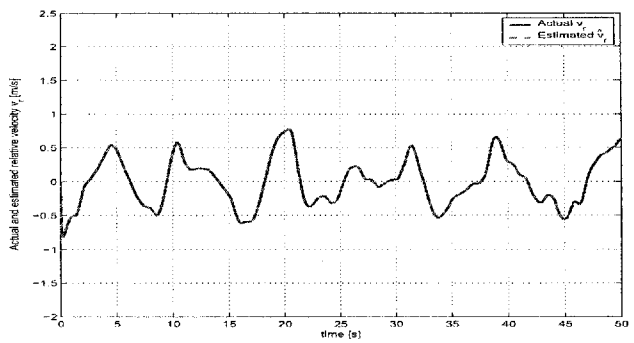

Figure 4.9: The actual relative velocity and its estimate in sway

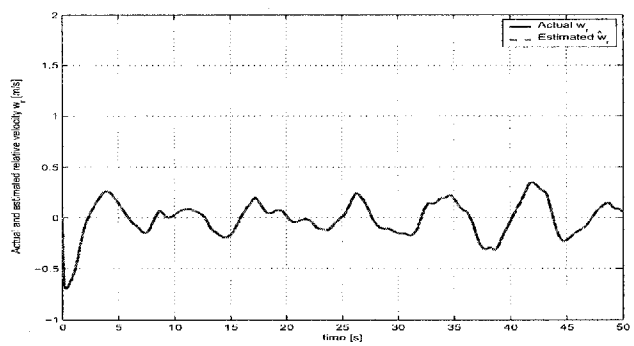

Figure 4.10: The actual relative velocity and its estimate in heave

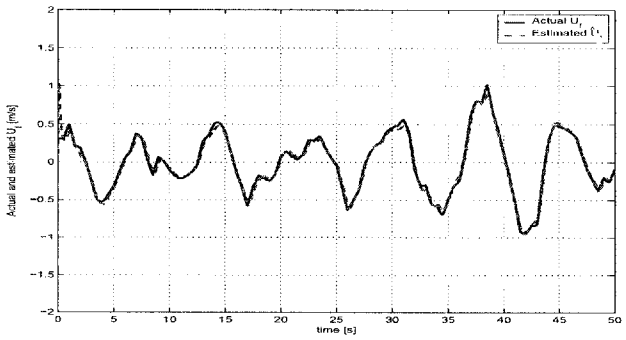

Figure 4.11: The actual wave velocity and its estimate in surge

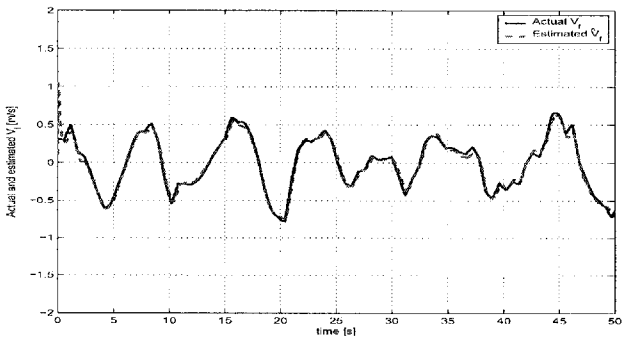

Figure 4.12: The actual wave velocity and its estimate in sway

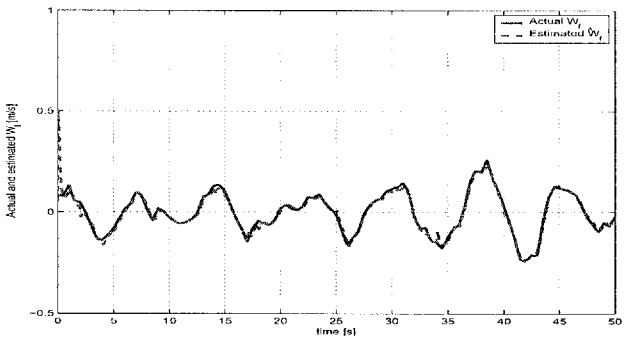

Figure 4.13: The actual wave velocity and its estimate in heave

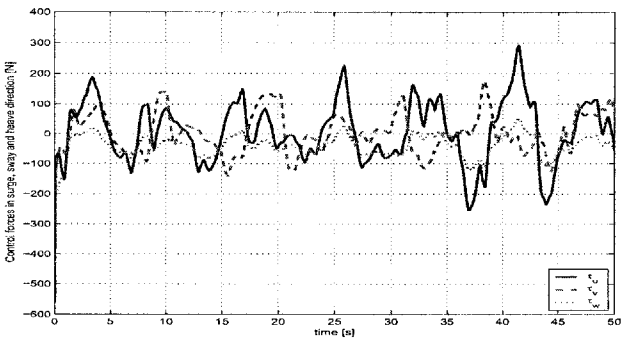

Figure 4.14: The control input forces in surge, sway and heave

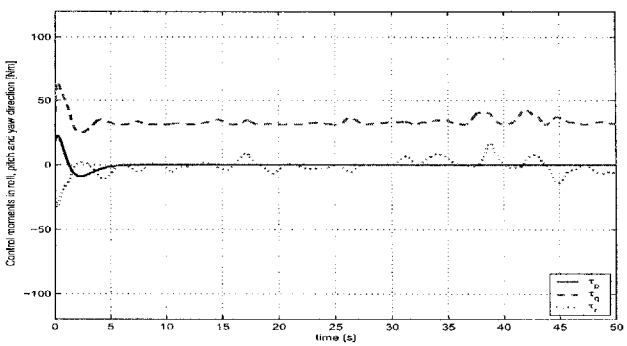

Figure 4.15: The control input moments in roll, pitch and yaw

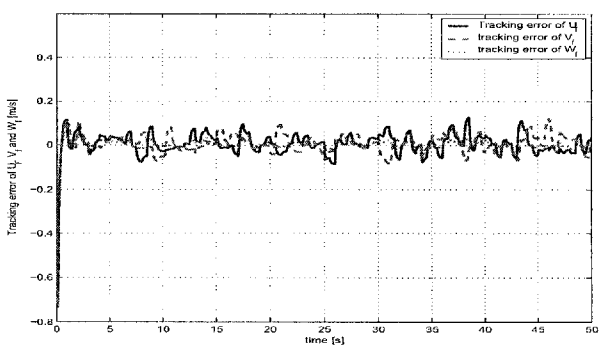

Figure 4.16: The estimation error of wave velocities in earth-fixed frame in surge, sway and heave directions

4.3 Output Feedback Control via Separation Principle

4.3.1 Model Simplification

In station keeping case, the relative speed of the vessel to the water is very small. As a consequence, the following simplification is valid for the AUV's 6 degree of freedom model under the assumption of the low relative velocity [101]. The effect of the Coriolis and centripetal term can be neglected, $C(\nu_r)\nu_r \approx 0$. The linear part of the damping will be dominating one, whereas high order terms can be neglected, $D(\nu_r)\nu_r \approx D\nu_r$ i.e., where D is a constant positive definite matrix. The dynamic model (2.62) can be simplified as

$$\begin{aligned} \dot{\eta}_0 &= A_0\eta_0 + B_0 J(\eta_2)\nu_r \\ M\dot{\nu}_r &= \tau - D\nu_r - g(\eta) \\ y &= C_0\eta_0 \end{aligned} \tag{4.84}$$

where $\eta_0 = [\ \xi^T \quad \eta^T\ ]^T$, $A_0 = \begin{bmatrix} \Omega & 0 \\ \Gamma & 0 \end{bmatrix}$, $\Omega = \begin{bmatrix} 0 & I \\ \Omega_{21} & \Omega_{22} \end{bmatrix}$, $\Gamma = \begin{bmatrix} 0 & I \\ 0 & 0 \end{bmatrix}$, $B_0 = \begin{bmatrix} 0 \\ I \end{bmatrix}$, and $C_0 = [0 \quad I]$.

4.3.2 Nonlinear Observer Design

In practice situation, not all the states will be available for measurement and thus observers are needed for state estimation. Here we briefly present the main result in previous chapter, which will be used in the subsequent development of an output feedback controller.

Consider the observer as follows:

$$\dot{\hat{\eta}}_0 = A_0\hat{\eta}_0 + B_0 J(\eta_2)\hat{\nu}_r + K\tilde{y} \tag{4.85}$$

$$\hat{y} = C_0\hat{\eta}_0 \tag{4.86}$$

$$M\dot{\hat{\nu}}_r = \tau - D\hat{\nu}_r - g(\eta_2) + J^T(\eta_2)K_3\tilde{y} \tag{4.87}$$

Here $\hat{\nu}_r$ and $\hat{\eta}_0$ are the estimates of ν_r and η_0, respectively, and $\tilde{y} = y - \hat{y}$ is the output estimation error. $K = \begin{bmatrix} K_1 \\ K_2 \end{bmatrix}$ with $K_1 \in \mathcal{R}^{6\times 6}$, $K_2 \in \mathcal{R}^{6\times 6}$, and $K_3 \in \mathcal{R}^{6\times 6}$ are the observer gain matrices.

The estimation error vectors are defined as $\tilde{\nu}_r = \nu_r - \hat{\nu}_r$, $\tilde{\eta}_0 = \eta_0 - \hat{\eta}_0$. So the error dynamics can be obtained by subtracting (4.85), (4.86) and (4.87) from (4.84).

$$\dot{\tilde{\eta}}_0 = A\tilde{\eta}_0 + BJ(\eta_2)\tilde{\nu}_r \tag{4.88}$$

$$\tilde{z} = C\tilde{\eta}_0 \tag{4.89}$$

$$M\dot{\tilde{\nu}}_r = -D\tilde{\nu}_r - J^T(\eta_2)\tilde{z} \tag{4.90}$$

where $A = [A_0 - KC_0]$, $B = B_0$, $C = K_3C_0$. Here we define $\varepsilon_z = -J^T(\eta_2)\tilde{z}$ and $\varepsilon_\nu = J(\eta_2)\tilde{\nu}_r$. The estimation error system (4.88)-(4.90) can be regarded as an interconnection of two passive block $\mathcal{H}_1$ and $\mathcal{H}_2$ with linear dynamics shown in Figure 4.17. In [64], this important property is exploited to design the observer and show the convergence of estimation error. Based on previous observer design technique in Chapter 3, we choose the following structures for observer gain

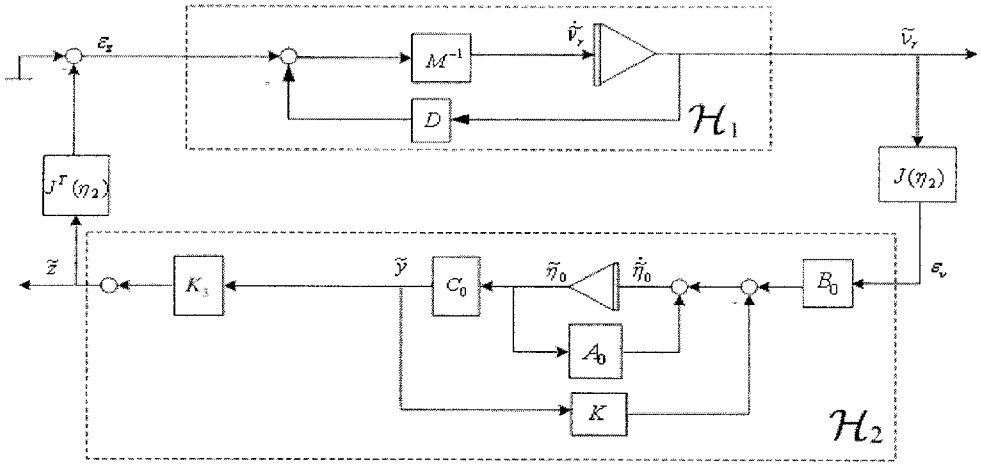

Figure 4.17: Dynamics of the position and relative velocity estimation errors.

matrices:

$$
\begin{aligned}
K_1 &= \begin{bmatrix} k_{11} & 0 & 0 & 0 & 0 & 0 \\ 0 & k_{12} & 0 & 0 & 0 & 0 \\ 0 & 0 & k_{13} & 0 & 0 & 0 \\ k_{21} & 0 & 0 & 0 & 0 & 0 \\ 0 & k_{22} & 0 & 0 & 0 & 0 \\ 0 & 0 & k_{23} & 0 & 0 & 0 \end{bmatrix} \\
K_2 &= \text{diag}\{k_{31}, k_{32}, k_{33}, k_{41}, k_{42}, k_{43}\} \\
K_3 &= \text{diag}\{k_1, k_2, k_3, k_4, k_5, k_6\},
\end{aligned}
\tag{4.91}
$$

where

$$
\begin{aligned}
k_{1i} &= 2\omega_{oi}(\zeta_{ni} - \zeta_i) \quad i = 1, 2, 3 \\
k_{2i} &= 2\omega_{oi}(\zeta_{ni}\omega_{ci} - \zeta_i k_{3i}) \quad i = 1, 2, 3 \\
k_{3i} &= 2\omega_{oi}(\zeta_{ni} - \zeta_i) + \omega_{ci} \quad i = 1, 2, 3 \\
k_{4i} &> 0 \quad i = 1, 2, 3
\end{aligned}
\tag{4.92}
$$

$$k_i > 0 \quad i = 1\ 6$$

Stability Analysis

To establish the observer convergence, we need to use the following Theorem:

Theorem 4.2 (Globally exponentially stable nonlinear observer) *Consider the AUV motion described by (4.85), the nonlinear observer (4.85)-(4.87) is globally exponentially stable if the observer gain matrices are chosen according to the structure in (4.91) with the parameters in (4.92).*

Proof With these observer gains, we can guarantee that all three decoupled observer error dynamics transfer functions can be designed to have phase greater then $-90°$. And thus the SPR requirement is satisfied. According to the Kalman-Yakubovich-Popov (KYP) lemma [54], there exist positive-definite matrices $P = P^T$ and $Q = Q^T$ such that

$$PA + A^T P = -Q, \tag{4.93}$$

$$B^T P = C \tag{4.94}$$

Consider the following Lyapunov function candidate:

$$V_{obs} = \tilde{\nu}_r^T M \tilde{\nu}_r + \tilde{\eta}_0^T P \tilde{\eta}_0 \tag{4.95}$$

Differentiation of V_{obs} along the trajectories of $\tilde{\nu}_r$ and $\tilde{\eta}_0$ in (4.88), (4.89) and (4.90) yields

$$\begin{aligned} \dot{V}_{obs} &= -2\tilde{\nu}_r^T D \tilde{\nu}_r + \tilde{\eta}_0^T (PA + A^T P)\tilde{\eta}_0 \\ &\quad +2\tilde{\nu}_r^T J^T(\eta_2) B^T P \tilde{\eta}_0 - 2\tilde{\nu}_r^T J^T(\eta_2)\tilde{z} \end{aligned} \tag{4.96}$$

Based on the definitions $C = K_3C_0$ and $B^TP = C$ and (4.89), we have $B^TP\tilde{\eta}_0 = K_3C_0\tilde{\eta}_0 = \tilde{z}$.

Application of Proposition 1 to (4.96) yields

$$\dot{V}_{obs} = -2\tilde{\nu}_r^T D\tilde{\nu}_r - \tilde{\eta_0}^T Q\tilde{\eta}_0 < 0 \tag{4.97}$$

Hence, $\tilde{\nu}_r$ and $\tilde{\eta}_0 = [\tilde{\xi}^T, \tilde{\eta}^T]^T$ converge exponentially to zero. This completes the proof of the Theorem 4.1.

4.3.3 State Feedback Control

In section 4.2, a passive observer was shown which ensures the globally exponential convergence of the estimation error. In this section we will design an output feedback controller via separation principle. We first present a state feedback controller that ensures GAS of the closed-loop system. Then we will use the estimated state instead of the true one for the state feedback control law. The stability proof the whole system is also presented.

In this part we prove that a state feedback controller globally asymptotically stabilizes the AUV system at the origin.

Theorem 4.3 (State Feedback control) Consider the AUV nonlinear model (4.84) and the control law

$$\begin{aligned} \tau^* &= g(\eta_2) - K_d(\nu_r + J^{-1}(\eta_2)\Gamma\xi) \\ &\quad -J^T K_p(\eta - \eta_d) - DJ^{-1}(\eta_2)\Gamma\xi \\ &\quad -M(\dot{J}^{-1}(\eta_2)\Gamma\xi + J^{-1}(\eta_2)\Gamma\Omega\xi) \end{aligned} \tag{4.98}$$

where K_d, K_p are positive definite controller gain matrices, then the closed-loop

system (4.84) and (4.98) is globally asymptotically stable (GAS).

Proof For station keeping in shallow water area, the AUVs must counteract the wave. We define $\bar{\nu}_r = \nu_r - \nu_{dr}, \bar{\eta} = \eta - \eta_d$, where $\nu_{dr} = -J^{-1}(\eta_2)\Gamma\xi$. The tracking error dynamics (4.84)-(4.98) is given by

$$M\dot{\bar{\nu}}_r = -(K_d + D)\bar{\nu}_r - J^T(\eta_2)K_p\bar{\eta} \tag{4.99}$$

$$\dot{\bar{\eta}} = J(\eta_2)\bar{\nu}_r \tag{4.100}$$

$$\bar{y} = \bar{\eta} \tag{4.101}$$

Consider the Lyapounov function candidate.

$$V_c = \frac{1}{2}(\bar{\nu}_r^T M\bar{\nu}_r + \bar{y}^T K_p\bar{y}) \tag{4.102}$$

which is clearly positive definite since M and K_p are positive definite matrices. Hence V_c qualifies as a Lyapunov function candidate for the closed-loop system (4.84) and (4.98). Furthermore, it is easy to verify that the time derivative of V_c along the trajectories of the closed-loop system is

$$\dot{V}_c = -\bar{\nu}_r^T(K_d + D)\bar{\nu}_r \tag{4.103}$$

The GAS of the origin $\bar{y} = 0$ follows by invoking the LaSalle's invariance principle.

4.3.4 The Separation Principle

Theorem 4.4 (GAS by Output Feedback Controller) The closed-loop system (4.84) with (4.85)-(4.87) and

$$\tau = g(\eta_2) - K_d(\hat{\nu}_r + J^{-1}(\eta_2)\Gamma\hat{\xi})$$

$$-J^T K_p(\hat{\eta} - \eta_d) - DJ^{-1}(\eta_2)\Gamma\hat{\xi} \\ -M(\dot{J}^{-1}(\eta_2)\Gamma\hat{\xi} + J^{-1}(\eta_2)\Gamma\Omega\hat{\xi}) \tag{4.104}$$

is GAS under the conditions of Theorem 4.2 and Theorem 4.3.

The proof will be shown in 2 steps. Firstly, we prove that a separation principle holds for the closed-loop system, for this we show that the estimation and tracking error dynamics can be decoupled yielding a cascaded system. Then we invoke a recent result from [71] on Lyapunov stability of cascaded nonlinear systems, which is detailed in Appendix B, for the stability proof of the closed-loop system.

At this point, we find it convenient to present the observation error-dynamics (4.88)-(4.90) in the state-space form

$$\begin{bmatrix} \dot{\tilde{\nu}}_r \\ \dot{\tilde{\xi}} \\ \dot{\tilde{\eta}} \end{bmatrix} = A_o \cdot \begin{bmatrix} \tilde{\nu}_r \\ \tilde{\xi} \\ \tilde{\eta} \end{bmatrix} \tag{4.105}$$

where

$$A_o = \begin{bmatrix} -M^{-1}D & 0 & -M^{-1}J^T(\eta_2)K_3 \\ 0 & \Omega & -K_1 \\ J(\eta_2) & \Gamma & -K_2 \end{bmatrix} \tag{4.106}$$

Define the observation and tracking error as $x_2 \triangleq \begin{bmatrix} \tilde{\nu}_r & \tilde{\xi} & \tilde{\eta} \end{bmatrix}^T$ and $x_1 \triangleq \begin{bmatrix} \bar{\nu}_r & \bar{\eta} \end{bmatrix}^T$, respectively, then we write the estimation error (4.88)-(4.90) and the tracking error dynamics (4.99)-(4.101), respectively, as $\dot{x}_2 \triangleq A_o(x_1)x_2$ in (4.105) and $\dot{x}_1 \triangleq A_c(x_1)x_1$ in (4.107)

$$\begin{bmatrix} \dot{\bar{\nu}}_r \\ \dot{\bar{\eta}} \end{bmatrix} = \begin{bmatrix} -M^{-1}(D + K_d) & -M^{-1}J^T(\eta_2)K_p \\ J(\eta_2) & 0 \end{bmatrix} \begin{bmatrix} \bar{\nu}_r \\ \bar{\eta} \end{bmatrix} \tag{4.107}$$

Notice that the control input (4.104) can be rewritten as $\tau = \tau^* + h(x_1)x_2$ with

$$\begin{aligned} h(x_1)x_2 &= K_d(\tilde{\nu}_r + J^{-1}(\eta_2)\Gamma\tilde{\xi}) \\ &\quad + J^T K_p\tilde{\eta} + DJ^{-1}(\eta_2)\Gamma\tilde{\xi} \\ &\quad + M(\dot{J}^{-1}(\eta_2)\Gamma\tilde{\xi} + J^{-1}(\eta_2)\Gamma\Omega\tilde{\xi}) \end{aligned} \tag{4.108}$$

Since the rotational angle η_2 is actually from $\bar{\eta} = \eta - \eta_d$, the system (4.84) in the closed-loop with (4.85)-(4.87) and (4.104) can be rewritten in the form

$$\Sigma_1' : \dot{x}_1 = A_c(x_1)x_1 + h(x_1)x_2 \tag{4.109}$$

$$\Sigma_2' : \dot{x}_2 = A_o(x_1)x_2 \tag{4.110}$$

which matches the cascaded form (B.1) and (B.2) in the appendix. The dynamics of Σ_2' is not decoupled from that of Σ_1' due to the presence of $J(\eta_2)$ in the matrix $A_o(x_1)$. To consider systems Σ_1', Σ_2' as a cascade we must prove that the system (4.109) and (4.110) is complete. That means the solutions $(x_1(t), x_2(t))$ can be continued for all $t \geq 0$. This allows us to consider $A_o(x_1)$ as a time-varying matrix $A_o(t) \triangleq A_o(x_1(t))$, that is we regard the AUV-observer system as a time-varying system dependent on the position error trajectories $x_1(t)$. Notice that $A_o(x_1)$ depends only on the rotational angle η_2. With an abuse of notation in the sequel we will write $A_o(t)$ instead of $A_o(x_1(t))$.

4.3.5 Completeness of Closed-Loop System

To prove the completeness of system (4.109) and (4.110), consider the Lyapunov function candidate

$$V(x) = \frac{1}{2}x_1^T P_c x_1 + \frac{1}{2}x_2^T P_o x_2 \tag{4.111}$$

where P_o is positive definite and $P_c \triangleq$block-diag$\{M, K_p\}$. Based on Theorem 4.1 and Theorem 4.2, the derivative of $V(x)$ along the closed-loop system trajectories is

$$\dot{V} = -x_1^T Q_c x_1 - x_2^T Q_o x_2 + x_1^T P_c h(x_1) x_2 \tag{4.112}$$

where Q_o is positive definite and we used (4.103) to define $Q_c \triangleq$block-diag$\{(D + K_d), 0\}$. Notice that there exists $\delta > 0$ such that $\|h(x_1)\| \leq \delta$ for all x_1 hence, since the first two terms on the right-hand side of (4.112) are negative we can write

$$\dot{V}(x) \leq p_{cM}\delta\|x_1\|\|x_2\| \tag{4.113}$$

where $p_{cM} < \infty$ is the largest eigenvalue of P_c. Using the Shwartz inequality we have that

$$\dot{V}(x(t)) \leq p_{cM}\delta\|x_1\|\|x_2\| \leq \frac{1}{2}p_{cM}\delta(\|x_1\|^2 + \|x_2\|^2) \tag{4.114}$$

From this it is clear that there also exists a constant c_1 such that $\dot{V}(x(t)) \leq c_1 V(x(t))$. It follows using the comparison equations method that there exist constant c_1, c_2 such that $V(t) \leq c_1 V(0)e^{c_2 t}$ that is, $V(t)$ is bounded for all t and since $V(x)$ is positive definite we obtain that the solutions $x(t)$ exist and can be continued for all $t \geq 0$.

4.3.6 Stability Analysis of Closed-Loop System

A key observation to this point is that the observer error dynamics is globally exponentially stable, uniformly in the tracking error trajectories $x_1(t)$. That is, even through system dynamics Σ_2' depends also on x_1 (specifically on the rotational angle η_2) the estimation error trajectories $x_2(t)$ tend to zero exponentially for any

trajectories $x_1(t)$. Second, we have proven that the solutions of the closed-loop system can be continued for all $t \geq 0$ thus the system Σ_2' can be written as

$$\Sigma_2' : \dot{x}_2 = A_o(x_1(t))x_2 \tag{4.115}$$

or simply

$$\Sigma_2' : \dot{x}_2 = A_o(t)x_2 \tag{4.116}$$

which, under the conditions of Theorem 4.2, is GES since $A_o(t)$ is Hurwitz for all $x_1(t)$, that is for all $t \geq 0$.

The stability proof is completed by observing that the system (4.109), (4.116) has a cascaded structure, hence we can invoke the Theorem B.1 in Appendix B and show that the cascaded closed-loop system (4.109), (4.116) satisfies the conditions of this theorem under the following assumptions.

Assumption 1: A constant c_1 that satisfies (B.3) is easily computed noticing

$$\left\| \frac{\partial V}{\partial x_1} \right\| \|x_1\| = max\{m_M, K_{pM}\}\|x_1\|^2 \tag{4.117}$$

where $m_M = \lambda_{max}(M)$ and $K_{pM} = \lambda_{max}(K_p)$, then it is easy to see that if c_1 satisfies

$$c_1 \geq \frac{max\{m_M, K_{pM}\}}{min\{m_m, K_{pm}\}} \tag{4.118}$$

where $m_m = \lambda_{min}(M)$ and $K_{pm} = \lambda_{min}(K_p)$, then the inequality (B.3) holds. Also from (4.117) it is clear that the inequality (B.4) is satisfied with $c_2 = max\{m_M, K_{pM}\}\mu$.

Assumption 2: On the growth rate on the tracking error x_1 is satisfied by choosing $\theta_1 \equiv$const, and $\theta_2 \equiv 0$.

Assumption 3: Holds since the observer-error dynamics is globally exponentially stable, uniformly in the tracking error $x_1(t)$, That is there exist positive constant λ_1 and λ_2 which depend on the initial conditions $x_1(t_0)$, such that $\|x_2(t)\| \leq \lambda_1\|x_2(t_0)\|e^{-\lambda_2(t-t_0)}$ and therefore we can take $\phi(\|x_2(t_0)\|) = (\lambda_1/\lambda_2)\|x_2(t_0)\|$

Thus, by invoking Theorem B.1, the global asymptotic stability (GAS) of system (4.84) in the closed-loop with (4.85)-(4.87) and (4.104) follows. This result will therefore guarantee that the estimation and the position error dynamics can be analyzed separately and therefore, that the observer and controller can be designed independently.

4.3.7 Simulation Results

To demonstrate the performance of the proposed observer and controller, simulation study is carried out based on the AUV model of the vehicle KAMBARA [94]. The AUV dynamics is described by (4.84) with the parameter values given in Appendix A.

The wave model parameters are chosen as $\zeta_i = 0.1$ and $\omega_i = 0.6283$ (i=1-3) corresponding to a wave period of 10s in surge, sway and heave. The amplitude of wave velocity relative to earth-fixed frame in surge, sway and heave are limited to 0.4m/s, 0.4m/s and 0.1m/s, respectively. The notch filter parameters are chosen as $\zeta_{ni} = 20$ and $\omega_i = 10$. From (4.92), we choose

$$\begin{aligned} K_1 &= \begin{bmatrix} 25.006 I_{3\times3} & 0 \\ 246.9211 I_{3\times3} & 0 \end{bmatrix} \\ K_2 &= \begin{bmatrix} 35.0063 I_{3\times3} & 0 \\ 0 & I_{3\times3} \end{bmatrix} \\ K_3 &= I_{6\times6} \end{aligned} \tag{4.119}$$

as numerical values for the observer.

The values for the controller are chosen as

$$K_d = 1000 I_{6\times 6},\ K_p = 2000 I_{6\times 6} \tag{4.120}$$

In the simulation study, we use the output feedback controller to achieve the station keeping. The initial position is $\eta = [2, 2, 5.5, 0.15, 0.15, 0.15]^T$ and $U_f = [0.1, 0.1, 0.1]^T$. The initial condition for the observer is $\hat{\eta} = [1.5, 1.5, 5, 0.1, 0.1, 0.1]^T$ and $\hat{U}_f = [0.2, 0.2, 0.05]^T$. The desired position of the vehicle is $\eta_d = [0.5, 1, 3, 0, 0, 0]^T$. The simulation results are shown in Figures 4.18-4.30.

Figures 4.18, 4.19 and 4.20 show the desired, actual and estimated position in surge, sway and heave directions. We can see that AUV can keep at one position with great accuracy by counteracting the wave disturbances in these directions. Figures 4.21, 4.22 and 4.23 show the actual, desired heading angles in roll, pitch and yaw. We can see that position and heading angle converge to the desired one exponentially. The actual and estimated relative velocities in surge, sway and heave directions are shown in 4.24, 4.25 and 4.26. The first-order wave velocities in surge, sway and heave directions and their estimates are shown in 4.27, 4.28 and 4.29. The exponential convergence of the wave disturbance estimation errors can be seen from Figure 4.30. We can see that the stochastic behavior of the wave disturbance is estimated as well even though the original wave model is driven by the zero mean white noise.

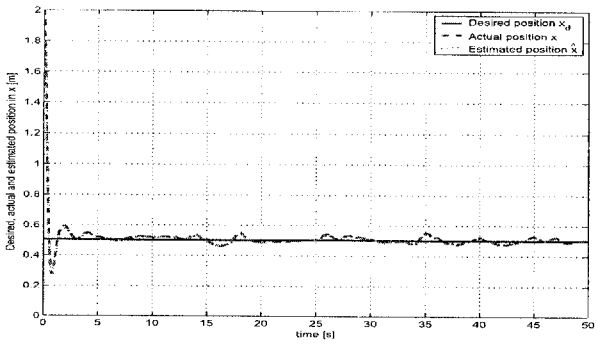

Figure 4.18: The desired, actual, and estimated position in surge

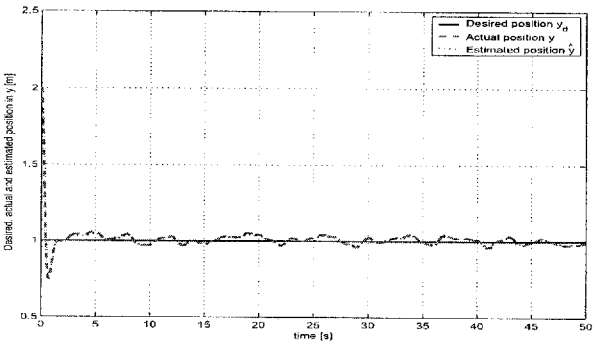

Figure 4.19: The desired, actual, and estimated position in sway

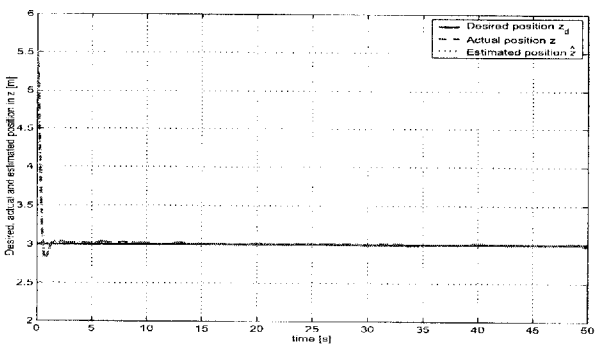

Figure 4.20: The desired, actual, and estimated position in heave

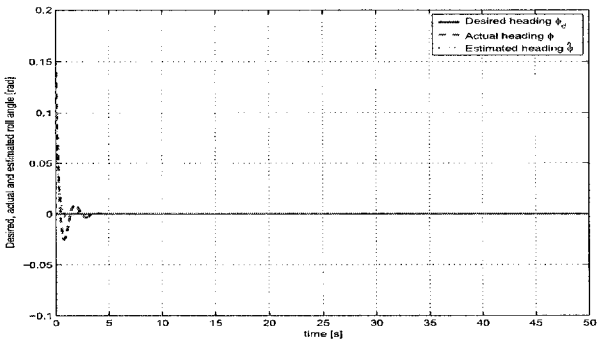

Figure 4.21: The desired, actual and estimated heading angle in roll

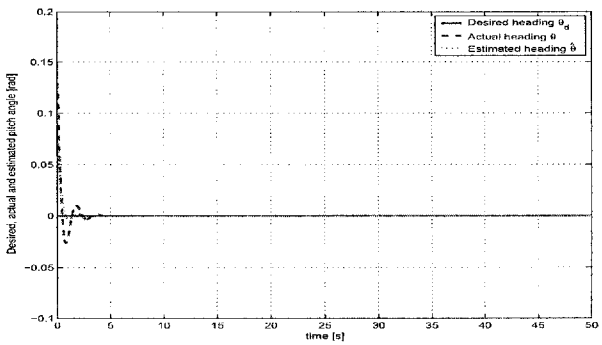

Figure 4.22: The desired, actual and estimated heading angle in pitch

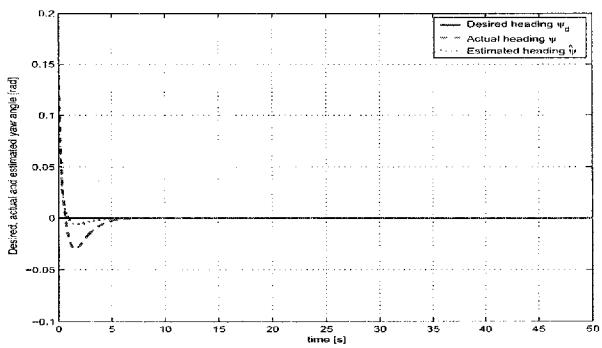

Figure 4.23: The desired, actual and estimated heading angle in yaw

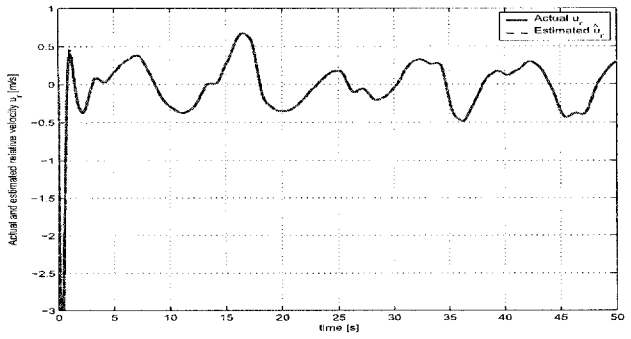

Figure 4.24: The actual relative velocity and its estimate in surge

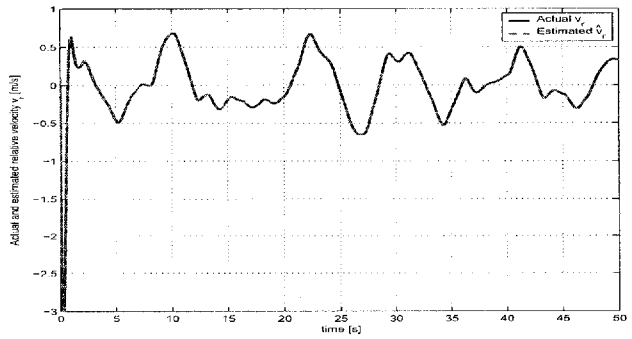

Figure 4.25: The actual relative velocity and its estimate in sway

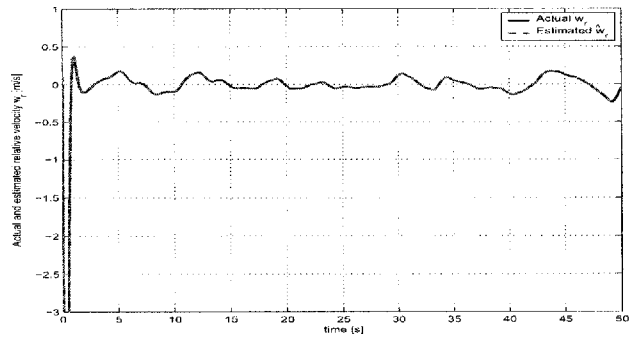

Figure 4.26: The actual relative velocity and its estimate in heave

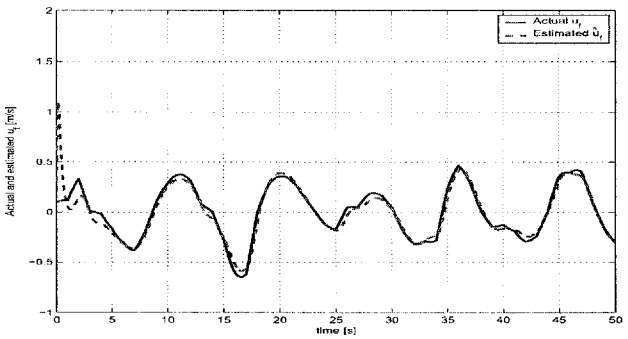

Figure 4.27: The actual wave velocity and its estimate in surge

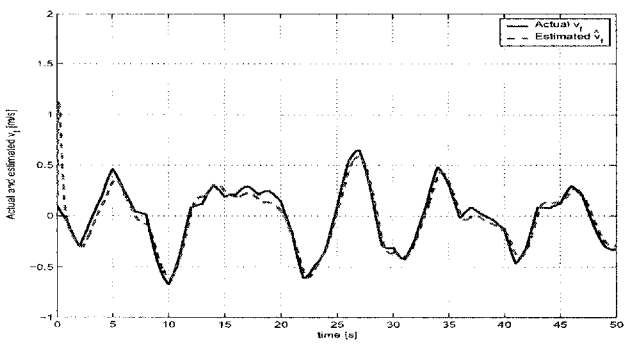

Figure 4.28: The actual wave velocity and its estimate in sway

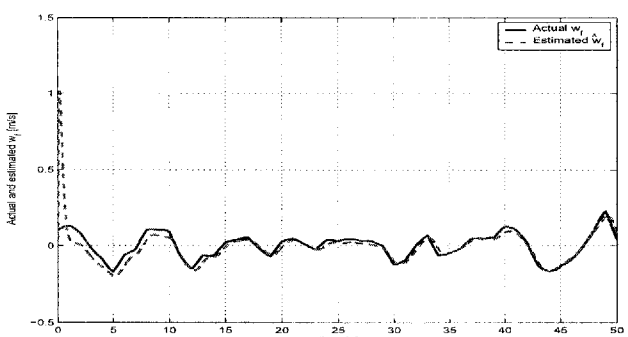

Figure 4.29: The actual wave velocity and its estimate in heave

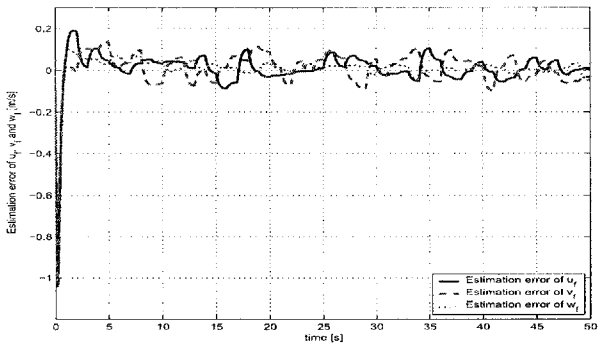

Figure 4.30: The estimation error of wave velocities in earth-fixed frame in surge, sway and heave directions

4.4 Conclusion

The nonlinear observer design in previous chapter is extended for station keeping control. The new observer can estimated the wave velocities and relative velocities based on the position and attitude measurement. Compared with other techniques, wave sensors are not needed for wave disturbance estimation. The relative velocities of AUV and the wave velocities in the earth-fixed frame are well estimated with exponential convergence. With the given nonlinear observer, backstepping is applied to a new system, in which the equations of unmeasured states have been replaced by the corresponding equations of their estimates from the observer. At each step of the procedure, observation errors are treated as disturbances and accounted for using nonlinear damping. The nonlinear output feedback controller is shown to maintain the AUV at fixed position by effectively counteracting high frequency wave disturbance. Convergence of the resulting nonlinear system was analyzed and simulations were performed to illustrate the behaviour of the proposed control scheme. Simulation results show that the control objectives were achieved successfully.

With a simplified model where station keeping vehicles hold, we designed another simple observer. The observer produces noise-free estimates of the position, the relative velocities and wave velocities which are used in a proportional- derivative

(PD) controller. The stability proof is based on a separation principle which holds for this simplified model. This separation principle is theoretically supported by recent results on cascaded nonlinear systems and standard Lyapunov theory.

Chapter 5

Dynamic Positioning Control Design

5.1 Introduction

Dynamic positioning systems have been designed and used primarily for drilling vessels and platforms and for support vessels in offshore oil industry since early 1960's. The first DP systems were designed using a notch filter and a conventional PID control [74]. The notch filter was used to remove sea wave components on the positioning measurements. The essence of the DP systems is to control the average position of the vessel, but to allow the vessel to move with the oscillatory components in the waves [34]. It is a compromise method between precise position control and energy efficiency. The thrust and rudder devices are not usually designed for counteracting the sea wave forces. If the filtering action is poor the thrusters will vary their outputs with the wave action and this causes energy wastage and wear and tear on the thrusters. This phenomenon is called thruster modulation.

Compared with station keeping problem in Chapter 4 which require absolutely fixed position by counteracting high frequency wave disturbance without concern-

ing energy issue, DP uses available control devices (such as rudder, propeller and vector thrusters) to keep the vessel to the desired position and concerning the energy efficiency problems by just counteracting the low frequency environmental forces [33, 34, 9, 98]. The control loops for dynamic positioning vessels include filters to remove the wave motion signals. The position control must only respond to the low frequency forces acting on the vessel. The filtering problems is to estimate the low frequency motions and filter out the high frequency motions due to wave so that the control can be designed. Even though the total position of the vessel was known exactly there would still be a need to estimate the low frequency motion and filter out the wave disturbance.

The second generation DP systems was later implemented using the LQ control strategy combined with Kalman filters [9]. Adaptive control [36] and robust control [51] were also introduced to deal with this problems by Grimble *et al.*. A linear LQG based controller [98] and a nonlinear PID controller [99] were designed by Sørensen et by Sørensen *et al.*. Grøvlen and Fossen [40] presented a uniform global asymptotical stability (UGAS) of a DP system (ship model, observer and control law) was proven by using observer backstepping. The results of this paper was extended and proved the GES of a DP system in [30] by using vectorial backstepping technique. These papers can be regarded as the first attempt to design a fully nonlinear DP-control system. Since wave filtering and bias estimation were not included, an UGES observer with wave filtering capabilities and bias estimation was designed using passivity by Fossen and Strand [33]. An extension of this observer with adaptive wave filtering was proposed in [102]. By using the separation principle of Panteley and Loria [85], the same observer in [33] was used with a PD-type control law and proved to be uniform globall asymptotically stabile (UGAS) for observer-controller systems for DP application by Loria *et al.* [71]. More recently, This result has been extended to the case where velocity and acceleration measurement are available and used for DP system [62].

The dynamic positioning system is mainly used in surface vessels or floating plat-

form. There is a rather rare application of DP systems for small AUVs. But it is actually very useful for mine countermeasure (MCM) application to save the energy and avoid wear and tear on thrusters.

In this chapter, we first introduce the dynamic model of AUVs for dynamic positioning (DP) in shallow water environment. Then based on the previous observer design method, we design a similar nonlinear observer to estimate the LF motion states and filter out wave disturbances. Similar to previous chapter, we propose an output feedback controller on observer backstepping technique in [56]. Simulation results that illustrate the performance of the control laws derived are also included. Finally, the chapter closes with some concluding remarks.

5.2 Formulation of Dynamic Positioning

The mathematical model of an AUV with 6DOF considering the influence of wave disturbances, Equation (2.67), has been presented in Chapter 2.

The essence of the DP problem is to control the average position of the vessel, but allow the vessel to move with the oscillatory components in the waves. In this case, the speed of the vehicle is very small. As a consequence, the following simplification is valid for the AUV's 6 degree of freedom model under the assumption of the low velocity [101]. The effect of the Coriolis and centripetal term can be neglected, $C(\nu)\nu \approx 0$. The linear part of the damping will be dominating one, whereas high order terms can be neglected, $D(\nu)\nu \approx D\nu$ i.e., where D is a constant positive definite matrix.

$$\begin{bmatrix} \dot{\xi}_1 \\ \dot{\xi}_2 \end{bmatrix} = \begin{bmatrix} 0 & I \\ \Omega_{21} & \Omega_{22} \end{bmatrix} \begin{bmatrix} \xi_1 \\ \xi_2 \end{bmatrix} + \begin{bmatrix} 0 \\ \Psi_1 \end{bmatrix} n_1$$

$$\begin{aligned} \eta_f &= \begin{bmatrix} 0 & I \\ 0 & 0 \end{bmatrix} \begin{bmatrix} \xi_1 \\ \xi_2 \end{bmatrix} = \Gamma\xi \\ y &= J(\eta)\nu + \eta_f = \eta + \eta_f \\ M\dot{\nu} &= \tau - D\nu - g(\eta) \end{aligned} \tag{5.1}$$

where $\eta_0 = [\ \xi^T \quad \eta^T\ ]^T$, $A_0 = \begin{bmatrix} \Omega & 0 \\ 0 & 0 \end{bmatrix}$, $\Omega = \begin{bmatrix} 0 & I \\ \Omega_{21} & \Omega_{22} \end{bmatrix}$, $B_0 = \begin{bmatrix} 0 \\ I \end{bmatrix}$, and $C_0 = [\Gamma \quad I]$.

In this chapter, we will design an output feedback controller $\tau = \tau(\hat{\nu}, \hat{\eta})$ without counteracting the wave disturbance to avoid the wear and tear on the actuators, where $(\hat{\nu}, \hat{\eta})$ is the estimate of the true states (ν, η), such that

$$\lim_{t\to\infty} \eta(t) = \eta_d \tag{5.2}$$

where η_d is the desired position and orientation vector.

5.3 Nonlinear Observer Design

Based on the results in Chapter 3, we briefly present the main result in previous chapter to estimate the unmeasurable states and filter out the wave frequency motion, which will be used in the subsequent development of an output feedback controller.

Consider the observer as follows:

$$\dot{\hat{\eta}}_0 = A_0\hat{\eta}_0 + B_0 J(\eta_2)\hat{\nu} + K\tilde{y} \tag{5.3}$$

$$\hat{y} = C_0\hat{\eta}_0 \tag{5.4}$$

$$M\dot{\hat{\nu}} = \tau - D\hat{\nu} - g(\eta_2) + J^T(\eta_2)K_3\tilde{y} \tag{5.5}$$

Here $\hat{\nu}$ and $\hat{\eta}_0$ are the estimates of ν and η_0, respectively, and $\tilde{y} = y - \hat{y}$ is the output estimation error. $K = \begin{bmatrix} K_1 \\ K_2 \end{bmatrix}$ with $K_1 \in \mathcal{R}^{6\times 6}$, $K_2 \in \mathcal{R}^{6\times 6}$, and $K_3 \in \mathcal{R}^{6\times 6}$ are the observer gain matrices.

The estimation error vectors are defined as $\tilde{\nu} = \nu - \hat{\nu}$, $\tilde{\eta}_0 = \eta_0 - \hat{\eta}_0$. So the error dynamics can be obtained by subtracting (5.3), (5.4) and (5.5) from (5.1).

$$\dot{\tilde{\eta}}_0 = A\tilde{\eta}_0 + BJ(\eta_2)\tilde{\nu} \tag{5.6}$$

$$\tilde{z} = C\tilde{\eta}_0 \tag{5.7}$$

$$M\dot{\tilde{\nu}} = -D\tilde{\nu} - J^T(\eta_2)\tilde{z} \tag{5.8}$$

where $A = [A_0 - KC_0]$, $B = B_0$, $C = K_3C_0$. Here we define $\varepsilon_z = -J^T(\eta_2)\tilde{z}$ and $\varepsilon_\nu = J(\eta_2)\tilde{\nu}$. The estimation error system (5.6)-(5.8) can be regarded as an interconnection of two passive block $\mathcal{H}_1$ and $\mathcal{H}_2$ with linear dynamics shown in Figure 5.1. In [64], this important property is exploited to design the observer and show the convergence of estimation error.

Proposition 5.1 (SPR velocity estimation error) *If the gain matrices in the observer (5.3), (5.4) and (5.5) are chosen with the following structures as follows:*

$$K_1 = \begin{bmatrix} k_{11} & 0 & 0 & 0 & 0 & 0 \\ 0 & k_{12} & 0 & 0 & 0 & 0 \\ 0 & 0 & k_{13} & 0 & 0 & 0 \\ k_{21} & 0 & 0 & 0 & 0 & 0 \\ 0 & k_{22} & 0 & 0 & 0 & 0 \\ 0 & 0 & k_{23} & 0 & 0 & 0 \end{bmatrix}$$

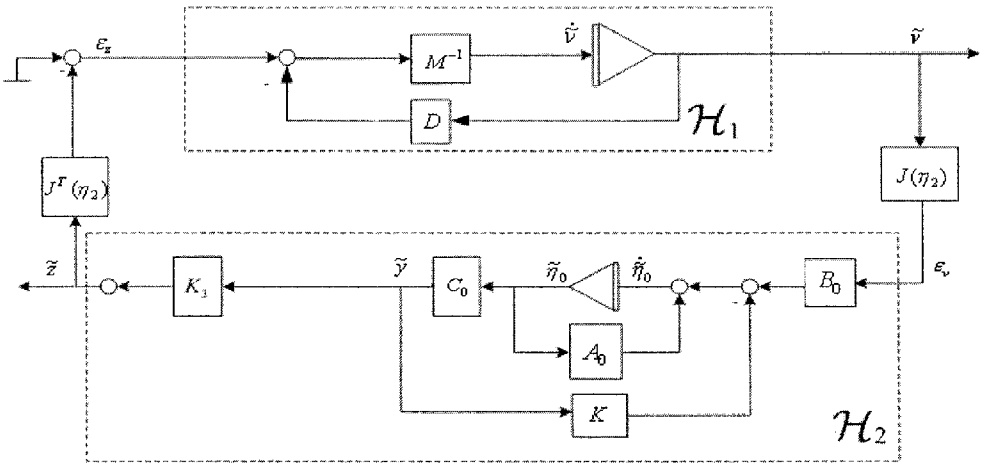

Figure 5.1: Dynamics of the LF position and velocity estimation errors.

$$
\begin{aligned}
K_2 &= diag\{k_{31}, k_{32}, k_{33}, k_{41}, k_{42}, k_{43}\} \\
K_3 &= diag\{k_1, k_2, k_3, k_4, k_5, k_6\},
\end{aligned}
\tag{5.9}
$$

with

$$
\begin{aligned}
k_{1i} &= -2\omega_{ci}(\zeta_{ni} - \zeta_i)\frac{1}{\omega_{oi}} \\
k_{2i} &= 2\omega_{oi}(\zeta_{ni} - \zeta_i) \\
k_{3i} &= \omega_{ci} \\
\zeta_{ni} &> \zeta_i;\ \omega_{ci} > \omega_{oi};\ K_3, k_{4i} > 0\ (i = 1, 2, 3)
\end{aligned}
\tag{5.10}
$$

then the mapping $\varepsilon_\nu \mapsto \tilde{z}$ in Figure 5.1 is strictly passive, that is its dynamics satisfies the Kalman-Yakubovich-Popov lemma [54].

Theorem 5.1 (Globally exponentially stable nonlinear observer) *Consider the AUV motion described by (5.1), the nonlinear observer (5.3)-(5.5) is globally exponentially stable in the sense of $\hat{\nu} \to \nu$ and $\hat{\eta}_0 \to \eta_0$ as $t \to \infty$.*

5.4 Output Feedback Control via Backstepping Technique

Here we present an output feedback controller which makes the overall observer-controller system stable by using observer backstepping technique in [56]. Backstepping makes use of a recursive procedure that breaks down the control problem for the full system into a sequence of designs for lower order systems [56, 54]. The observer backstepping method in this section is based on the work of Aarset *et al.* [2], which is an extension of the results in Fossen and Grøvlen [30]. The results in [2, 30] focused on dynamic positioning control of ships in horizontal plane which concerned energy efficiency problem. In this section, the observer backstepping control technique is used for dynamic positioning of an AUV in 3D space without counteracting the high frequency wave disturbance.

5.4.1 Observer Backstepping Controller Design

Step 1 Since we can only measure the position and heading angle, we need to use the estimated states for control purposes. The previous observer design can guarantee observer error $\tilde{\eta}$, $\tilde{\eta}_f$ and $\tilde{\nu}$ converge to zero exponentially. So $\hat{\eta} - \eta_d$ will be used for observer backstepping design.

Define the error variable z_1 as

$$z_1 = \hat{\eta} - \eta_d + K_I \int_0^t (\hat{\eta} - \eta_d) d\tau = \dot{e}_I + K_I e_I \tag{5.11}$$

where $K_I > 0$ is the diagonal integration gain matrix used to eliminate steady state errors and $\dot{e}_I = \hat{\eta} - \eta_d$. Using Equations (5.3) and (5.5) in the observer design, we obtain the following expression by differentiating (5.11)

$$\dot{z}_1 = J(\eta_2)\hat{\nu} + K_2\tilde{y} - \dot{\eta}_d + K_I(\hat{\eta} - \eta_d) \tag{5.12}$$

The virtual control vector is chosen as $\gamma_1 = J(\eta_2)\hat{\nu} = z_2 + \beta_1$ with the stabilizing function $\beta_1 = -(E_1 + F_1)z_1 + \dot{\eta}_d - K_I(\hat{\eta} - \eta_d)$.

So Equation (5.12) results in

$$\dot{z}_1 = -(E_1 + F_1)z_1 + z_2 + K_2\tilde{y} \tag{5.13}$$

where E_1 is a strictly positive diagonal feedback design matrix expressed as $E_1 = \text{diag}\{e_1, e_2, e_3, e_4, e_5, e_6\}$ and F_1 is a strictly positive diagonal damping matrix defined as:

$$F_1 = \text{diag}\{e_1 k_{21}^2, e_2 k_{22}^2, e_3 k_{23}^2, e_4 k_{24}^2, e_5 k_{25}^2, e_6 k_{26}^2\} \tag{5.14}$$

The damping term $-F_1 z_1$ is used to compensate the disturbance like term $K_2\tilde{y}$.

Step 2 From previous definition, z_2 can be expressed as

$$z_2 = \gamma_1 - \beta_1 = J(\eta_2)\hat{\nu} + (E_1 + F_1)z_1 - \dot{\eta}_d + K_I(\hat{\eta} - \eta_d) \tag{5.15}$$

Time differentiation of z_2 is:

$$\begin{aligned}
\dot{z}_2 &= \dot{\gamma}_1 - \dot{\beta}_1 \\
&= \dot{J}(\eta_2)\hat{\nu} + J(\eta_2)\dot{\hat{\nu}} \\
&\quad +(E_1 + F_1)\dot{z}_1 - \ddot{\eta}_d + K_I(\dot{\hat{\eta}} - \dot{\eta}_d) \\
&= \dot{J}(\eta_2)\hat{\nu} + J(\eta_2)M^{-1}(\tau - D\hat{\nu} - g(\eta_2) + J^T(\eta_2)K_3\tilde{y}) \\
&\quad -(E_1 + F_1)^2 z_1 + (E_1 + F_1)z_2 + (E_1 + F_1)K_2\tilde{y} \\
&\quad -\ddot{\eta}_d + K_I(J(\eta_2)\hat{\nu} + K_2\tilde{y} - \dot{\eta}_d)
\end{aligned} \tag{5.16}$$

By defining Λ as

$$\begin{aligned}\Lambda &= \dot{J}(\eta_2)\hat{\nu} + J(\eta_2)M^{-1}(-D\hat{\nu} - g(\eta_2) + J^T(\eta_2)K_3\tilde{y}) \\ &\quad -(E_1+F_1)^2 z_1 + (E_1+F_1)z_2 \\ &\quad -\ddot{\eta}_d + K_I(J(\eta_2)\hat{\nu} - \dot{\eta}_d)\end{aligned} \tag{5.17}$$

Equation (4.54) can be written as

$$\begin{aligned}\dot{z}_2 &= J_1(\eta_2)M_1^{-1}\tau_1 + \Lambda \\ &\quad +((E_1+F_1)K_2 + K_I K_2)\tilde{y}\end{aligned} \tag{5.18}$$

Because all the terms in $(E_1+F_1)K_2 + K_I K_2$ is diagonal matrix, we define a term $\Theta = (E_1+F_1)K_2 + K_I K_2$ as

$$\Theta = \text{diag}\{\theta_1, \theta_2, \theta_3, \theta_4, \theta_5, \theta_6\} \tag{5.19}$$

The following choice of feedback controller is made

$$\tau_1 = -M_1 J_1^{-1}(\eta_1)(\Lambda + (E_2+F_2)z_2 + z_1) \tag{5.20}$$

where E_2 is a strictly positive feedback design matrix usually chosen to be diagonal and expressed as $E_2 = \text{diag}\{e_1, e_2, e_3, e_4, e_5, e_6\}$. The F_2 is a strictly positive diagonal damping matrix. The damping term $-F_2 z_2$ is used to compensate the disturbance like term $\Theta\tilde{y}$.

So the resulting z_2-error dynamics is

$$\dot{z}_2 = -(E_2+F_2)z_2 - z_1 + \Theta\tilde{y}. \tag{5.21}$$

The strictly positive diagonal damping matrix F_2 is defined as

$$F_2 = \text{diag}\{e_1\theta_1^2, e_2\theta_2^2, e_3\theta_3^2, e_4\theta_4^2, e_5\theta_5^2, e_6\theta_6^2\} \tag{5.22}$$

By combining Equations (5.6)-(5.8), (5.13) and (5.21), the resulting error dynamics of the whole system can be written as

$$\dot{z} = -(E_z + F_z)z + Ez + W\tilde{y} \tag{5.23}$$

$$\dot{\tilde{\eta}}_0 = A\tilde{\eta}_0 + BJ(\eta_2)\tilde{\nu} \tag{5.24}$$

$$M\dot{\tilde{\nu}} = -D\tilde{\nu} - J(\eta_2)C\tilde{\eta}_0 \tag{5.25}$$

where $z = [z_1^T, z_2^T]^T$ and $E_z = \begin{bmatrix} E_1 & 0 \\ 0 & E_2 \end{bmatrix}$, $F_z = \begin{bmatrix} F_1 & 0 \\ 0 & F_2 \end{bmatrix}$, $E = \begin{bmatrix} 0 & 1 \\ -1 & 0 \end{bmatrix}$, $W = \begin{bmatrix} K_2 \\ \Theta \end{bmatrix}$.

5.4.2 Stability Analysis

A Lyapunov function candidate for the control law is

$$V_{con} = \frac{1}{2}z^T z + e_I^T K_I E_1 e_I. \tag{5.26}$$

So the Lyapunov function candidate for the whole system is

$$\begin{aligned} V &= V_{con} + V_{obs} \\ &= \frac{1}{2}z^T z + e_I^T K_I E_1 e_I + \tilde{\nu}^T M\tilde{\nu} + \tilde{\eta}_0^T P\tilde{\eta}_0. \end{aligned} \tag{5.27}$$

The time derivation of Equation (5.27) is

$$\begin{aligned}\dot{V} &= \dot{V}_{con} + \dot{V}_{obs} \\ &= z^T\dot{z} + 2e_I^T K_I E_1 \dot{e}_I - 2\tilde{\nu}^T D\tilde{\nu} - \tilde{\eta}_0^T Q\tilde{\eta}_0 \\ &= -z_1^T E_1 z_1 - z_1^T F_1 z_1 + z_1^T K_2 \tilde{y} \\ &\quad -z_2^T E_2 z_2 - z_2^T F_2 z_2 + z_2^T \Theta\tilde{y} \\ &\quad +2e_{1I}^T K_I E_1 \dot{e}_{1I} - 2\tilde{\nu}^T D\tilde{\nu} - \tilde{\eta}_0^T Q\tilde{\eta}_0\end{aligned} \tag{5.28}$$

Adding the following zero terms

$$\begin{aligned}&\frac{1}{4}(\tilde{\eta}_0^T C_0^T G_1 C_0 \tilde{\eta}_0 - \tilde{\eta}_0^T C_0^T G_1 C_0 \tilde{\eta}_0) = 0 \\ &\frac{1}{4}(\tilde{\eta}_0^T C_0^T G_1 C_0 \tilde{\eta}_0 - \tilde{\eta}_0^T C_0^T G_1 C_0 \tilde{\eta}_0) = 0\end{aligned} \tag{5.29}$$

with $G_1 = \text{diag}\{\frac{1}{e_1}, \frac{1}{e_2}, \frac{1}{e_3}, \frac{1}{e_4}, \frac{1}{e_5}, \frac{1}{e_6}\}$, and $C_0\tilde{\eta}_0 = \tilde{y}$ into (5.28) and considering the relation [2]

$$\begin{aligned}&-z_1^T F_1 z_1 + z_1^T K_2 \tilde{y} - \frac{1}{4}\tilde{\eta}_0^T C_0^T G_1 C_0 \tilde{\eta}_0 \leq 0 \\ &-z_2^T F_2 z_2 + z_2^T \Theta\tilde{y} - \frac{1}{4}\tilde{\eta}_0^T C_0^T G_1 C_0 \tilde{\eta}_0 \leq 0,\end{aligned} \tag{5.30}$$

So the Equation (5.28) can be written as

$$\begin{aligned}\dot{V}_1 &\leq -z_1^T E_1 z_1 + \frac{1}{4}\tilde{\eta}_0^T C_0^T G_1 C_0 \tilde{\eta}_0 \\ &\quad -z_2^T E_2 z_2 + \frac{1}{4}\tilde{\eta}_0^T C_0^T G_1 C_0 \tilde{\eta}_0 \\ &\quad +2e_I^T K_I E_1 \dot{e}_I - 2\tilde{\nu}^T D\tilde{\nu} - \tilde{\eta}_0^T Q\tilde{\eta}_0 \\ &\leq -(\dot{e}_I + K_I e_I)^T E_1 (\dot{e}_I + K_I e_I) + 2e_I^T K_I E_1 \dot{e}_I\end{aligned}$$

$$
\begin{aligned}
& -z_2^T E_2 z_2 - 2\tilde{\nu}^T D\tilde{\nu} \\
& -\tilde{\eta}_0^T (Q - \frac{1}{2} C_0^T G_1 C_0)\tilde{\eta}_0 \\
\leq\ & -\dot{e}_I E_1 \dot{e}_I - e_I^T K_I^T E_1 K_I e_I - z_2^T E_2 z_2 \\
& -2\tilde{\nu}^T D\tilde{\nu} - \tilde{\eta}_0^T (Q - \frac{1}{2} C_0^T G_1 C_0)\tilde{\eta}_0 \\
<\ & 0 \qquad \forall \tilde{\eta}_0 \neq 0, \tilde{\nu}_1 \neq 0.
\end{aligned} \tag{5.31}
$$

The $\dot{V}_1$ can be made negative definite by choosing the positive definite matrix $Q > \frac{1}{2} C_0^T G_1 C_0$. So according to the Lyapunov stability theory, the AUV system with observer (5.3)-(5.5) and controller law (5.20) is GES.

5.4.3 Simulation Results

To demonstrate the performance of the proposed observer, simulation study is carried out based on the AUV model of the vehicle KAMBARA [94]. The AUV dynamics is described by (5.1) with the parameter values given in Appendix A.

The wave model parameters are chosen as $\zeta_i = 0.1$ and $\omega_i = 0.6283$ (i=1-3) corresponding to a wave period of 10s in surge, sway and heave. The amplitude of WF displacement in the earth-fixed frame in surge, sway and heave are limited to 0.5m, 0.5m and 0.2m, respectively. The notch filter parameters are chosen as $\zeta_{ni} = 5$ and $\omega_i = 5$. From (5.10), we choose

$$
\begin{aligned}
K_1 &= \begin{bmatrix} 6.1573 I_{3\times 3} & 0_{3\times 3} \\ 30.0130 I_{3\times 3} & 0_{3\times 3} \end{bmatrix} \\
K_2 &= \begin{bmatrix} 11.1573 I_{3\times 3} & 0_{3\times 3} \\ 0_{3\times 3} & I_{3\times 3} \end{bmatrix} \\
K_3 &= I_{6\times 6}
\end{aligned} \tag{5.32}
$$

as numerical values for the observer. In simulation, the wave model is driven by the zero mean Gaussian white noise although it was assumed to be zero in the stability analysis. This is to demonstrate the good performance of the observer in the presence of stochastic noise.

The parameters in controllers are chosen as $E_1 = 2I_{6\times6}$, $E_2 = 2I_{3\times3}$, $F_1 = 0.01K_2^2 = \begin{bmatrix} 1.2449I_{3\times3} & 0_{3\times3} \\ 0_{3\times3} & 0.01I_{3\times3} \end{bmatrix}$, $F_2 = 0.01\Theta^2 = \begin{bmatrix} 22.431I_{3\times3} & 0_{3\times3} \\ 0_{3\times3} & 0.0906I_{3\times3} \end{bmatrix}$.

In the simulation study, we use the output feedback controller to achieve the station keeping. The initial position is $\eta = [2, 2, 5.5, 0.15, 0.15, 0.15]^T$ and $U_f = [0.1, 0.1, 0.1]^T$. The initial condition for the observer is $\hat{\eta} = [1.5, 1.5, 5, 0.1, 0.1, 0.1]^T$ and $\hat{U}_f = [0.2, 0.2, 0.05]^T$. The desired position of the vehicle is $\eta_d = [0.5, 1, 3, 0, 0, 0]^T$. The simulation results are shown in Figures 5.2-5.14.

Figures 5.2, 5.3 and 5.4 show the desired, actual and estimated LF position in surge, sway and heave directions. We can see that AUV can keep at one position with great accuracy by counteracting the wave disturbances in these directions. Figures 5.5, 5.6 and 5.7 show the actual, desired heading angles in roll, pitch and yaw. We can see that position and heading angle converge to the desired one exponentially. The actual and estimated LF velocities in surge, sway and heave directions are shown in Figures 5.8, 5.9 and 5.10. The WF position in surge, sway and heave directions and their estimates are shown in Figures 5.11, 5.12 and 5.13. The exponential convergence of the WF position estimation errors can be seen from Figure 5.14. We can see that the stochastic behavior of the wave disturbance is estimated as well even though the original wave model is driven by the zero mean white noise.

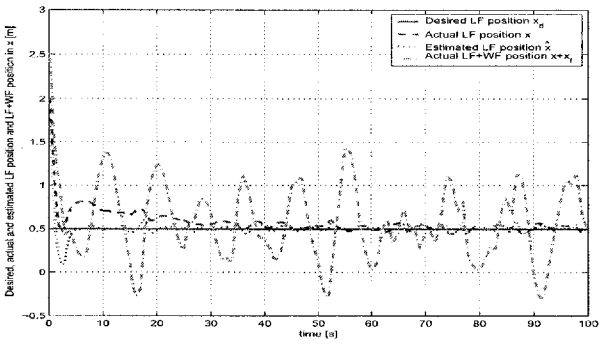

Figure 5.2: The desired, actual, estimated LF position and measured position in surge

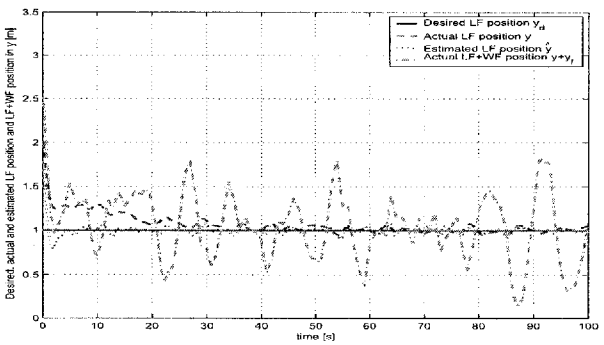

Figure 5.3: The desired, actual, estimated LF position and measured position in sway

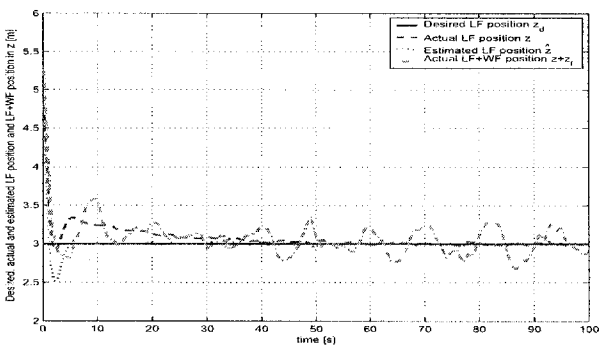

Figure 5.4: The desired, actual, estimated LF position and measured position in heave

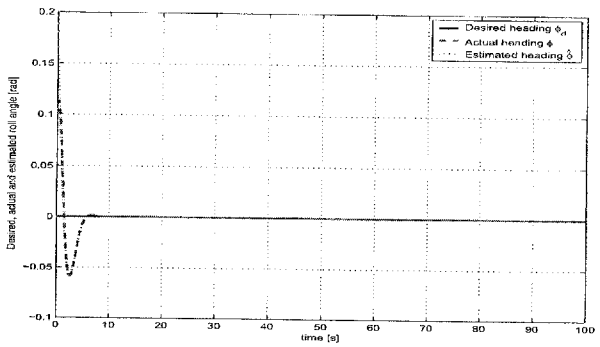

Figure 5.5: The desired, actual and estimated roll angle

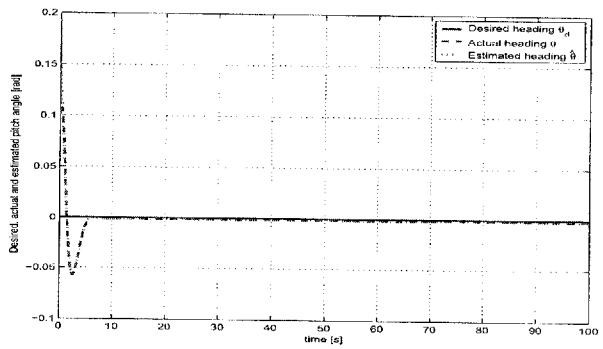

Figure 5.6: The desired, actual and estimated pitch angle

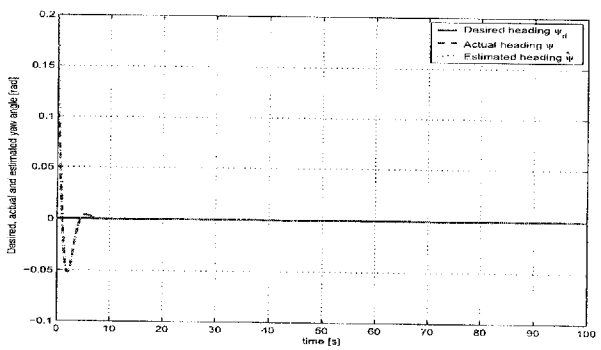

Figure 5.7: The desired, actual and estimated yaw angle

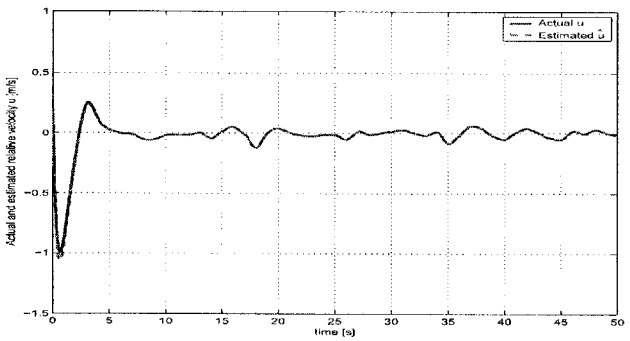

Figure 5.8: The actual LF velocity and its estimates in surge

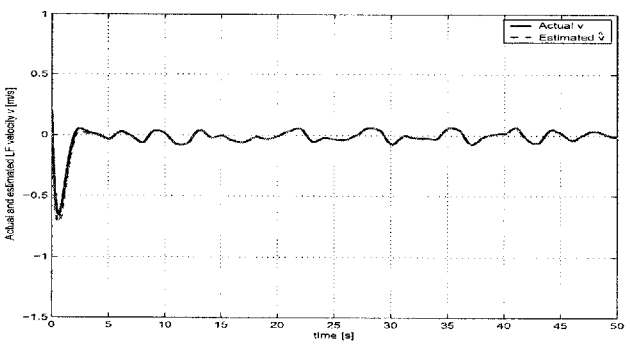

Figure 5.9: The actual LF velocity and its estimates in sway

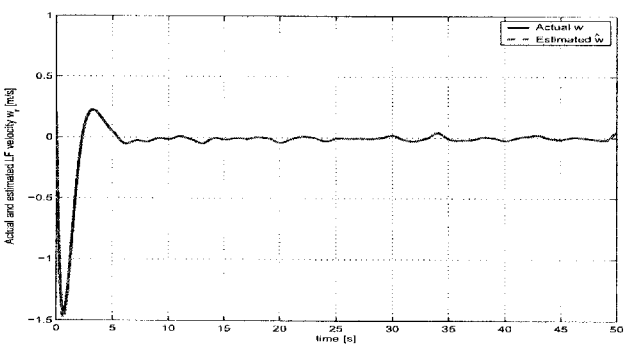

Figure 5.10: The actual LF velocity and its estimates in heave

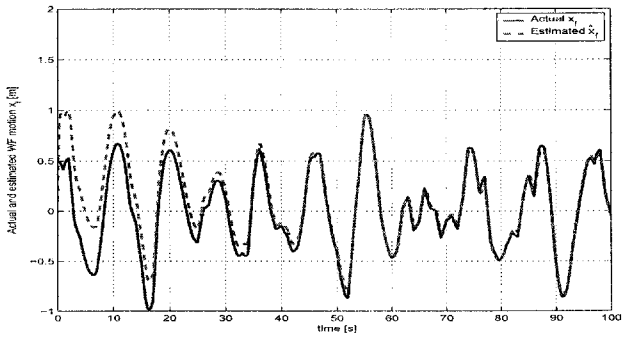

Figure 5.11: The actual WF position and its estimates in surge

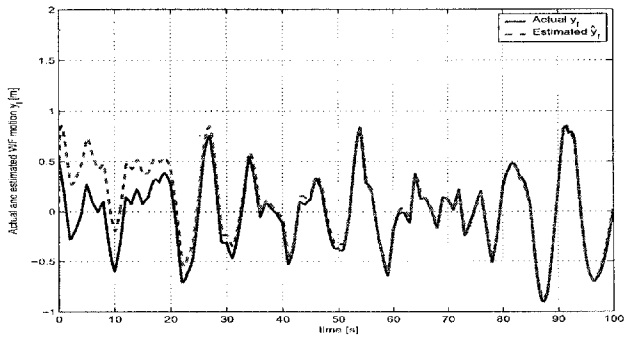

Figure 5.12: The actual WF position and its estimates in sway

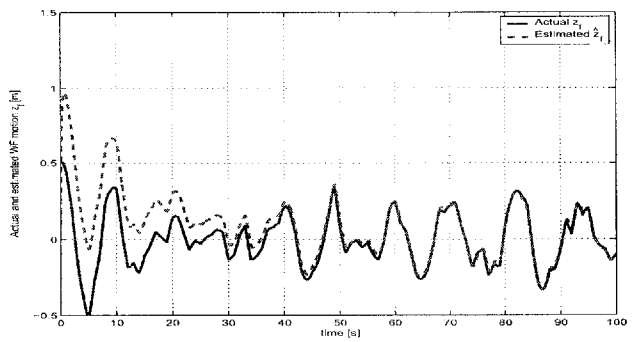

Figure 5.13: The actual WF position and its estimates in heave

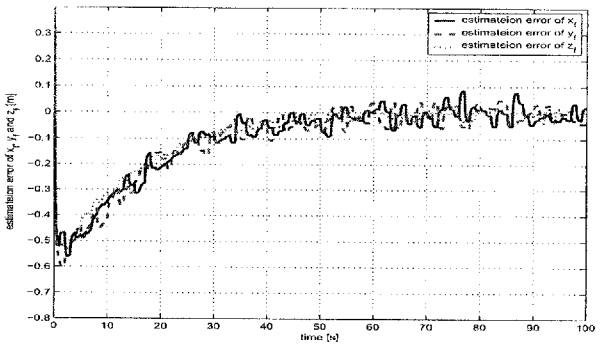

Figure 5.14: The estimation error of WF position in earth-fixed frame in surge, sway and heave directions

5.5 Conclusion

A solution was presented to the problem of dynamic positioning of AUVs operating in shallow water environment considering energy efficiency. Without lose of generality, we use a simplified model where dynamic positioning AUVs hold. Based on the observer technique, a nonlinear observer is briefly presented. The observer provide estimations of LF velocities of AUV and to filter out WF motion. An output feedback controller is then designed using observer backstepping technique. Also using the Lyapunov stability analysis, convergence of the resulting nonlinear system was analyzed and simulations were performed to illustrate the behavior of the proposed control scheme. Simulation results show that the control objectives were achieved successfully. Future research will address the application of the new control strategy developed for more general AUV model concerning energy efficiency in the next chapter.

Chapter 6

Nonlinear Tracking Control Design

6.1 Introduction

This chapter addresses the problem of nonlinear tracking control of AUVs in shallow water environment. Most usual control system designs for AUVs usually consider only constant disturbances, such as low frequency current disturbances or parameter uncertainties. Significant oscillation disturbances due to wave motion will be introduced into the position movement of the AUV operating in shallow water environment. When considering energy efficiency of a specified mission, it is not desirable to counteract the high frequency oscillatory movement due to wave. It is critical to design the controller to avoid wear and tear on thrusters.

Numerous studies have been done for the tracking control problems of marine vehicles. An overview of some different methods on controller design can be found in [29, 14]. But the control problems of marine vehicles considering the wave disturbance explicitly have been studied by only a few authors.

Paulsen presented an output feedback controller with a wave filter for yaw angle regulation of nonlinear marine vehicles in [86]. In this paper, the controller incorporated a wave filter without using velocity feedback. Vik [108] developed an observer-controller structure design for yaw angle regulation of nonlinear dynamics of marine vehicles and proved the semi-global exponential stability based on the ideas in [11]. Both of these work in [86, 108] considered a one-degree of freedom nonlinear model with wave disturbance. Using the idea of [11], an observer-controller structure design for tracking control of ships with a 3 degrees of freedom nonlinear model without wave disturbance is presented in [87].

In this chapter, we will design a nonlinear output feedback controller by using observer backstepping technology. The observer designed in Chapter 3 will be used in this output feedback controller.

6.2 Nonlinear Observer Based Backstepping Control Design

For translational motion control, the control objective is to make the AUV's LF motion to track the desired trajectory $\eta_{\mathbf{d}} = \left[\begin{array}{ccc} \eta_d, & \dot{\eta}_d, & \ddot{\eta}_d \end{array} \right]^T$ in the earth-fixed frame without counteracting the high frequency disturbance due to wave. Using the estimated LF motion, here we present an output feedback controller to solve this task by using observer backstepping technique [56].

For rotational motion, there is no need to use the observer backstepping controller because we can directly measure the orientation angle and rotational rate with great accuracy by using gyro compass. We use a separate general backstepping control technique for the orientation angle control.

Backstepping makes use of a recursive procedure that breaks down the control problem for the full system into a sequence of designs for lower order systems

[56, 54]. The observer backstepping method in this section is based on the work of Aarset *et al.* [2], which is an extension of the results in Fossen and Grøvlen [30]. The results in [2, 30] are applicable for dynamic positioning control of ships using a simplified model. In this chapter, the backstepping control technique is used for the tracking control of an AUV with general 6 DOF model taking into account disturbance due to wave.

6.2.1 Controller Design for Translational Motion

Step 1 Since $\alpha_1 = \eta_1$ is combined with the wave motion and cannot be measured directly, the tracking error $\alpha_1 - \alpha_d$ is rewritten in terms of estimation of $\hat{\alpha}_1$. Since the observer guarantees $\hat{\alpha}_1 \to \alpha_1$, the tracking error $\hat{\alpha}_1 - \alpha_d$ is used for observer backstepping design.

Define the error variable z_1 as

$$z_1 = \hat{\alpha}_1 - \alpha_d + K_I \int_0^t (\hat{\alpha}_1 - \alpha_d) d\tau = \dot{e}_{1I} + K_I e_{1I} \tag{6.1}$$

where $K_I > 0$ is the diagonal integration gain matrix used to eliminate steady state errors and $\dot{e}_{1I} = \hat{\alpha}_1 - \alpha_d$. Using Equations (3.30) in the observer design, we obtain the following by differentiating (6.1)

$$\dot{z}_1 = J_1(\eta_2) M_1^{-1} J_1^{-1}(\eta_2) \hat{\alpha}_2 + K_3 \tilde{y}_1 - \dot{\alpha}_d + K_I(\hat{\alpha}_1 - \alpha_d) \tag{6.2}$$

The virtual control vector is chosen as $\gamma_1 = J_1(\eta_2) M_1^{-1} J_1^{-1}(\eta_2) \hat{\alpha}_2 = z_2 + \beta_1$ with the stabilizing function

$$\beta_1 = -(E_1 + F_1) z_1 + \dot{\alpha}_d - K_I(\hat{\alpha}_1 - \alpha_d).$$

So Equation (6.2) results in

$$\dot{z}_1 = -(E_1 + F_1) z_1 + z_2 + K_3 \tilde{y}_1 \tag{6.3}$$

where E_1 is a strictly positive diagonal feedback design matrix expressed as $E_1 = \text{diag}\{e_1, e_2, e_3\}$ and F_1 is a strictly positive diagonal damping matrix defined as:

$$F_1 = \begin{bmatrix} e_1 k_{31}^2 & 0 & 0 \\ 0 & e_2 k_{32}^2 & 0 \\ 0 & 0 & e_3 k_{33}^2 \end{bmatrix} \tag{6.4}$$

The damping term $-F_1 z_1$ is used to compensate the disturbance like term $K_3 \tilde{y}$.

Step 2 Time differentiation of z_2 is:

$$\begin{aligned} \dot{z}_2 &= \dot{\gamma}_1 - \dot{\beta}_1 \\ &= J_1(\eta_2)S(\eta_2)M_1^{-1}J_1^T(\eta_2)\hat{\alpha}_2 + J_1(\eta_2)M_1^{-1}S^T(\eta_2)J_1^T(\eta_2)\hat{\alpha}_2 \\ &\quad + J_1(\eta_2)M_1^{-1}J_1^T(\eta_2)J_1(\eta_2)(-D_1(\hat{\nu}_1)\hat{\nu}_1 - g_1(\eta_2) + \tau_1 + M_1^{-1}J_1^{-1}K_4(\eta_2)\tilde{y}_1) \\ &\quad + (E_1 + F_1)\dot{z}_1 - \ddot{\alpha}_d + K_I(\dot{\hat{\alpha}}_1 - \dot{\alpha}_d) \\ &= J_1(\eta_2)S(\eta_2)M_1^{-1}J_1^T(\eta_2)\hat{\alpha}_2 + J_1(\eta_2)M_1^{-1}S^T(\eta_2)J_1^T(\eta_2)\hat{\alpha}_2 \\ &\quad + J_1(\eta_2)M_1^{-1}J_1^T(\eta_2)J_1(\eta_2)(-D_1(\hat{\nu}_1)\hat{\nu}_1 - g_1(\eta_2) + \tau_1 + M_1^{-1}J_1^{-1}K_4(\eta_2)\tilde{y}_1) \\ &\quad + (E_1 + F_1)(-(E_1 + F_1)z_1 + z_2 + K_3\tilde{y}_1) - \ddot{\alpha}_d \\ &\quad + K_I(J_1(\eta_2)M_1^{-1}J_1^T(\eta_2)\hat{\alpha}_2 + K_3\tilde{y}_1 - \dot{\alpha}_d) \end{aligned} \tag{6.5}$$

By defining Λ_1 as

$$\begin{aligned} \Lambda_1 &= J_1(\eta_2)S(\eta_2)M_1^{-1}J_1^T(\eta_2)\hat{\alpha}_2 + J_1(\eta_2)M_1^{-1}S^T(\eta_2)J_1^T(\eta_2)\hat{\alpha}_2 \\ &\quad + J_1(\eta_2)M_1^{-1}(-D_1(\hat{\nu}_1)\hat{\nu}_1 - g_1(\eta_2) + M_1^{-1}J_1^{-1}K_4(\eta_2)\tilde{y}_1) \\ &\quad + (E_1 + F_1)(-(E_1 + F_1)z_1 + z_2) - \ddot{\alpha}_d \\ &\quad + K_I(J_1(\eta_2)M_1^{-1}J_1^T(\eta_2)\hat{\alpha}_2 - \dot{\alpha}_d) \end{aligned} \tag{6.6}$$

Equation (6.5) can be written as

$$\begin{aligned} \dot{z}_2 &= J_1(\eta_2)M_1^{-1}\tau_1 + \Lambda_1 \\ &\quad +((E_1 + F_1)K_3 + K_I K_3)\tilde{y}_1 \end{aligned} \tag{6.7}$$

Because all the terms in $(E_1 + F_1)K_3 + K_I K_3$ is diagonal matrix, we define a term $\Theta = (E_1 + F_1)K_3 + K_I K_3$ as

$$\Theta = \begin{bmatrix} \theta_1 & 0 & 0 \\ 0 & \theta_2 & 0 \\ 0 & 0 & \theta_3 \end{bmatrix}. \tag{6.8}$$

The following choice of feedback controller is made

$$\tau_1 = -M_1 J_1^{-1}(\eta_1)(\Lambda_1 + (E_2 + F_2)z_2 + z_1) \tag{6.9}$$

where E_2 is a strictly positive diagonal feedback design matrix expressed as $E_2 = \text{diag}\{e_3, e_4, e_5\}$. The F_2 is a strictly positive diagonal damping matrix. The damping term $-F_2 z_2$ is used to compensate the disturbance like term $\Theta\tilde{y}_1$.

So the resulting z_2-error dynamics is

$$\dot{z}_2 = -(E_2 + F_2)z_2 - z_1 + \Theta\tilde{y}_1. \tag{6.10}$$

The strictly positive diagonal damping matrix F_2 is defined as

$$F_2 = \begin{bmatrix} e_4\theta_1^2 & 0 & 0 \\ 0 & e_5\theta_2^2 & 0 \\ 0 & 0 & e_6\theta_3^2 \end{bmatrix} \tag{6.11}$$

By combining Equations (3.36)-(3.38) and (6.10), the resulting error dynamics of the whole system can be written as

$$\dot{z} = -(E_z + F_z)z + Ez + W\tilde{y}_1 \tag{6.12}$$

$$\dot{\tilde{\eta}}_0 = A\tilde{\eta}_0 + BJ_1(\eta_2)M_1^{-1}J_1^{-1}(\eta_2)\tilde{\alpha}_2 \tag{6.13}$$

$$\dot{\tilde{\alpha}}_2 = J_1(\eta_2)(-D_1(\nu_1)\nu_1 + D_1(\hat{\nu}_1)\hat{\nu}_1) - J_1(\eta_2)M_1^{-1}J_1^{-1}(\eta_2)C\tilde{\eta}_0 \tag{6.14}$$

where $z = [z_1^T, z_2^T]^T$ and $E_z = \begin{bmatrix} E_1 & 0 \\ 0 & E_2 \end{bmatrix}$, $F_z = \begin{bmatrix} F_1 & 0 \\ 0 & F_2 \end{bmatrix}$, $E = \begin{bmatrix} 0 & 1 \\ -1 & 0 \end{bmatrix}$, $W = \begin{bmatrix} K_3 \\ \Theta \end{bmatrix}$.

A Lyapunov function candidate for the control law is

$$V_{con} = \frac{1}{2}z^T z + e_{1I}^T K_I E_1 e_{1I}. \tag{6.15}$$

So the Lyapunov function candidate for the whole system is

$$\begin{aligned} V_1 &= V_{con} + V_{obs} \\ &= \frac{1}{2}z^T z + e_{1I}^T K_I E_1 e_{1I} + \tilde{\alpha}_2^T \tilde{\alpha}_2 + \tilde{\eta}_0^T P \tilde{\eta}_0. \end{aligned} \tag{6.16}$$

The time derivation of Equation (6.16) is

$$\begin{aligned} \dot{V}_1 &= \dot{V}_{con} + \dot{V}_{obs} \\ &= z^T\dot{z} + 2e_{1I}^T K_I E_1 \dot{e}_{1I} + 2\tilde{\nu}_1^T M_1^T(-D_1(\nu_1)\nu_1 + D_1(\hat{\nu}_1)\hat{\nu}_1) - \tilde{\eta}_0^T Q\tilde{\eta}_0 \\ &= -z_1^T E_1 z_1 - z_1^T F_1 z_1 + z_1^T K_3 \tilde{y}_1 \\ &\quad -z_2^T E_2 z_2 - z_2^T F_2 z_2 + z_2^T \Theta \tilde{y}_1 \\ &\quad +2e_{1I}^T K_I E_1 \dot{e}_{1I} + 2\tilde{\nu}_1^T M_1^T(-D_1(\nu_1)\nu_1 + D_1(\hat{\nu}_1)\hat{\nu}_1) - \tilde{\eta}_0^T Q\tilde{\eta}_0 \end{aligned} \tag{6.17}$$

Adding the following zero terms

$$\begin{aligned}\frac{1}{4}(\tilde{\eta}_0^T C_y^T G_1 C_y \tilde{\eta}_0 - \tilde{\eta}_0^T C_y^T G_1 C_y \tilde{\eta}_0) = 0\\ \frac{1}{4}(\tilde{\eta}_0^T C_y^T G_2 C_y \tilde{\eta}_0 - \tilde{\eta}_0^T C_y^T G_2 C_y \tilde{\eta}_0) = 0\end{aligned} \tag{6.18}$$

with $G_1 = \begin{bmatrix} \frac{1}{e_1} & 0 & 0 \\ 0 & \frac{1}{e_2} & 0 \\ 0 & 0 & \frac{1}{e_3} \end{bmatrix}$, $G_2 = \begin{bmatrix} \frac{1}{e_4} & 0 & 0 \\ 0 & \frac{1}{e_5} & 0 \\ 0 & 0 & \frac{1}{e_6} \end{bmatrix}$, $C_y = \begin{bmatrix} 0 & I & I \end{bmatrix}$ and $C_y\tilde{\eta}_0 = \tilde{y}$ into (6.17), and considering the relation [2]

$$\begin{aligned}-z_1^T F_1 z_1 + z_1^T K_3 \tilde{y}_1 - \frac{1}{4}\tilde{\eta}_0^T C_y^T G_1 C_y \tilde{\eta}_0 \leq 0\\ -z_2^T F_2 z_2 + z_2^T \Theta \tilde{y}_1 - \frac{1}{4}\tilde{\eta}_0^T C_y^T G_2 C_y \tilde{\eta}_0 \leq 0,\end{aligned} \tag{6.19}$$

So the Equation (6.17) can be written as

$$\begin{aligned}\dot{V}_1 \leq\ & -z_1^T E_1 z_1 + \frac{1}{4}\tilde{\eta}_0^T C_y^T G_1 C_y \tilde{\eta}_0 \\ & -z_2^T E_2 z_2 + \frac{1}{4}\tilde{\eta}_0^T C_y^T G_2 C_y \tilde{\eta}_0 \\ & +2e_{1I}^T K_I E_1 \dot{e}_{1I} - 2\tilde{\nu}_1^T M_1^T D_1 \tilde{\nu}_1 - \tilde{\eta}_0^T Q \tilde{\eta}_0 \\ \leq\ & -(\dot{e}_{1I} + K_I e_I)^T E_1 (\dot{e}_{1I} + K_I e_{1I}) + 2e_{1I}^T K_I E_1 \dot{e}_{1I} \\ & -z_2^T E_2 z_2 - 2\tilde{\nu}_1^T M_1^T D_1 \tilde{\nu}_1 \\ & -\tilde{\eta}_0^T (Q - \frac{1}{4}C_y^T G_1 C_y - \frac{1}{4}C_y^T G_2 C_y)\tilde{\eta}_0 \\ \leq\ & -\dot{e}_{1I} E_1 \dot{e}_{1I} - e_{1I}^T K_I^T E_1 K_I e_{1I} - z_2^T E_2 z_2 \\ & -2\tilde{\nu}_1^T M_1^T D_1 \tilde{\nu}_1 \\ & -\tilde{\eta}_0^T (Q - \frac{1}{4}C_y^T G_1 C_y - \frac{1}{4}C_y^T G_2 C_y)\tilde{\eta}_0 \\ <\ & 0 \qquad \forall \tilde{\eta}_0 \neq 0, \tilde{\nu}_1 \neq 0.\end{aligned} \tag{6.20}$$

The $\dot{V}_1$ can be made negative definite by choosing the positive definite matrix $Q > \frac{1}{4}C_y^T G_1 C_y + \frac{1}{4}C_y^T G_2 C_y$. So according to the Lyapunov stability theory, the AUV system with observer (3.30)-(3.32) and controller law (6.9) is GES.

6.2.2 Controller Design for Rotational Motion

Because we can measure the orientation angle and rotational rate with great accuracy by using the gyro compass, there is no need to use the observer backstepping controller. We use the general backstepping control technique for the orientation angle control.

Consider the dynamics of the orientational model.

$$\dot{\eta}_2 = J_2(\eta_2)\nu_2 \tag{6.21}$$

$$\dot{\nu}_2 = M_2^{-1}(-C_1(\nu_1)\nu_1 - C_2(\nu_2)\nu_2 - D_2(\nu_2)\nu_2 - g_2(\eta_2) + \tau_2) \tag{6.22}$$

$$y_2 = \eta_2 \tag{6.23}$$

where $J_2(\eta_2)$ is the kinematic transformation matrix and both η_2 and ν_2 are assumed measured.

Step 1 Similar with previous design, we first define the error variable z_3 as

$$z_3 = \eta_2 - \eta_{2d} + K_I \int_0^t (\eta_2 - \eta_{2d})d\tau = \dot{e}_{2I} + K_I e_{2I} \tag{6.24}$$

where $K_I > 0$ still has the same definition as previous and $\dot{e}_{2I} = \eta_2 - \eta_{2d}$. Based on (6.21), we get the following by differentiating (6.24)

$$\dot{z}_3 = J_2(\eta_2)\nu_2 - \dot{\eta}_{2d} + K_I(\eta_2 - \eta_{2d}) \tag{6.25}$$

The virtual control vector is chosen as $\gamma_2 = J_2(\eta_2)\nu_2 = z_4 + \beta_2$ with the stabilizing function

$$\beta_2 = -E_3 z_3 + \dot{\eta}_{2d} - K_I(\eta_2 - \eta_{2d}).$$

So Equation (6.25) results in

$$\dot{z}_3 = -E_3 z_3 + z_4 \tag{6.26}$$

where E_3 is a strictly positive diagonal feedback design matrix.

Step 2 By differentiate z_4, we get

$$\begin{aligned}
\dot{z}_4 &= \dot{\gamma}_2 - \dot{\beta}_2 \\
&= \dot{J}_2(\eta_2)\nu_2 + J_2(\eta_2)\dot{\nu}_2 + E_3\dot{z}_3 - \ddot{\eta}_{2d} + K_I(\dot{\eta}_2 - \dot{\eta}_{2d}) \\
&= \dot{J}_2(\eta_2)\nu_2 + J_2(\eta_2)M_2^{-1}(\tau_2 - C_1(\nu_1)\nu_1 - C_2(\nu_2)\nu_2 - D_2(\nu_2)\nu_2 - g_2(\eta_2)) \\
&\quad + E_3(-E_3 z_3 + z_4) - \ddot{\eta}_{2d} + K_I(J_2(\eta_2)\nu_2 - \dot{\eta}_{2d})
\end{aligned} \tag{6.27}$$

By defining Λ_2 as

$$\begin{aligned}
\Lambda_2 &= \dot{J}_2(\eta_2)\nu_2 + J_2(\eta_2)M_2^{-1}(-C_2(\nu_2)\nu_2 - D_2(\nu_2)\nu_2 - g_2(\eta_2)) \\
&\quad + E_3(-E_3 z_3 + z_4) - \ddot{\eta}_{2d} + K_I(J_2(\eta_2)\nu_2 - \dot{\eta}_{2d})
\end{aligned} \tag{6.28}$$

Equation (6.27) can be rewritten as

$$\dot{z}_4 = J_2(\eta_2)M_2^{-1}\tau_2 - J_2(\eta_2)M_2^{-1}C_1(\nu_1)\nu_1 + \Lambda_2 \tag{6.29}$$

We can easily choose the following controller

$$\tau_2 = -M_2 J_2^{-1}(\eta_2)(\Lambda_2 + E_4 z_4 + z_3) + C_1(\hat{\nu}_1)\hat{\nu}_1 \tag{6.30}$$

So the resulting z_4 error dynamics is

$$\dot{z}_4 = -E_4 z_4 - z_3 - J_2(\eta_2) M_2^{-1}(C_1(\nu_1)\nu_1 - C_1(\hat{\nu}_1)\hat{\nu}_1) \tag{6.31}$$

where F_4 is a strictly positive feedback matrix usually chosen to be diagonal form.

Defining the following Lyapunov function candidate

$$V_2 = \frac{1}{2} z_3^T z_3 + \frac{1}{2} z_4^T z_4 \tag{6.32}$$

So the time derivation of Equation (6.33) is

$$\dot{V}_2 = -z_3^T E_3 z_3 - z_4^T E_4 z_4 - z_4 J_2(\eta_2) M_2^{-1}(C_1(\nu_1)\nu_1 - C_1(\hat{\nu}_1)\hat{\nu}_1) < 0 \quad \forall z_3 \neq 0, z_4 \neq 0 (6.33$$

Based on the previous GES property of observer design, so the GES is guaranteed.

6.2.3 Simulation Results

To demonstrate the performance of the proposed observer and controller design, simulation study is carried out using the AUV model of the vehicle KAMBARA [94]. The parameter values of the AUV dynamics described by (3.3) and (3.4) are shown in Appendix A.

The wave model parameters in (3.5) are chosen as $\zeta_i = 0.1$ and $\omega_{oi} = 0.7854$ (i=1-3) corresponding to a wave period of 8s in surge, sway and heave. The desired notch filter parameters are chosen as $\zeta_{ni} = 5$ and $\omega_{ci} = 5$. From (4.43), we select $K_1 = -62.3886 I_{3\times3}$, $K_2 = 7.6969 I_{3\times3}$, $K_3 = 5 I_{3\times3}$ and $K_4 = 0.1 I_{3\times3}$.

The controller parameters are chosen as $E_1 = 0.2 I_{3\times3}$, $F_1 = 0.2 K_3^2 = 5 I_{3\times3}$, $E_2 = 0.2 I_{3\times3}$, $F_2 = 0.2\Theta^2 = 192.2 I_{3\times3}$, $E_3 = 0.6 I_{3\times3}$ and $E_4 = 2 I_{3\times3}$.

For illustration, the desired trajectory is

$$\begin{aligned} x_d &= 20sin(0.05t) \\ y_d &= 20(1 - cos(0.05t)) \\ z_d &= 5 - 0.04t \quad (t <= 50s) \\ z_d &= 3 \qquad (t > 50s). \end{aligned} \tag{6.34}$$

Accordingly, $\alpha_d = [x_d, y_d, z_d]^T$, while $\dot{\alpha}_d$ and $\ddot{\alpha}_d$ are derived numerically.

The initial condition of the KAMBARA is $\nu_1 = [0,0,0]^T$, $\nu_2 = [0.1,0.1,0.1]^T$, $\eta_1 = [0,0.5,5.5]^T$ and $\eta_2 = [0.3,0.3,0.3]^T$. The initial condition of the observer is $\hat{\alpha}_1 = [0.5,-1,5.8]^T$ and $\hat{\alpha}_2 = [0.1,0.1,0.1]^T$. The desired orientational angles are $\eta_{2d} = [0,0.1,0.2]^T$. In simulation the wave model is driven by the zero-mean Gaussian white noise although it is assumed to be zero in the previous stability analysis. This is to demonstrate the good performance of the observer in the presence of random noise. The amplitude of the WF displacement in surge, sway and heave are limited to $1m, 1m$ and $0.2m$, respectively. In addition, to test the robustness of our design, we introduce WF disturbances on AUV rotational motion with limit of 1deg, 1deg, 1deg in roll, pitch and yaw respectively. The simulation results are shown in Figures 6.1-6.13.

Figure 6.1 show the actual and desired trajectory and the measured trajectory. The desired trajectory is in the counter clockwise direction. We can see that the LF position estimates $\hat{x}, \hat{y}$ and the actual LF position x, y converge to the desired trajectory, despite the presence of position measurement noises and the wave disturbances. Figures 6.2, 6.3 and 6.4 show the desired, actual and estimated LF position and measured positions in surge, sway and heave. We can see that the estimated LF position converges to the actual LF position and follow the desired LF position. We can see that there is a small error between the estimated and

desired position due to the observer dynamic response to the time varying desired trajectory. Figures 6.5, 6.6 and 6.7 show the actual and desired heading angles in roll, pitch and yaw. We can see that excellent tracking of heading angle is obtained. The corresponding actuator forces and moments are shown in Figures 6.8 and 6.9. The WF motions in surge, sway and heave directions and their estimations are shown in Figures 6.10, 6.11 and 6.12. We can see the random effect of white noise which drive the wave model from Figs 6.10, 6.11 and 6.12. The exponential convergence of the wave disturbance estimation errors can be verified from Figure 6.13. We can see that the stochastic behavior of the wave disturbance is estimated well even though the white noise was assumed to be zero in the original wave model in the stability analysis.

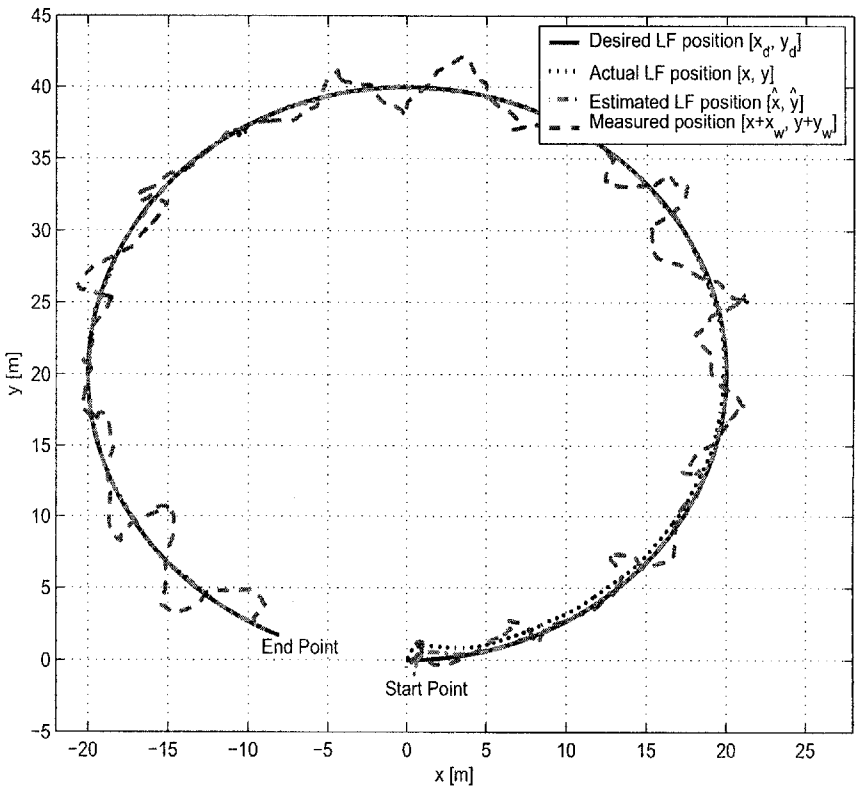

Figure 6.1: The desired, actual, estimated LF trajectory and measured trajectory

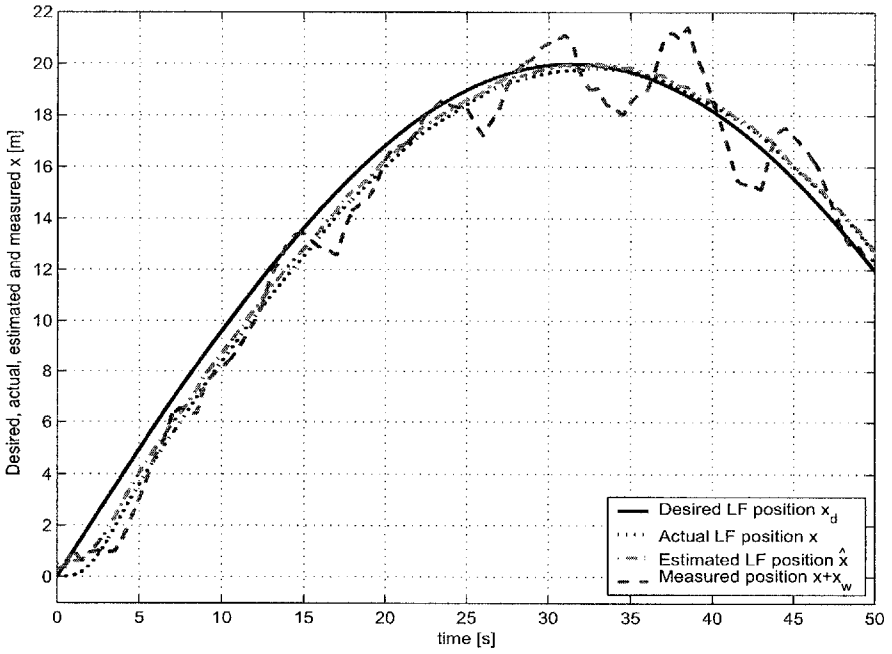

Figure 6.2: The desired, actual, estimated LF trajectory and measured trajectory in surge

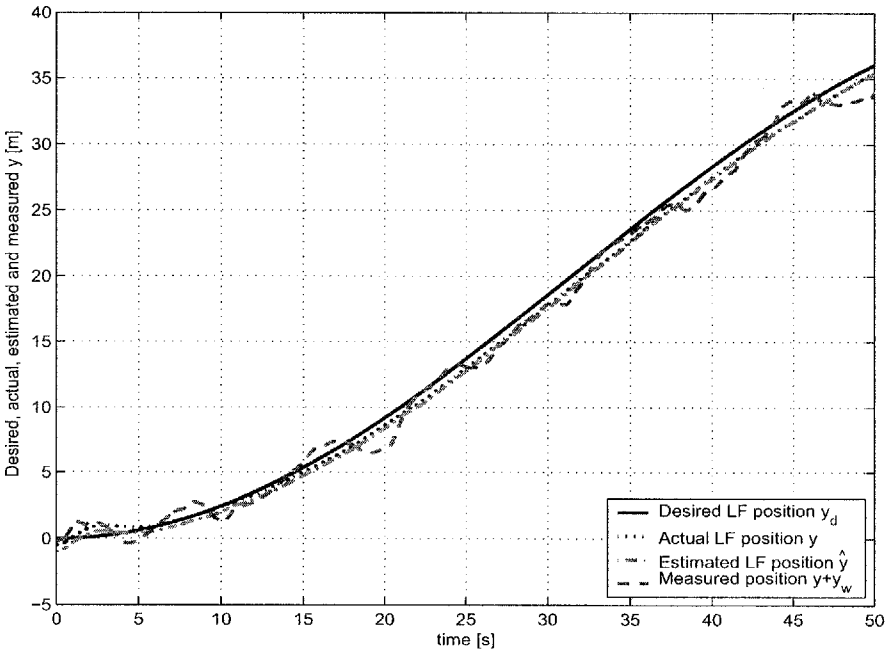

Figure 6.3: The desired, actual, estimated LF trajectory and measured trajectory in sway

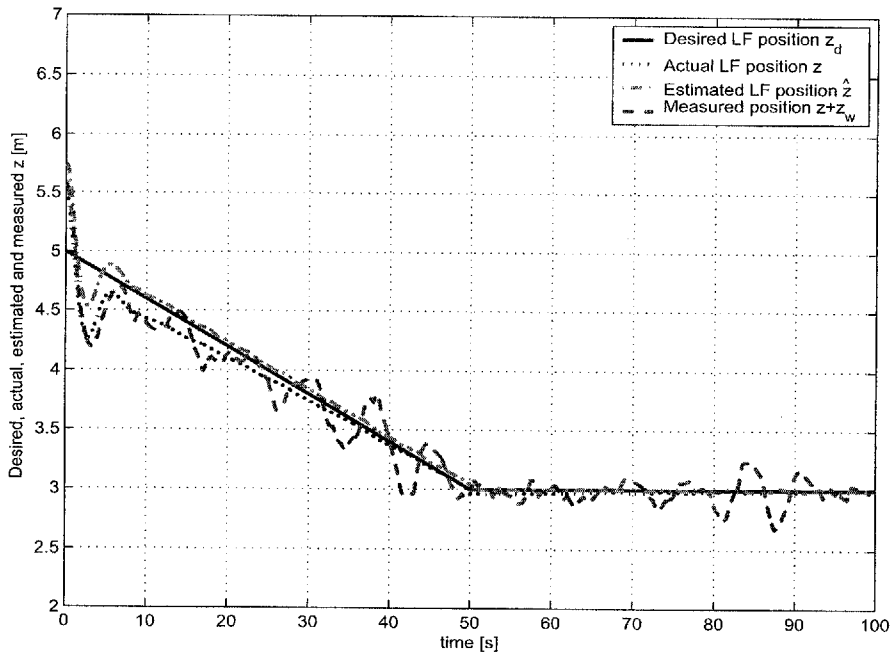

Figure 6.4: The desired, actual, estimated LF trajectory and measured trajectory in heave

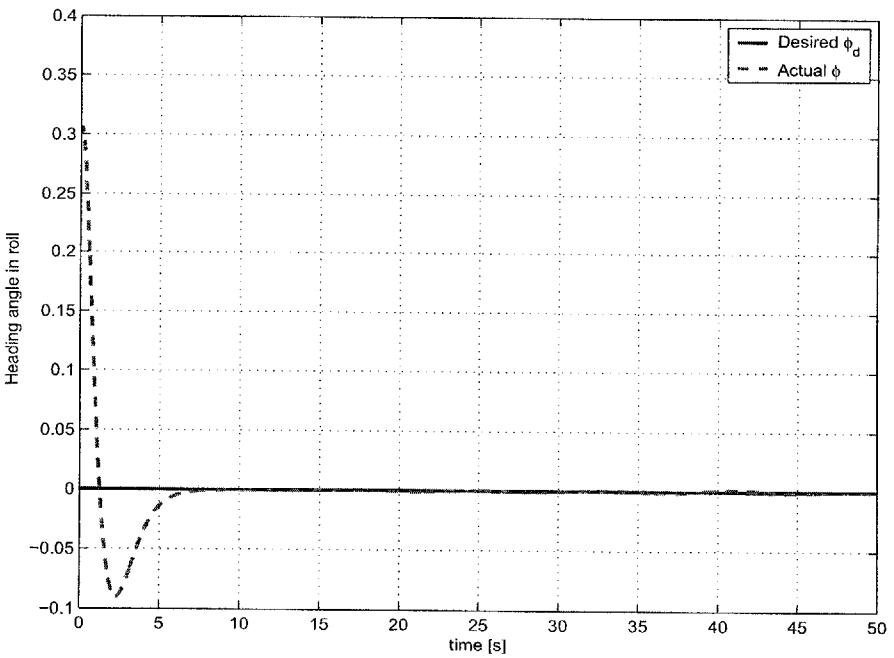

Figure 6.5: The desired and actual heading angle of AUV in roll

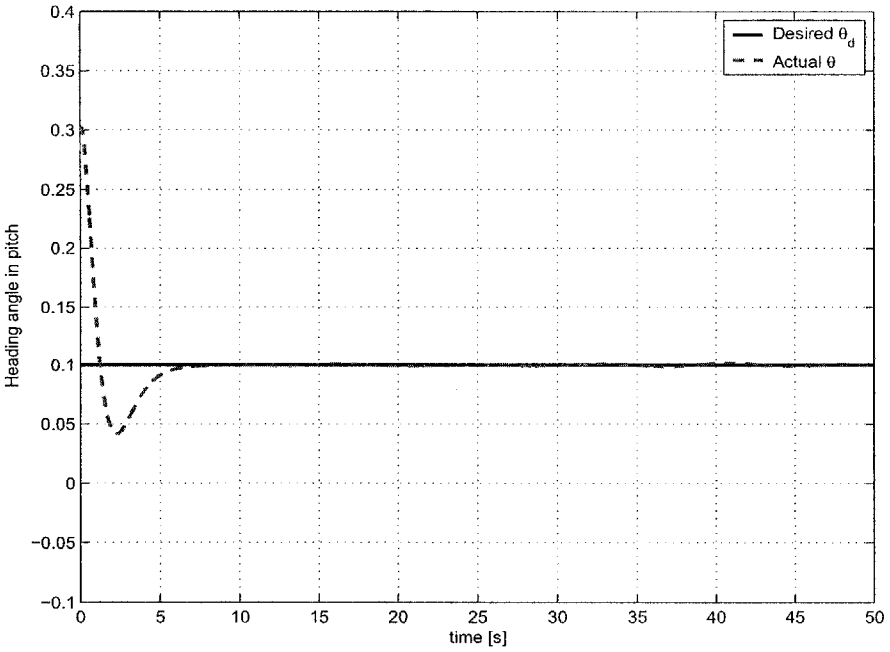

Figure 6.6: The desired and actual heading angle of AUV in pitch

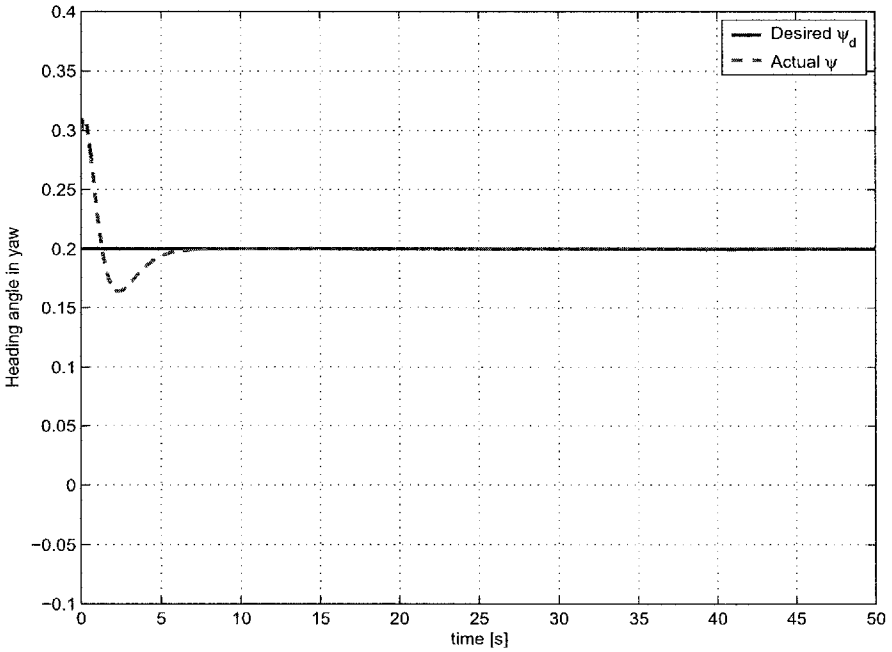

Figure 6.7: The desired and actual heading angle of AUV in yaw

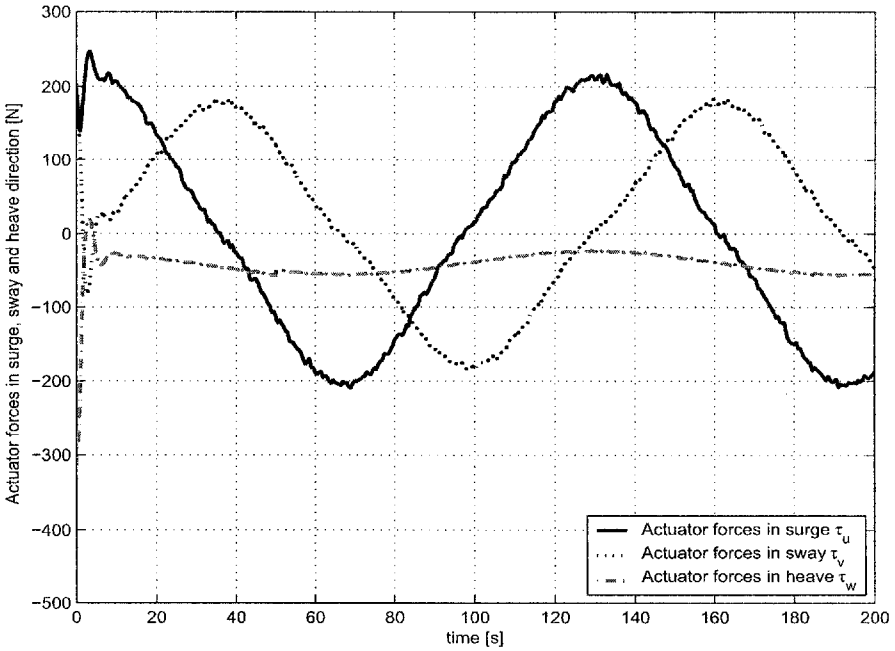

Figure 6.8: The actuator forces in surge, sway and heave

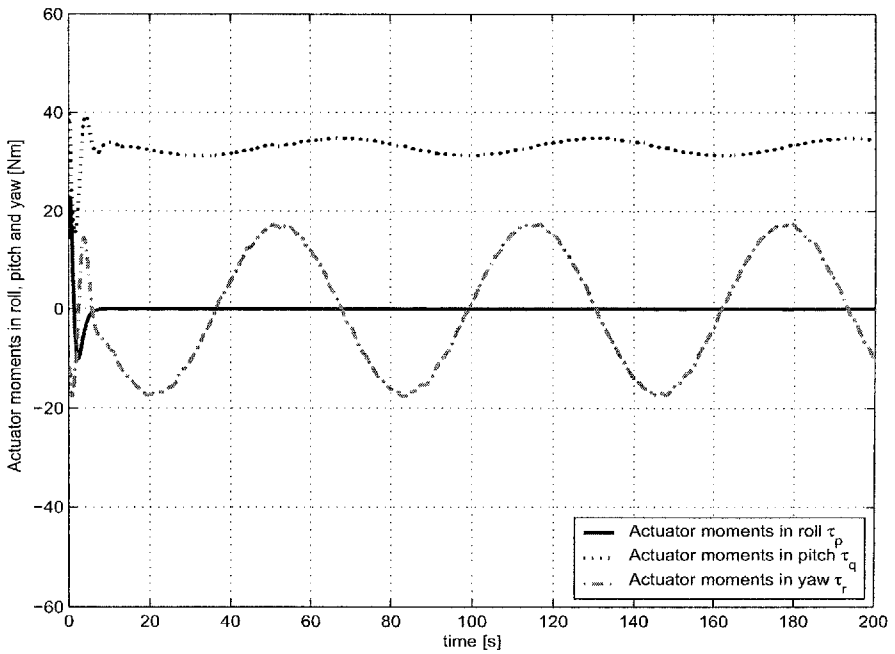

Figure 6.9: The actuator moments in roll, pitch and yaw

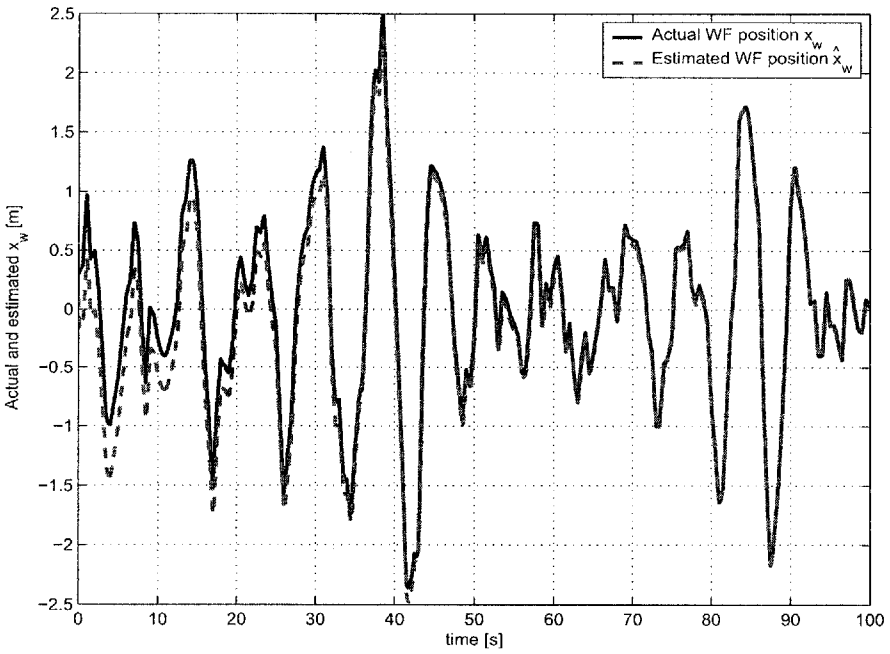

Figure 6.10: The actual and estimated WF position in surge

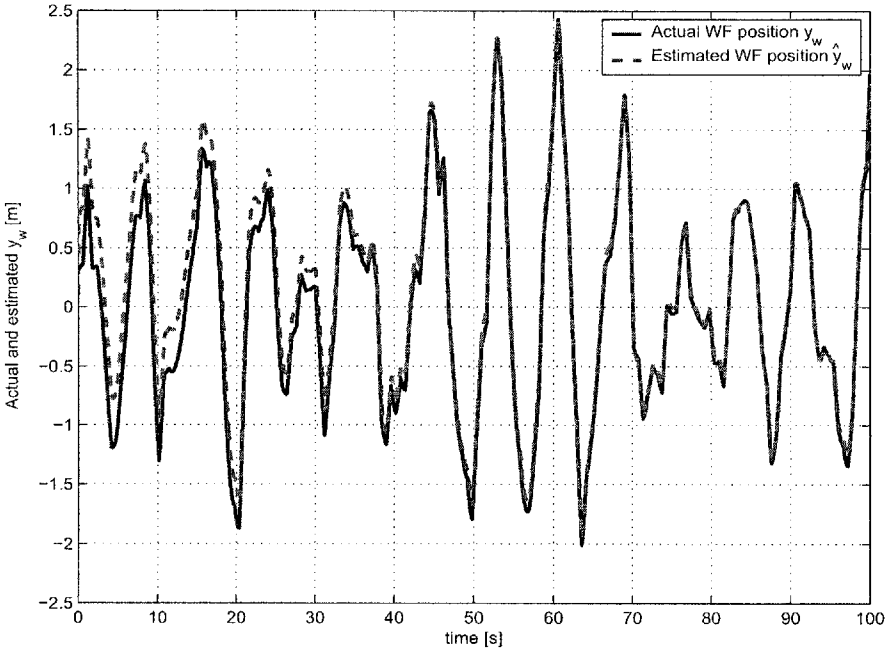

Figure 6.11: The actual and estimated WF position in sway

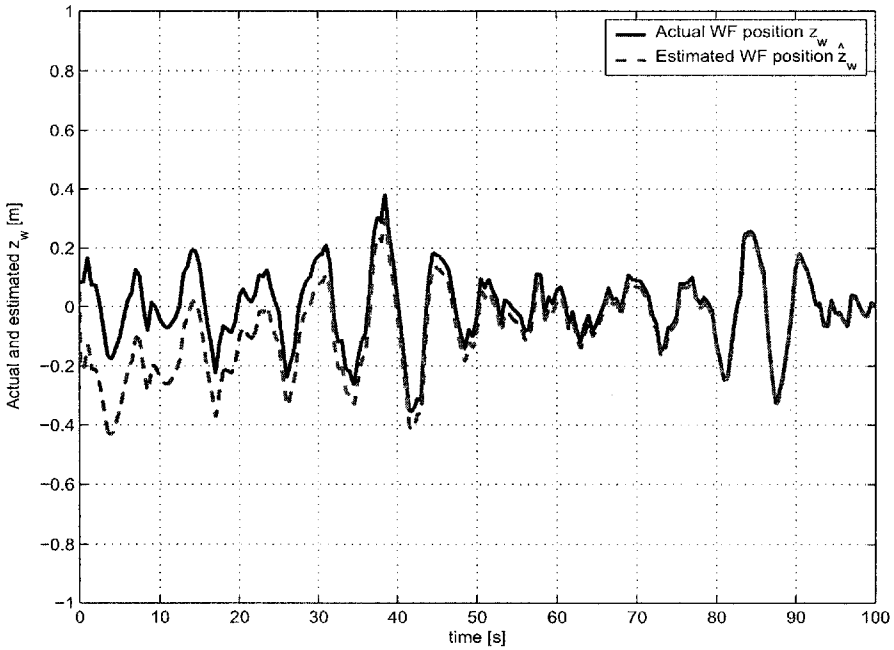

Figure 6.12: The actual and estimated WF position in heave

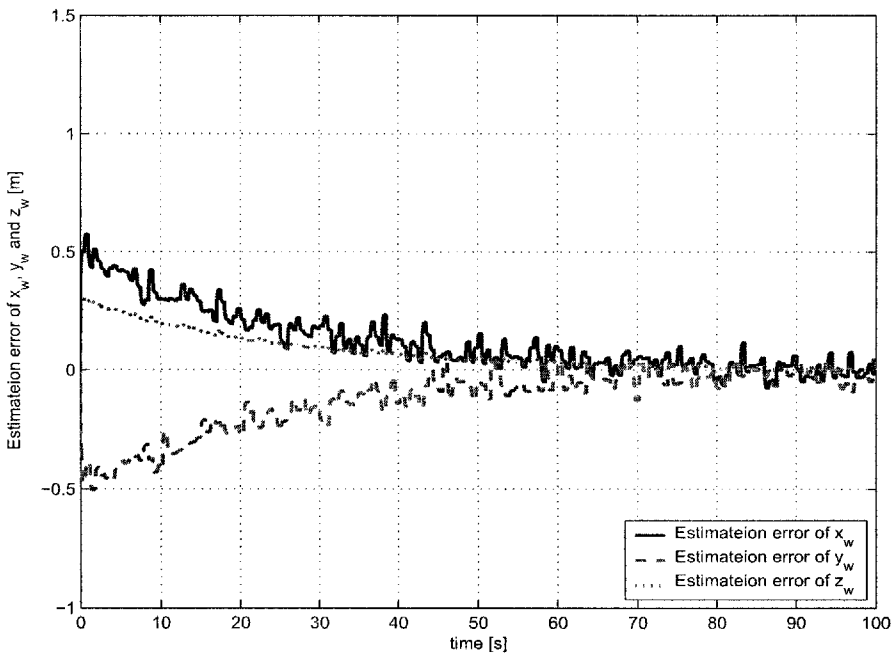

Figure 6.13: The estimation error of WF position in earth-fixed frame in surge, sway and heave

6.3 Conclusion

In this chapter, an output feedback controller is designed for tracking control of an AUV in shallow water area concerning energy efficiency. Based on the previous results in Chapter 3 where the LF positions and velocities of the vehicle, along with the WF positions in the earth-fixed frame are estimated with exponential convergence. An output feedback controller is subsequently designed using the observer backstepping technique for translational motion control, where the unavailable state information is replaced with estimates from the nonlinear observer. The nonlinear output feedback controller is shown to track the desired LF position in the earth-fixed frame without introducing WF disturbance into the feedback control loop. The total system is proven to be GES through Lyapunov stability analysis. A general backstepping controlled is designed for rotational motion of AUVs. Simulation results of a representative AUV show that the output feedback controller indeed performs well with stability and robustness. We also should note that this control strategy can be automatically reduced for dynamic positioning when the desired position is fixed point.

Chapter 7

Conclusion and Recommendations

This chapter concludes the main results in this research work and it also suggests some open questions for future work.

7.1 Conclusion

Autonomous underwater vehicles (AUVs) face a lot of challenges in shallow water environment. There are different mission requirements when the AUVs are operating in shallow water environment, such as station keeping, dynamic positioning and tracking. AUVs usually lack the capability to measure the external disturbances directly. In addition, due to limited power onboard AUVs, we also need to consider energy efficiency actuator control for dynamic positioning and tracking mission. In some tasks when the station keeping mission is required, we need to ensure precise control at a fixed location despite the presence of wave disturbance.

To complete these missions, external wave disturbance information should be obtained with good accuracy. For low cost AUVs, nonlinear observer is an alternative option to replace the expensive ADV sensor which is used in station keeping (SK) application in [92]. The observers can be used to estimate the wave velocities and

relative velocities for SK to meet precise control requirement or to filter out the wave-frequency (WF) positions from position measurements for dynamic positioning (DP) and trajectory tracking applications with energy efficiency requirement.

To facilitate the stability proof of the observer design, we introduced a coordinate transformation to remove the Coriolis and centripetal terms in the dynamic model. Based on the transformed model, we designed a nonlinear observer for tracking control assuming known wave model and an adaptive observer for unknown constant wave parameters. This technique can be utilized to estimate wave velocities for SK application or filter out WF positions for DP and tracking applications. The stability issue of these observers are proved and demonstrated by simulation results. Based on the observer design, we can design various output feedback controller to meet different application requirements. The observer backstepping technique allowed us to design various output feedback controller with GES stability to meet different mission requirement. The major contributions in this work have been published at international conferences and the most recent results are under review for publication in several journals.

Collectively, these results demonstrate that we have made useful advances to solve problem of AUVs operating in shallow water environments.

7.2 Recommendations for Further Research

A few further research topics are suggested as follows:

- Although the disturbances considered in this thesis are shallow water wave disturbances, we should also consider more about the effect of general wave disturbances, such as unknown time varying wave model and current forces. One topic for further research is to extend these results for AUVs considering shallow wave and slowly time varying current together. The system identifi-

cation of the 6DOF models for AUVs in shallow water area with field data is recommended. This is particularly important to validate the fidelity of the AUV and wave disturbance models.

- Sea trial and validation of the proposed control methods should be conducted to test the performance. For station keeping, the test results should also be benchmarked against Riedel's work [91] in which the expensive ADVOcean sensor was used. For dynamic positioning, the AUVs can move to the surface to completer DP mission. We can compare the results with other surface ship DP applications [33, 74].

- Throughout the thesis, it was assumed that the AUVs are fully actuated via the thrust force and torque. Although there are many published research results on underactuated underwater vehicles [4, 5, 20], the tracking control and station keeping control of underactuated AUVs in shallow water environment remain an open problems.

- As demonstrated by the adaptive observer simulations, estimation results of the adaptive observer can be more accurate than fixed nonlinear observer for unknown wave model. One topic for further research is to identify other model parameters that vary with the environmental conditions and to extend the use of adaptive techniques in the observer and controller designs. Another topic is there exists the possibility of parameter drift instability when the time-varying unknown parameter is considered [59]. Further study should be conducted for this issue.

Author's Publications

(1) S. Liu, D. Wang, and E. K. Poh, "A nonlinear observer for AUVs in shallow water environment", in *Proceedings of IEEE International Conference on Intelligent Robots and Systems*, (Sendai, Japan), pp. 1130–1135, September 2004.

(2) S. Liu, D. Wang, E. K. Poh, and C. S. Chia, "Nonlinear output feedback controller design for tracking control of ODIN in wave disturbance condition", in *Proceedings of OCEANS 2005 MTS/IEEE*, (Washington,DC), October 2005.

(3) S. Liu, D. Wang, E. K. Poh, and Y. Wang, "Dynamic positioning of AUVs in shallow water environment: observer and controller design", in *Proceedings of 2005 IEEE/ASME International Conference on Advanced Intelligent Mechatronics*, (Monterey,CA), p. 705C710, July 2005.

(4) S. Liu, D. Wang, and E. K. Poh, "Station keeping of AUVs in shallow water environment: Observer and controller design", in *Proceedings of Third International Conference on Computational Intelligence, Robotics and Autonomous Systems*, (Singapore), December 2005.

(5) S. Liu, D. Wang, and E. K. Poh, "Nonlinear adaptive observer design for tracking control of AUVs in wave disturbance condition", in *Proceedings of OCEANS 2006 MTS/IEEE*, (Singapore), May 2006.

(6) S. Liu, D. Wang, and E. K. Poh, "Nonlinear Output Feedback Tracking

Control for AUVs in Shallow Wave Disturbance Condition", *International Journal of Control*, to appear.

(7) S. Liu, D. Wang, and E. K. Poh, "Output feedback control design for station keeping of AUVs in shallow water environment", under review.

Bibliography

[1] O. M. Aamo, M. Arcak, T. I. Fossen, and P. V. Kokotović. Global output tracking control of a class of Euler-Lagrange systems with monotonic nonlinearities in the velocities. *International Journal of Control*, 74(7):649–658, 2001.

[2] M. F. Aarset, J. P. Strand, and T. I. Fossen. Nonlinear vectorial observer backstepping with integral action and wave filtering for ships. In *Proceedings of the IFAC Conference on Control Applications in Marine Systems (CAMS'98)*, pages 83–89, Fukuoka, Japan, 1998.

[3] M. Abkowitz. *Stability and Motion Control of Ocean Vehicles*. MIT Press, Massachusetts, 1972.

[4] A. P. Aguiar and A. M. Pascoal. Dyanmic positioning and way-point tracking of the underactuated AUVs in the presence of ocean currents. In *Proc. of the 41th IEEE Conf. on Decision and Control*, pages 4178–4183, Las Vegas, NV USA, December 2002.

[5] F. Alonge and F. M. Raimondi. Trajectory tracking of underactuated underwater vehicles. In *Proceedings of 40th IEEE Conference on Decision and Control*, pages 4421–4426, Orlando FL, December 2001.

[6] P. E. An, M. Dhanak, L. K. Shay, S. Smith, and J. VanLeer. Coastal oceanography using a small AUV. *Journal of Atmospheric and Oceanic Technology*, 18(2):215–234, 2001.

[7] K. Asakawa, J. Kojima, Y. Kato, S. Matsumoto, N. Kato, A. Teruyuki, and T. Iso. Design concept and experimental results of the autonomous underwater vehicle AQUA EXPLORER 2 for the inspection of underwater cables. *Advanced Robotics*, 16(1):27–42, 2002.

[8] J.M. Bachkosky, T. Brancati, D.R. Conley, and J.W. Douglass *et al.* Unmanned vehicles in mine countermeasures. Technical report, Naval Research Advisory Committee, November 2000.

[9] Jens G. Balchen, N. A. Jenssen, and S. Sælid. Dynamic positioning using Kalman filtering and optimal control theory. In *Prepr. IFAC Symposium on Automation in Offshore Oil Field Operation*, pages 183–186, Amsterdam, Holland, 1976.

[10] P. Batista, C. Silvestre, and P. Oliveira. A sensor based homing strategy for autonomous underwater vehicles. In *14th Mediterranean Conference on Control and Automation*, Ancona, Italy, 2006.

[11] H. Berghuis and H. Nijmeijer. A passivity approach to controller-observer design for robots. *IEEE Transactions on Robotics and Automation*, 9(6):740–754, 1993.

[12] K. F. Bowden. *Physical Oceanography of Coastal Waters.* Ellis Horward, 1983.

[13] S. K. Choi and J. Yuh. Experimental study on a learning control system with bound estimation for underwater robots. In *Proceedings of 1996 IEEE International Conference on Robotics and Automation*, pages 2160–2165, Minneapolis, MN, April 1996.

[14] P. J. Craven, R. Sutton, and R. S. Burns. Control strategies for unmanned underwater vehicles. *The Journal of Navigation*, 51(1):79–105, 1998.

[15] J. P. V. S. Cunha, R. R. Costa, and L. Hsu. Design of a high performance variable structure position control of ROV's. *IEEE Journal of Oceanic Engineering*, 20(1):42–55, 1995.

[16] F. Dabe. Remora, a new concept for AUVs in mine warfare. In *Proceedings of OCEANS 2004 MTS/IEEE*, pages 851–855, Kobe, Japan, November 2004.

[17] R. G. Dean and R. A. Dalrymple. *Water Wave Mechanics for Engineers and Scientists.* World Scientific, 1991.

[18] P. A. DeBitetto. Fuzzy logic for depth control of unmanned undersea vehicles. In *Proceedings of the 1994 Symposium on Autonomous Underwater Vehicle Technology*, pages 233–241, Cambridge, MA, July 1994.

[19] K. D. Do, Z. P. Jiang, J. Pan, and H. Nijmeijer. A global output-feedback controller for stabilization and tracking of underactuated odin: A spherical underwater vehicle. *Automatica*, 40(1):117–124, 2004.

[20] K. D. Do, J. Pan, and Z. P. Jiang. Robust and adaptive path following for underactuated autonomous underwater vehicle. *Oceanic Engineering*, 31(16):1967–1997, 2004.

[21] O. Doucy, D. Brutzman, and A. J. Healey. Near surface manoeuvring and station-keeping for an autonomous underwater vehicle. In *NATO Symposium, Applied Vehicle Technology Panel*, Ankara, Turkey, 2000.

[22] J. Yuh (ed). *Underwater Robotic Vehicles: Design and Control.* TSI Press, 1995.

[23] H. Eda and C. L. Crane. Steering characteristics of ships in calm water and waves. *Transaction of Society of Naval Architects and Marine Engineers (SNAME)*, 73(3):135–177, 1965.

[24] G. Ellis. *Observers in Control Systems: A Practical Guide.* Academic Press, San Diego, 2002.

[25] O. M. Faltisen1990. *Sea Loads on Ships and Offshore Structures.* Cambridge University Press, 1990.

[26] J. Ferguson, A. Pope, B. Butler, and R. Verrall. Theseus AUV - two record breaking missions. *Sea Technology*, 40(2):65–70, 1999.

[27] T. I. Fossen. *Nonlinear modeling and control of underwater vehicles.* PhD thesis, Norwegian Institude of Technology, 1991.

[28] T. I. Fossen. *Guidance and Control of Ocean Vehicles.* John Wiley & Sons, New York, 1994.

[29] T. I. Fossen. *Marine Control Systems: Guidance, Navigation and Control of Ships, Rigs and Underwater Vehicles.* Marine Cybernetics, 2002.

[30] T. I. Fossen and Å. Grøvlen. Nonlinear output feedback control of dynamically positioned ships using vectorial observer backstepping. *IEEE Transactions on Control Systems Technology*, 6(1):121–128, 1998.

[31] T. I. Fossen and S. Sagatun. Adaptive control of nonlinear systems: A case study of underwater robotic systems. *International Journal of Systems Science*, 8(3):393–412, 1991.

[32] T. I. Fossen and S. I. Sagatun. Adaptive control of nonlinear underwater robotic systems. In *Proc. of the 1991 IEEE Int. Conference on Robotics and Automation*, pages 1687–1694, Sacramento, California, 1991.

[33] T. I. Fossen and J. P. Strand. Passive nonlinear observer design for ships using Lyapunov methods: experimental result with a supply vessel. *Automatica*, 35(1):3–16, 1999.

[34] J. Fotakis, M. J. Grimble, and B. Kouvaritakis. A comparison of characteristic locus and optimal designs for dynamic ship positioning systems. *IEEE Transactions on Automatic Control*, 27(6):1143–1157, 1982.

[35] C. L. Frey and S. L. Wood. Development of an autonomous underwater vehicle for sub-ice environmental monitoring in Prudhoe Bay, Alaska. In *Proceedings of OCEANS 2003 MTS/IEEE*, pages 1161–1173, San Diego, California, USA, September 2003.

[36] P. T.-K. Fung and M. J. Grimble. Dynamic ship positioning using a self-tuning Kalman filtering. *IEEE Transactions on Automatic Control*, 28(3):339–350, 1983.

[37] K. R. Goheen and E. R. Jefferys. Multivariable self-tuning autopilots for autonomous and remotely operated underwater vehicles. *IEEE Journal of Oceanic Engineering*, 15(3):144–151, 1990.

[38] G. Grenon, P. E. An, S. M. Smith, and A. J. Healey. Enhancement of the inertial navigation system for the Morpheus autonomous underwater vehicles. *IEEE Journal of Oceanic Engineering*, 26(4):548–560, October 2001.

[39] G. Griffiths, N. W. Millard, S. D. McPhail, P. Stevenson, J. R. Perrett, M. Peabody, A. T. Webb, and D. T. Meldrum. Towards environmental monitoring with the Autosub autonomous underwater vehicle. In *Proceedings of the 1998 International Symposium on Underwater Technology*, pages 121–125, Tokyo, Japan, Apri 1998.

[40] Å. Grøvlen and T. I. Fossen. Nonlinear control of dynamic positioned ships using only position feedback: An observer backstepping approach. In *Proc. of the 35th IEEE Conf. on Decision and Control*, pages 3388 3393, Kobe, Japan, 1996.

[41] J. Guo, F. C. Chiu, and C. C. Huang. Design of a sliding mode fuzzy controller for the guidance and control of an autonomous underwater vehicle. *Ocean Engineering*, 30(16):2137–2155, 2003.

[42] P. E. Hagen, N. Stcøkersen, K. Vestgård, and P. Kartvedt. The HUGIN 1000 autonomous underwater vehicle for military applications. In *Proceedings of*

OCEANS 2003 MTS/IEEE, pages 1141–1145, San Diego, California, USA, September 2003.

[43] K. Hamilton and J. Evans. Subsea pilotless inspection using an autonomous underwater vehicle (SPINAV): concepts and results. In *Proceedings of IEEE OCEANS 2005 Europe*, pages 775–781, Brest, France, June 2005.

[44] A. J. Healey. Model-based maneuvering controls for autonomous underwater vehicles. *ASME Journal of Dynamics Systems,Measurement, and Control*, 114(4):614–622, December 1992.

[45] A. J. Healey and D. Lienard. Multivariable sliding mode control for autonomous diving and steering of unmanned underwater vehicles. *IEEE Journal of Oceanic Engineering*, 18(3):327–339, 1993.

[46] P. C. Hughes. *Spacecraft Attitude Dynamics.* John Wiley and Sons, New York, 1986.

[47] K. Ishii, T. Fujii, and T. Ura. Neural network system for online controller adaptation and its application to underwater robot. In *Proc. 1998 IEEE Int. Conference on Robotics and Automation*, pages 756–761, 1998. vol. 1.

[48] B. Jalving. Depth accuracy in seabed mapping with underwater vehicles. In *Proceedings of OCEANS 99 MTS/IEEE*, pages 973–978, Seattle,Washington, September 1999.

[49] Z. P. Jiang and I. Kanellakopoulos. Global output-feedback tracking for a benchmark nonlinear system. *IEEE Transactions on Automatic Control*, 45(5):1023–1027, 2000.

[50] J. Jouffroy and J. Lottin. On the use of contraction theory for the design of nonlinear observers for ocean vehicles. In *Proceedings of the American Control Conference*, pages 2647–2652, Anchorage, Alaska, 2002.

[51] M. R. Katebi, M. J. Grimble, and Y. Zhang. H_∞ robust control design for dynamic ship positioning. In *IEE Proceedings on Control Theory and Applications*, pages 110–120, 1997.

[52] N. Kato. Applications of fuzzy algorithm to guidance and control of underwater vehicles. In J. Yuh, editor, *Underwater Robotic Vehicles: Design and Control*. TSI, Albuquerque, 1995.

[53] H. Kermorgant. Architecture of AUV systems for harbour protection and mine countermeasure. In *Proceedings of IEEE OCEANS 2005 Europe*, pages 1400–1405, Brest, France, June 2005.

[54] H. K. Khalil. *Nonlinear System*. Prentice Hall, NJ, 1996. 2nd ed.

[55] B. Kinsman. *Wind Waves: Their Generation and Propagation on the Ocean Surface*. Dover Pubns, 1984.

[56] M. Krstić, I. Kanellakopoulos, and P. V. Kokotović. *Nonlinear and Adaptive Control Design*. John Wiley & Sons, Inc, New York, 1995.

[57] M. Kumagai, T. Ura, Y. Kuroda, and R. Walker. A new autonomous underwater vehicle designed for lake environment monitoring. *Advanced Robotics*, 16(1):17–26, 2002.

[58] N. H. Kussat, C. D. Chadwell, and R. Zimmerman. Absolute positioning of an autonomous underwater vehicle using GPS and acoustic measurements. *IEEE Journal of Oceanic Engineering*, 30(1):153–164, January 2005.

[59] D. A. Lawrence, W. A. Sethares, and W. Ren. Parameter drift instability in disturbance-free adaptive systems. *IEEE Transactions on Automatic Control*, 38(3):584–587, 1993.

[60] J. H. Li and P. K. Lee. Design of an adaptive nonlinear controller for depth control of an autonomous underwater vehicle. *Ocean Engineering*, 32(17-18):2165–2181, December 2005.

[61] J. H. Li and P. K. Lee. A neural network adaptive controller design for free-pitch-angle diving behavior of an autonomous underwater vehicle. *Robotics and Autonomous Systems*, 52(2-3):132–147, August 2005.

[62] K. P. Lindegaard. *Acceleration Feedback in Dynamic Positioning.* PhD thesis, Norwegian University of Science and Technology, 2003.

[63] K. P. Lindegaard and T. I. Fossen. A model based wave filter for surface vessels using position, velocity and partial acceleration feedback. In *Proceedings of 40th IEEE Conference on Decision and Control*, pages 946–951, Orlando FL, December 2001.

[64] S. Liu, D. Wang, and E. K. Poh. A nonlinear observer for AUVs in shallow water environment. In *Proceedings of IEEE International Conference on Intelligent Robots and Systems*, pages 1130–1135, Sendai, Japan, September 2004.

[65] S. Liu, D. Wang, and E. K. Poh. Station keeping of AUVs in shallow water environment: Observer and controller design. In *Proceedings of Third International Conference on Computational Intelligence, Robotics and Autonomous Systems*, Singapore, December 2005.

[66] S. Liu, D. Wang, and E. K. Poh. Nonlinear adaptive observer design for tracking control of AUVs in wave disturbance condition. In *Proceedings of OCEANS 2006 MTS/IEEE*, Singapore, June 2006.

[67] S. Liu, D. Wang, and E. K. Poh. Nonlinear output feedback tracking control for AUVs in shallow wave disturbance condition. Under review, 2006.

[68] S. Liu, D. Wang, and E. K. Poh. Output feedback control design for station keeping of AUVs in shallow water environment. Under review, 2006.

[69] S. Liu, D. Wang, E. K. Poh, and C. S. Chia. Nonlinear output feedback controller design for tracking control of ODIN in wave disturbance condition. In *Proceedings of OCEANS 2005 MTS/IEEE*, Washington,DC, October 2005.

[70] J. Lorentz and J. Yuh. A survey and experimental study of neural network AUV control. In *Proc. of the 1996 Symposium on Autonomous Underwater Vehicle Technology*, pages 109–116, 1996.

[71] A. Loria, T. I. Fossen, and E. Panteley. A separation principle for dynamic positioning of ships: theoretical and experimental results. *IEEE Transactions on Control Systems Technology*, 8(2):332–343, 2000.

[72] J.-F Lots, D.M. Lane, E. Trucco, and F. Chaumette. A 2D visual servoing for underwater vehicle station keeping. In *Proceedings of 2001 IEEE International Conference on Robotics and Automation*, pages 2767–2772, Seoul, Korea, May 2001.

[73] M. Morgado, P. Oliveira, C. Silvestre, and J.F. Vasconcelos. USBL/INS tightly-coupled integration technique for underwater vehicles. In *9th International Conference on Information Fusion (ICIF 2006)*, pages 1–8, July 2006.

[74] J. M. Morgan. *Dynamic Positioning of Offshore Vessels.* Petroleum, Tulsa, OK, 1978.

[75] W. Naeem, R. Sutton, and S. M. Ahmad. LQG/LTR control of an autonomous underwater vehicle using a hybrid guidance law. In *Proceedings of the 1st IFAC Workshop on Guidance and Control of Underwater Vehicles GCUV '03*, pages 35–40, Wales, UK, April 2003.

[76] Y. Nakamura and S. Savant. Nonlinear tracking control of autonomous underwater vehicles. In *Proc. of the 1992 IEEE International Conference on Robotics and Automation*, pages A4–A9, Nice, France, 1992.

[77] K. Nasahashi, T. Ura, A. Asada, T. Obara, T. Sakamaki, K. Kim, and K. Okamura. Underwater volcano observation by autonomous underwater vehicle "r2D4". In *Proceedings of IEEE OCEANS 2005 Europe*, pages 557–562, Brest, France, June 2005.

[78] S. Negahdaripour, X. Xu, and L. Jin. Direct estimation of motion from sea floor images for automatic station-keeping of submersible platforms. *IEEE Journal of Oceanic Engineering*, 24(3):370–382, July 1999.

[79] J. N. Newman. *Marine Hydrodynamics*. MIT Press, Massachusetts, 1977.

[80] T. Nicosevici, R. Garcia, M. Carreras, and M. Villanueva. A review of sensor fusion techniques for underwater vehicle navigation. In *Proceedings of OCEANS 2004 MTS/IEEE*, pages 1600 – 1605, Kobe,Japan, November 2004.

[81] J. Nie, J. Yuh, E. Kardash, and T. I. Fossen. On-board sensor-based adaptive control of small uuvs in very shallow water. *International Journal of Adaptive Control and Signal Processing*, 14(4):441–452, 2000.

[82] H. Nijmeijer and T. I. Fossen, editors. *New Directions in Nonlinear Observer Design*. Springer-Verlag, 1999.

[83] SNAME (The Society of Naval Architects and Marine Engineers). Nomenclature for treating the motion of a submerged body through a fluid. *Technical Research Bulletin*, 73(3):1–5, 1950.

[84] R. Ortega, A. Loria, P. J. Nicklasson, and H. Sira-Ramirez. *Passivity-Based Control of Euler-Lagrange Systems*. Springer, 1998.

[85] E. Panteley and A. Loria. On global uniform asymptotic stability of nonlinear time-varying systems in cascade. *Systems and Control Letters*, 33(2):131–138, 1998.

[86] M. Paulsen, O. Egeland, and T. I. Fossen. A passive output feedback controller with wave filter for marine vehicles. *International Journal of Robust and Nonlinear Control*, 8(15):1239–1253, 1998.

[87] K. Y. Pettersen and H. Nijmeijer. Output feedback tracking control for ships. In H. Nijmeijer and T. I. Fossen, editors, *New Directions in Nonlinear Observer Design*, pages 311–334, London, UK, 1999. Springer-Verlag.

[88] C. Puaut. Hydrodynamic analysis of an underwater body including free-surface effects. Master's thesis, Florida Atlantic University, 2001.

[89] R. Reid, A. Tugcu, and B. Mears. The use of wave filter design in Kalman filter state estimation of the automatic steering problem of a tanker in a seaway. *IEEE Transactions on Automatic Control*, 29(7):577–584, July 1984.

[90] K. Reif, F. Sonnemann, and R. Unbehauen. Nonlinear state observation using H_∞-filtering Riccati design. *IEEE Transactions on Automatic Control*, 44(1):203–208, January 1999.

[91] J. S. Riedel. *Seaway Learning and Motion Compensation in Shallow Waters for Small AUVs.* PhD thesis, Naval Postgraduate School, 1999.

[92] J. S. Riedel. Shallow water station keeping of an autonomous underwater vehicle: The experimental results of a disturbance compensation controller. In *Proceedings IEEE Oceans 2000*, pages 1017–1024, Providence, RI, September 2000.

[93] S. Sælid, N. A. Jenssen, and J. G. Balchen. Design and analysis of a dynamic positioning system based on Kalman filtering and optimal control. *IEEE Transactions on Automatic Control*, 28(3):331–339, 1983.

[94] C. Silpa-Anan. Autonomous underwater robot: Vision and control. Master's thesis, The Australian National University, 2001.

[95] J. J. E. Slotine, J. K. Hedrick, and E. A. Misawa. On sliding observers for nonlinear systems. *Journal of Dynamic Systems, Measurement, and Control*, 109(3):245–252, September 1987.

[96] S. M. Smith and S. E. Dunna. The Ocean Voyager II: an AUV designed for coastal oceanography. In *Proceedings of the 1994 Symposium on Autonomous Underwater Vehicle Technology*, pages 139–148, Cambridge, MA, July 1994.

[97] S. M. Smith, G. J. S. Rae, and D. T. Anderson. Applications of fuzzy logic to the control of an autonomous underwater vehicle. In *2nd IEEE International Conference on Fuzzy Systems*, pages 1099–1106, 1993. vol. 2.

[98] A. J. Sørensen, S. I. Sagatun, and T. I. Fossen. Design of a dynamic positioning system using model-based control. *Journal of Control Engineering Practice*, 4(3):359–368, 1996.

[99] A. J. Sørensen and J. P. Strand. Positioning of small-waterplane-area marine constructions with roll and pitch damping. *Journal of Control Engineering Practice*, 8(2):205–213, February 2000.

[100] R. M. Stanislaw. *Ocean Surface Waves: Their Physics and Prediction.* World Scientific, 1965.

[101] J. P. Strand. *Nonlinear Position Control System Design for Marine Vessels.* PhD thesis, Norwegian University of Science and Technology, 1999.

[102] J. P. Strand and T. I. Fossen. Nonlinear passive observer design for ships with adaptive wave filtering. In H. Nijmeijer and T. I. Fossen, editors, *New Directions in Nonlinear Observer Design*, pages 113–134, London, UK, 1999. Springer-Verlag.

[103] S. S. Tabaii, F. El-Hawary, and M. El-Hawary. Hybrid adaptive control of autonomous underwater vehicle. In *Proceedings of the 1994 Symposium on Autonomous Underwater Vehicle Technology*, pages 275–282, Cambridge, MA, July 1994.

[104] M. S. Triantafyllou and M. A. Grosenbaugh. Robust control for underwater vehicle systems with time delays. *IEEE Journal of Oceanic Engineering*, 16(1):146–151, January 1991.

[105] K. P. Valavanis, D. Gracanin, M. Matijasevic, R. Kolluru, and G. A. Demetriou. Control architectures for autonomous underwater vehicles. *IEEE Control Systems Magazine*, 17(6):48–64, 1997.

[106] P. van de Ven, C. Flanagan, and S. Toal. Neural network control of underwater vehicles. *Engineering Applications of Artificial Intelligence*, 18(5):533–547, August 2005.

[107] S. van der Zwaan and J. Santos-Victor. Real-time vision-based station keeping for underwater robots. In *Proceedings of MTS/IEEE OCEANS 2001 Conference*, pages 1058–1065, Honolulu, HI, November 2001.

[108] B. Vik and T. I. Fossen. Semi-global exponential output feedback control of ships. *IEEE Transactions on Control Systems Technology*, 5(3):360–370, 1997.

[109] J. S. Wang and C. S. G. Lee. Self-adaptive recurrent neuro-fuzzy control of an autonomous underwater vehicle. *IEEE Transactions on Robotics and Automation*, 19(2):283–295, April 2003.

[110] C. C. Canudas De Wit and J. J. E. Slotine. Sliding observers for robot manipulators. *Automatica*, 27(5):859–864, September 1991.

[111] D. R. Yoerger and J. E. Slotine. Robust trajectory control of underwater vehicles. *IEEE Journal of Oceanic Engineering*, 10(4):462–470, 1985.

[112] J. Yuh. Modeling and control of underwater robotic vehicles. *IEEE Trans. on Systems, Man, and Cybernetics*, 20(6):1475–1483, 1990.

[113] J. Yuh. A neural net controller for underwater robotic vehicles. *IEEE Journal of Oceanic Engineering*, 15(3):161–166, 1990.

[114] J. Yuh. Learning control for underwater robotic vehicles. *IEEE Control Systems Magazine*, 14(2):39–46, 1994.

[115] J. Yuh, J. Nie, and C. S. G. Lee. Experimental study on adaptive control of underwater robots. In *Proc. of the 1999 IEEE International Conference on Robotics & Automation*, pages 393–398, Detroit, Michigan, 1999.

Appendix A

A.1 Parameter Used in Simulation

To demonstrate the performance of the proposed observer and controller design in this thesis, the parameters of KAMBARA [94] in Australian National University is used for the all the simulations. The AUV dynamics is described by (3.3) and (3.4) with the parameter values given as follows.

$$M_1 = \text{diag}\{175.4, 140.8, 140.8\}$$

$$M_2 = \text{diag}\{14.08, 12.98, 16.07\}$$

$$C_1(\nu_1) = \begin{bmatrix} 0 & 140.8w & -140.8v \\ -140.8w & 0 & 175.4u \\ 140.8v & -175.4u & 0 \end{bmatrix}$$

$$C_2(\nu_2) = \begin{bmatrix} 0 & 16.07r & -12.98q \\ -16.07r & 0 & 14.08p \\ 12.98q & -14.08p & 0 \end{bmatrix}$$

$$D_1(\nu_1) = \text{diag}(120 + 90|u|, 90 + 90|v|, 150 + 120|w|)$$

$$D_2(\nu_2) = \text{diag}(15 + 10|p|, 15 + 12|q|, 18 + 15|r|)$$

$$g_1(\eta_2) = \begin{bmatrix} (W - B)sin\theta \\ -(W - B)cos\theta sin\phi \\ -(W - B)cos\theta cos\phi \end{bmatrix}$$

$$g_2(\eta_2) = \begin{bmatrix} -z_b B cos\theta sin\phi \\ -z_b B sin\theta - x_b B cos\theta cos\phi \\ x_b B cos\theta sin\phi \end{bmatrix}$$

where $W = 1148N$ and $B = 1108N$ are the gravity force and buoyancy force of KAMBARA, respectively. $r_B = [-0.017\ 0\ -0.115]^T$ is the distance of the center of buoyancy relative to the gravity center of the vehicle $r_G = [0\ 0\ 0]^T$.

Appendix B

B.1 Separation Principle

Consider the time varying system

$$\Sigma_1' : \dot{x}_1 = f_1(t, x_1) + g(t, x)x_2 \tag{B.1}$$

$$\Sigma_2' : \dot{x}_2 = f_2(t, x_2) \tag{B.2}$$

where $x_1 \in \mathcal{R}^n$, $x_2 \in \mathcal{R}^m$, $x \triangleq \text{col}[x_1, x_2]$. The function $f_1(t, x_1)$ is continuously differentiable in (t, x_1) and $f_2(t, x_2)$, $g(t, x)$ are continuous in their arguments, and locally Lipschitz.

Theorem B.1 If the following assumptions 1-3 below are satisfied, the cascaded system (B.1), (B.2) is globally uniformly asymptotically stable. [71]

(1) The system $\dot{x}_1 = f_1(t, x_1)$ is globally uniformly asymptotically stable with a Lyapunov function $V(t, x_1)$, $V : \mathcal{R} \geq 0 \times \mathcal{R}^n \to \mathcal{R} \geq 0$ positive definite (that is $V(t, 0) = 0$ and $V(t, x_1) > 0$ for all $x_1 \neq 0$) and proper (that is, radially undounded) which satisfies

$$\left\| \frac{\partial V}{\partial x_1} \right\| \|x_1\| \leq c_1 V(t, x_1) \qquad \forall \|x_1\| \geq \mu \tag{B.3}$$

where $c_1, \mu > 0$. We also assume that $(\partial V/\partial x_1)(t, x_1)$ is bounded uniformly in t for all $\|x_1\| \leq \mu$, that is, there exists a constant $c_2 > 0$ such that for all $t \geq t_0 \geq 0$

$$\left\|\frac{\partial V}{\partial x_1}\right\| \|x_1\| \leq c_2 \qquad \forall \|x_1\| \geq \mu \tag{B.4}$$

(2) The function $g(t, x)$ satisfies

$$\|g(t, x)\| \leq \theta_1(\|x_2\|) + \theta_2(\|x_2\|)\|x_1\| \tag{B.5}$$

where $\theta_1, \theta_2 : \mathcal{R} \geq 0 \rightarrow \mathcal{R} \geq 0$ are continuous.

(3) Equation $\dot{x}_2 = f_2(t, x_2)$ is globally uniformly asymptotically stable for all $t_0 \geq 0$,

$$\int_{t_0}^{\infty} \|x_2(t, t_0, x_2(t_0))\| dt \leq \phi(\|x_2(t_0)\|) \tag{B.6}$$

where function $\phi(\cdot)$ is a class $\mathcal{K}$ function.